KONINKLIJKE NEDERLANDSCHE AKADEMIE VAN WETENSCHAPPEN

PROCEEDINGS

VOLUME LII

No. 4

1949
NORTH-HOLLAND PUBLISHING COMPANY
(N.V. Noord-Hollandsche Uitgevers Mij.)
AMSTERDAM

CONTENTS

Chemistry. — *Phase determination in direct Fourier-synthesis of crystal structures.* By J. M. BIJVOET.

(Communicated at the meeting of March 26, 1949.)

A direct Fourier synthesis of the electrondensity in crystals is based on the fact that the amplitude of a density wave is proportional to that of the X-ray beam reflected by the corresponding netplane. The phases of the reflected waves being lost in ordinary X-ray methods [1]), the phase relations between the different density components remain unknown at this stage.

The method of isomorphous substitution $A_1R \rightarrow A_2R$ introduces, along familiar lines, known reference waves, viz. the density components of the A-configuration (for atomic scattering power A_2-A_1; we suppose this configuration to be centrosymmetrical and its determination accomplished).

The reference waves being known, their superposition effect on the density waves of the A_1R structure reveals their mutual phase differences, i.e. the unknown phases φ_{hkl} of the density waves of the A_1R structure relative to the centre of symmetry of the A-configuration:

$$F^2_{hkl\,A_2R} = F^2_{hkl\,A_1R} + F^2_{hkl\,A_2-A_1} + 2\,|F_{hkl}|_{A_1R}\,F_{hkl\,A_2-A_1}\cos\varphi_{hkl\,A_1R}\,.$$

Here $|F_{A_1R}|$ is derived from the diffraction-intensities of A_1R; $|F_{A_2R}|$ idem for crystal A_2R; $F_{A_2-A_1}$ is calculated for the A-configuration of atomic scattering power A_2-A_1.

Now this procedure gives us φ_{hkl} *except for its sign,* thus performing the phase (sign) determination only for the case of a centrosymmetrical A_1R structure (projection). Otherwise a synthesis with both φ_{hkl} and $-\varphi_{hkl}$ can be resorted to, resulting in a duplicated structure-model [2]).

Now we wish to call attention to the fact that in this non-symmetrical case there is, in principle, a general way of determining the sign of φ_{hkl}. We can use the abnormal scattering of an atom for a wavelength just beyond its K-absorption limit. This effect is made use of already in X-ray analysis to discriminate between atoms of scattering power nearly equal under normal conditions [3]). Even the abnormal phase shift has been used, as long ago as 1930, by COSTER in a manner similar to that proposed here [4]). Let the abnormal phase shift introduced at atom A be δ. Then the

---

[1]) C.f. those methods in which the scattered beam is made to interfere with the drect beam, i.a. H. OTT, Ann. Physik **31**, 264 (1938), D. GABOR, Nature **161**, 777 (1948).

[2]) C.f. C. BOKHOVEN, J. C. SCHOONE, J. M. BIJVOET, Proc. Kon. Ned. Akad. v. Wetensch., Amsterdam, **52**, 120 (1949).

[3]) See R. W. JAMES, The Cryst. State II (1948) Chapter IV (1).

[4]) D. COSTER, K. S. KNOL and J. A. PRINS, Z. f. Physik, **63**, 345 (1930).

phase differences $\pm \varphi_{hkl}$ between the density waves concerned result in the phase differences $\varphi_{hkl} + \delta$ resp. $-\varphi_{hkl} + \delta$ for the scattered radiation, and so will become distinguishable. At present we are testing the applicability of his method in an actual analysis.

It will be clear that by the above method it also becomes possible to attribute the *d* or *l* structure to an optically active compound on actual grounds and not merely by basic convention as in organic chemistry.

Van 't Hoff Laboratorium der
Rijksuniversiteit, Utrecht.

Mathematics. — *Contradictoriteit der elementaire meetkunde.* By L. E. J. BROUWER.

(Communicated at the meeting of March 26, 1949.)

In een vroegere mededeeling [1]) is de contradictoriteit der aequivalentie der relaties „>0" en „$\circ>0$" aangetoond [2]). Hieruit volgt tevens de contradictoriteit der aequivalentie der relaties „≥ 0" en „òf $=0$ òf $\circ>0$". Immers laatstgenoemde aequivalentie zou eerstgenoemde impliceeren.

Beschouwen we de *snijpuntsstelling der Euclidische planimetrie*, luidende dat voor elke twee lijnen a en l van het Euclidische vlak, die nòch kunnen samenvallen nòch evenwijdig kunnen zijn, een gemeenschappelijk punt kan worden aangewezen. Nemen we een rechthoekig coördinatenstelsel aan, en kiezen we voor a de X-as en voor l uitsluitend lijnen door het punt $P(0, 1)$ met richtingscoëfficiënt ≤ 0 en ≥ -1, dan leert de snijpuntsstelling in het bijzonder, dat voor elke lijn l door P met richtingscoëfficiënt <0 en ≥ -1 een snijpunt S met de X-as kan worden aangewezen, derhalve een natuurlijk getal $n(l)$ kan worden aangegeven zoodanig dat $x_S < 2^{n(l)}$, derhalve voor de richtingscoëfficiënt $\varrho(l)$ van l de relatie $\varrho(l) < -2^{-n(l)}$, dus de relatie $\varrho(l) <\circ\ 0$ geldt. Daar derhalve uit de snijpuntsstelling der planimetrie de contradictoor gebleken aequivalentie der relaties „<0" en „$<\circ\ 0$" volgt, *is de snijpuntsstelling der Euclidische planimetrie eveneens contradictoor gebleken.*

De hieruit voortvloeiende *contradictoriteit der Euclidische planimetrie* is evenwel door deze uitsluitend in de verte plaatsvindende manifestatie nauwelijks afdoende gedemonstreerd, terwijl de *snijpuntsstelling der projectieve planimetrie*, luidende dat voor elke twee lijnen van het projectieve vlak, die niet kunnen samenvallen, een gemeenschappelijk punt kan worden aangewezen, hierdoor nog niet wordt aangetast.

Beschouwen we wederom [1]) den met het eenheidscontinuum samenvallenden puntwaaier J. Zij f een willekeurig punt van J, verstaan we onder a_f de assertie, die f rationaal verklaart, en beschouwen we de soort σ der sequenties $S(\gamma, a_f)$ en de soort η der correspondeerende tweezijdige dempingsgetallen $E(\gamma, a_f)$, waarbij γ steeds voorstelt de tweevleugelige aanstuiving met kern 0 en telgetallen $(-1)^n 2^{-n}$ $(n = 1, 2, \ldots)$, doch f vrij varieert binnen J, met dien verstande dat het n^{de} element $k_n^{(\mu_n)}$ van f steeds na $c_n(\gamma, a_f)$ doch vóór $c_{n+1}(\gamma, a_f)$ wordt geschapen.

---

[1]) Proc. Kon. Ned. Akad. v. Wetensch., Amsterdam, **52**, p. 122 (1949).

[2]) Als resultaat der mededeeling is de non-aequivalentie van $>$ en $\circ>$ geformuleerd. De bewijsgang levert echter het verder strekkende resultaat der non-aequivalentie van „>0" en „$\circ>0$".

Zouden nu te eeniger tijd de relaties „$\neq 0$" en „òf < 0 òf > 0" voor het continuum aequivalent blijken, dan zou daarmee in het bijzonder voor elk element e van η kunnen worden aangetoond:

hetzij $e < 0$, in welk geval de onmogelijkheid van $e \circ > 0$, dus de absurditeit der rationaliteit van f zou zijn gebleken,

hetzij $e > 0$, in welk geval de onmogelijkheid van $e <\circ 0$, dus de niet-contradictoriteit der rationaliteit van f zou zijn gebleken.

Derhalve zou het eenheidscontinuum zijn *gesplitst* in twee puntkernsoorten, in elk van welke een element zou kunnen worden aangewezen, hetgeen onmogelijk is [3]). Zoodat van de aequivalentie der relaties „$\neq 0$" en „òf < 0 òf > 0" voor het continuum de absurditeit is gebleken.

Hieruit volgt tevens de contradictoriteit der aequivalentie van „$a = a$" en „òf $a \leq 0$ òf $a \geq 0$" voor het continuum. Immers laatstgenoemde aequivalentie zou eerstgenoemde impliceeren.

Beschouwen we een Euclidisch vlak met een rechthoekig coördinatenstelsel. Zij a de X-as, m de lijn $x = 1$, α een willekeurig reëel getal $\neq 0$, β de absolute waarde van α, P het punt $(-1, 2\beta)$, Q het punt $(1, \alpha)$, l de verbindingslijn der punten P en Q, γ een zoowel van $\frac{1}{3}$ als van 3 verwijderd liggend reëel getal. Dan snijdt de verbindingslijn van P met het punt $(\gamma, 0)$ de lijn m in het punt $\left(1, 2\beta\frac{\gamma-1}{\gamma+1}\right)$, dat met Q slechts kan samenvallen, als hetzij $2\beta\,\frac{\gamma-1}{\gamma+1} = \beta$, hetzij $2\beta\,\frac{\gamma-1}{\gamma+1} = -\beta$, d.w.z. als hetzij $\beta(\gamma-3) = 0$, hetzij $\beta(3\gamma-1) = 0$, welke vergelijkingen beide valsch zijn, zoodat het onmogelijk is, dat de verbindingslijn l van P en Q de X-as a snijdt in het punt $(\gamma, 0)$.

Mocht derhalve voor de lijnen l en a een snijpunt kunnen worden aangewezen, dan is dit òf het punt $(\frac{1}{3}, 0)$, òf het punt $(3, 0)$. In het eerste geval is α noodzakelijk < 0, in het laatste geval > 0.

Gold dus de snijpuntsstelling der projectieve planimetrie, kon derhalve voor iedere $\alpha \neq 0$ een gemeenschappelijk punt van a en l worden aangewezen, dan zouden de relaties „$\neq 0$" en „òf < 0 òf > 0" voor het continuum aequivalent zijn. Zoodat wegens de contradictoriteit dezer aequivalentie *eveneens de snijpuntsstelling der projectieve planimetrie contradictoor is gebleken,* waarmee zoowel van de Euclidische als van de projectieve planimetrie de contradictoriteit afdoende is gedemonstreerd.

Verwacht mag worden dat, met behulp van uit vrije variatie van f voortvloeiende soorten van dempingsgetallen door α_f, ook van andere reeds onjuist gebleken theorieën der klassieke wiskunde de contradictoriteit zal kunnen worden vastgesteld.

---

[3]) Vgl. Mathem. Annalen **97**, p. 66, noot [10]).

Mathematics. — *Approximate division of an angle into equal parts.* By J. G. VAN DER CORPUT and H. MOOIJ.

(Communicated at the meeting of March 26, 1949.)

The editors [1]) of Mathematica *A* published an approximate construction of the trisection, due to M. MARTENS, a former head-master. Although this construction is very accurate for acute angles (with an error smaller than 21′ 24″), it is surpassed in this respect by the very simple construction given by S. C. VAN VEEN [2]), of which the error for acute angles is less than 2′ 36″.

These articles led H. MOOIJ to deal in his thesis [3]) with the problem of dividing a given angle approximately into a number of equal parts and even of the approximate construction of $r\,\alpha$, where α is a given angle and r denotes a number between zero and one, which can be constructed with a pair of compasses and a ruler.

MOOIJ's construction is based on the following theorem.

First theorem.

Describe a circle, the centre of which coincides with the vertex O of the given angle $AOB = 2\alpha \leqq 180°$.

Suppose that the circle intersects the legs of the angle at A and B.

Let C be the middle of the segment AB. Produce AB to D in such a way, that

$$CD = \frac{r^2+3}{4r}\,AC.$$

Describe a circle with D as centre and $\frac{3-3r^2}{4r}\,AC$ as radius, which intersects the smaller arc AB at E. Then $\angle COE$ is approximately equal to $r\,\alpha$ and the difference is smaller than

$$\tfrac{4}{3}\,r\,(1-r^2)\,(\operatorname{tg}\tfrac{1}{2}\,\alpha + \tfrac{1}{4}\sin\alpha - \tfrac{3}{4}\,\alpha).$$

Thus the trisection ($r = \frac{1}{3}$) gives the following construction, which is identical to VAN VEEN's.

Describe a circle with the unit as radius, the centre O of which is the vertex of the given angle $AOB = 2\alpha \leqq 180°$. Assume that the circle intersects the legs of the given angle 2α at A and B. Let C be the middle of AB. Produce AB to D such that

$$CD = \frac{7}{3}\,AC.$$

---

1) Trisectie, Mathematica A 6 (1937—38), p. 1—4.

2) S. C. VAN VEEN, Benaderde trisectie, Mathematica A 7 (1938—39), p. 229—237.

3) H. MOOY, Over de didactiek van de meetkunde benevens benaderingsconstructies ter verdeling van een hoek in gelijke delen, Thesis Amsterdam 1948.

Describe a circle with D as centre and AB as radius, which intersects the smaller arc AB at E. Then $\angle COE$ is approximately equal to $\frac{1}{3}\alpha$ and the difference is smaller than

$$\tfrac{3}{8}\tfrac{2}{1}(\operatorname{tg}\tfrac{1}{2}\alpha+\tfrac{1}{4}\sin\alpha-\tfrac{3}{4}\alpha).$$

In this article the proof of the results found by MOOIJ will again be given. Further we shall give a second approximate construction of $r\alpha$, which is a little more complicated, but gives a more accurate approximation.

The new construction is based on the following theorem.

Second theorem.

Describe a circle with the unit as radius, the centre O of which coincides with the vertex of the given angle $AOB=2\alpha\leqq 180°$.

Assume the circle intersects the legs of the given angle at A and B; let C be the middle of AB. Produce AB to D such that

$$CD=\frac{1}{4r}(3+r^2)AC+\frac{1}{240\,r}(1-r^2)(9-r^2)\,AC^3. \quad . \quad . \quad (1)$$

Describe a circle with D as centre and the radius

$$\frac{3}{4r}(1-r^2)AC+\frac{1}{240\,r}(1-r^2)(9-r^2)\,AC^3. \quad . \quad . \quad . \quad . \quad (2)$$

If this circle intersects the smaller are AB of circle O at E, then $\angle COE$ is approximately equal to $r\alpha$ and the difference is smaller than

$$\tfrac{4}{3}r(\operatorname{tg}\tfrac{1}{2}\alpha+\tfrac{1}{4}\sin\alpha+\tfrac{3}{8}\tfrac{3}{0}\sin^3\alpha-\tfrac{3}{8}\tfrac{3}{0}\alpha\sin^2\alpha-\tfrac{3}{4}\alpha).$$

As for the trisection ($r=\frac{1}{3}$) we get the following approximate construction.

Describe a circle with the unit as radius, the centre O of which is the vertex of the given angle $OAB=2\alpha\leqq 180°$.

Assume that the circle intersects the legs of the given angle 2α at A and B and that C is the centre of AB. Produce AB to D, such that

$$CD=\tfrac{7}{3}AC+\tfrac{8}{8}\tfrac{8}{1}AC^3.$$

Describe a circle with D as centre and with

$$2\,AC+\tfrac{8}{8}\tfrac{8}{1}AC^3$$

as radius. This circle intersects the smaller arc AB at E. Than $\angle COE$ is approximately equal to[1] α and the difference is smaller than

$$\tfrac{4}{9}(\operatorname{tg}\tfrac{1}{2}\alpha+\tfrac{1}{4}\sin\alpha+\tfrac{3}{8}\tfrac{3}{0}\sin^3\alpha-\tfrac{3}{8}\tfrac{3}{0}\alpha\sin^2\alpha-\tfrac{3}{4}\alpha).$$

This construction becomes somewhat simpler, if the factor $(9-r^2)$ in the second term of (1) en (2) is replaced by 9.

If $r=\frac{1}{3}$, we get

$$CD=\tfrac{7}{3}AC+\tfrac{1}{1}\tfrac{1}{0}AC^3 \quad . \quad . \quad . \quad . \quad . \quad . \quad . \quad (3)$$

and the radius of the circle with D as centre becomes

$$2AC + \tfrac{1}{10} AC^3. \quad \ldots\ldots\ldots \quad (4)$$

This approximation is extraordinarily accurate. In order to have a survey of the accuracy of the approximation of the trisection, we give the following tables, referring to the three constructions I, II and III; here I denotes VAN VEEN's construction (which also occurs in MOOIJ's thesis); II is the construction according to the formulae (1) en (2) and finally III is the simpler construction in which the formulae (3) and (4) are applied.

Difference from $1/3\,\alpha$.

2α	I	II	III
180°	1° 35′ 17″	1° 4′ 9.5″	1° 3′ 7,1″
120°	11′ 19″	4′ 21,2″	4′ 16,9″
90°	2′ 38″	37,3″	35,7″
60°	18″	2,29″	2,25″

For the proof of the above assertions we need the following lemma

Lemma.

Assume the real numbers A, B, C and D satisfy the inequalities

$$A^2 + B^2 \geqq C^2; \quad A^2 + B^2 > D^2; \quad C \neq D$$

and the real number t satisfies

$$A \sin t + B \cos t = D.$$

Then the equation

$$A \sin x + B \cos x = C \quad \ldots\ldots\ldots \quad (5)$$

has at least one real solution x for which the inequality

$$|x - t| < \frac{2\,|C - D|}{\sqrt{A^2 + B^2 - C^2} + \sqrt{A^2 + B^2 - D^2}}$$

holds and for which $x-t$ has the same sign as

$$\frac{C - D}{A \cos t - B \sin t}.$$

Moreover

$$A \cos t - B \sin t = \pm \sqrt{A^2 + B^2 - D^2} \neq 0.$$

For the proof we substitute $x = t + u$ in (5) and we introduce z determined by

$$\operatorname{tg} \tfrac{1}{2} u = z \qquad (-\pi < u < \pi).$$

Equation (5) becomes

$$A \sin (t + u) + B \cos (t + u) = C,$$

whence

$$A\left(\frac{1-z^2}{1+z^2}\sin t+\frac{2z}{1+z^2}\cos t\right)+B\left(\frac{1-z^2}{1+z^2}\cos t-\frac{2z}{1+z^2}\sin t\right)=C,$$

consequently

$$z^2(A\sin t+B\cos t+C)-2z(A\cos t-B\sin t)-(A\sin t+B\cos t-C)=0,$$

hence

$$(D+C)z^2+2(B\sin t-A\cos t)z+C-D=0. \quad . \; . \quad (6)$$

The discriminant of this quadratic equation is

$$\Delta=(B\sin t-A\cos t)^2-(C^2-D^2)$$

and therefore

$$\Delta=A^2+B^2-C^2\geqq 0.$$

The roots of (6) are

$$\operatorname{tg}\tfrac{1}{2}u=\frac{A\cos t-B\sin t\pm\sqrt{A^2+B^2-C^2}}{C+D}$$
$$=\frac{A^2+B^2-D^2-A^2-B^2+C^2}{(C+D)(A\cos t-B\sin t\mp\sqrt{A^2+B^2-C^2})}.$$

The sign of $\pm\sqrt{A^2+B^2-C^2}$ can be taken equal to that of $A\cos t-B\sin t$ and then the sign of $\operatorname{tg}\frac{1}{2}u$ is the same as that of

$$\frac{C-D}{A\cos t-B\sin t}.$$

According to our convention u lies between $-\pi$ and π, so that $\frac{1}{2}u$ has the same sign as $\operatorname{tg}\frac{1}{2}u$, thus

$$|\tfrac{1}{2}u|<|\operatorname{tg}\tfrac{1}{2}u|=\frac{|C-D|}{\sqrt{A^2+B^2-C^2}+|A\cos t-B\sin t|}$$
$$=\frac{|C-D|}{\sqrt{A^2+B^2-C^2}+\sqrt{A^2+B^2-D^2}}$$

where $u=x-t$. This establishes the proof.

For the proof of the first theorem we put

$$AO=1;\ \angle COE=x;\ CD=p\sin\alpha;\ DE=q\sin\alpha \text{ and } \angle BDE=y.$$

By projecting OED on OC and on AD, we get the relations

$$\cos x-q\sin\alpha\sin y=\cos\alpha$$

and

$$\sin x+q\sin\alpha\cos y=p\sin\alpha.$$

By eliminating y we obtain

$$p\sin\alpha\sin x+\cos\alpha\cos x=1+\tfrac{1}{2}(p^2-q^2-1)\sin^2\alpha,$$

thus

$$A \sin x + B \cos x = C,$$

where

$$A = p \sin \alpha; \quad B = \cos \alpha \text{ and } C = 1 + \tfrac{1}{2}(p^2 - q^2 - 1) \sin^2 \alpha. \quad . \quad (7)$$

We have to determine A and C in such a way, that x is approximately equal to $r\alpha$; therefore we put

$$A \sin r\alpha + B \cos r\alpha = D. \quad . \quad . \quad . \quad . \quad . \quad . \quad . \quad (8)$$

Then, according to the above lemma,

$$|r\alpha - x| < \frac{2|C-D|}{\sqrt{A^2+B^2-C^2} + \sqrt{A^2+B^2-D^2}}. \quad . \quad . \quad . \quad (9)$$

Expanding $\cos r\alpha$ and $\sin r\alpha$ in powers of $\sin \alpha$, we get

$$\left.\begin{aligned} \cos r\alpha &= 1 - \frac{r^2}{2!}\sin^2\alpha - \frac{r^2(2^2-r^2)}{4!}\sin^4\alpha - \frac{r^2(2^2-r^2)(4^2-r^2)}{6!}\sin^6\alpha - \ldots \\ \sin r\alpha &= r\sin\alpha + \frac{r(1^2-r^2)}{3!}\sin^3\alpha + \frac{r(1^2-r^2)(3^2-r^2)}{5!}\sin^5\alpha + \ldots \end{aligned}\right\} \quad (10)$$

From the relations (7) and (10) it follows that (8) becomes

$$D = p\sin\alpha\left\{r\sin\alpha + \frac{r(1^2-r^2)}{3!}\sin^3\alpha + \ldots\right\} + \cos\alpha\cos r\alpha.$$

Differentiation of (10) gives

$$r\cos r\alpha = r\cos\alpha\left\{1 + \frac{1^2-r^2}{2!}\sin^2\alpha + \frac{(1^2-r^2)(3^2-r^2)}{4!}\sin^4\alpha + \ldots\right\}.$$

By substituting this result in the above value of D, we get

$$\left.\begin{aligned} D = p\sin\alpha &\left\{r\sin\alpha + \frac{r(1^2-r^2)}{3!}\sin^3\alpha + \frac{r(1^2-r^2)(3^2-r^2)}{5!}\sin^5\alpha + \ldots\right\} + \\ &+ (1-\sin^2\alpha)\left\{1 + \frac{1^2-r^2}{2!}\sin^2\alpha + \frac{(1^2-r^2)(3^2-r^2)}{4!}\sin^4\alpha + \ldots\right\}. \end{aligned}\right\} \quad (11)$$

Putting

$$a_h = \{(2h-1)^2 - \varrho\}\, a_{h-1}; \quad a_0 = 1; \quad \psi(h) = -(2h-1+\varrho) + 2prh$$

and replacing $\sin\alpha$ by s and r^2 by ϱ, we find

$$D = \sum_{h=0}^{\infty} \frac{s^{2h}\, a_{h-2}\{(2h-3)^2 - \varrho\}}{(2h)!}\, \psi(h) \quad . \quad . \quad . \quad . \quad . \quad (12)$$

In order to get a good approximation of $r\alpha$, we choose p and q in such a way, that the expansion of $C-D$ begins with $\sin^6\alpha$. This gives

$\tfrac{1}{2}(p^2-q^2-1) = pr - 1 + \tfrac{1}{2}(1-r^2)$ and

$$\frac{pr(1^2-r^2)}{3!} + \frac{(1^2-r^2)(3^2-r^2)}{4!} - \frac{1^2-r^2}{2!} = 0,$$

hence

$$p = \frac{r^2+3}{4r} \text{ and } q = \frac{3-3r^2}{4r}. \quad \ldots\ldots \quad (13)$$

In what follows an upperbound is given for the error, provided that r lies between 0 and 1. Substituting in (12) the value of p given by (13), we get

$$\psi(h) = -2h+1-\varrho+\frac{r^2+3}{2r}hr = \tfrac{1}{2}(h-2)(\varrho-1)$$

hence

$$D = \sum_{h=0}^{\infty} \frac{s^{2h}\, a_{h-2}\,\{(2h-3)^2-\varrho\}}{2\,.\,(2h)!}(h-2)(\varrho-1).$$

In $C-D$ the terms with s^0; s^2 and s^4 disappear, hence

$$C-D = -\sum_{h=3}^{\infty} \frac{s^{2h}\, a_{h-2}\,\{(2h-3)^2-\varrho\}}{2\,.\,(2h)!}(h-2)(\varrho-1)$$
$$= (1-\varrho)^2(3^2-\varrho)\,U\,s^6,$$

where

$$U = \frac{1}{2\,.\,6!}+\frac{2\,(5^2-\varrho)\,5^2}{2\,.\,8!}+\frac{3\,.\,(5^2-\varrho)\,(7^2-\varrho)\,5^4}{2\,.\,10!}+\ldots.$$

By virtue of $0 \leqq \varrho \leqq 1$ the inequality $U \leqq U_0$ is evident, consequently

$$C-D \leqq s^6(1-\varrho)^2(3^2-\varrho)\,U_0$$

where U_0 denotes the value of U at the point $\varrho = 0$. Hence

$$C-D \leqq (1-\varrho)^2\left(1-\tfrac{1}{9}\varrho\right)(C-D)_0, \quad \ldots\ldots \quad (14)$$

where $(C-D)_0$ denotes the value which $C-D$ takes for $\varrho = 0$.

The denominator of the right hand side of (9) contains the terms $\sqrt{A^2+B^2-C^2}$ and $\sqrt{A^2+B^2-D^2}$. Here

$$A^2+B^2-C^2 = p^2s^2+\cos^2\alpha-\{1+\tfrac{1}{2}(p^2-q^2-1)s^2\}^2$$
$$= q^2s^2-\tfrac{1}{4}(p^2-q^2-1)^2s^4.$$

Substitution of the values of p and q, found in (13), gives

$$A^2+B^2-C^2 = \frac{9(1-\varrho)^2}{16\varrho}s^2-\frac{(1-\varrho)^2}{16}s^4,$$

hence

$$\sqrt{A^2+B^2-C^2} = \frac{3(1-\varrho)}{4r}s\sqrt{1-\frac{\varrho}{9}s^2}. \quad \ldots\ldots \quad (15)$$

By putting $t = r\alpha$ in the last formula of our lemma and substituting (7), we obtain

$$\pm\sqrt{A^2+B^2-D^2} = p\sin\alpha\cos r\alpha-\cos\alpha\sin r\alpha \quad \ldots \quad (16)$$

With the aid of the series (10), by substituting $p = \frac{r^2+3}{4r}$, and, putting $c_0 = 1$ and $c_h = (4h^2-\varrho)\, c_{h-1}$ $(h \geqq 1)$, we get

$$\pm \sqrt{A^2+B^2-D^2} = \frac{r(1-\varrho)}{4}\left\{3\varrho\, s - \frac{s^3}{3!} + \frac{2^2-\varrho}{5!}\, s^5 + \frac{3(4^2-\varrho)(2^2-\varrho)}{7!}\, s^7 + \ldots\right\}$$

$$= \frac{r(1-\varrho)}{4} \sum_{h=1}^{\infty} \frac{(2h-5)\, c_{h-2}}{(2h-1)!}\, s^{2h-1}.$$

The right hand side is $\geqq 0$, consequently

$$\sqrt{A^2+B^2-D^2} \geqq \frac{3(1-\varrho)}{4r}\, s\left(1 - \frac{\varrho}{18}\, s^2\right)$$

and a fortiori

$$\sqrt{A^2+B^2-D^2} > \frac{3(1-\varrho)}{4r}\, s \sqrt{1 - \frac{\varrho}{9}\, s^2} \quad . \quad . \quad . \quad . \quad (17)$$

The relations (9), (14), (15) en (17) give

$$|ra-x| < \frac{2(1-\varrho)^2 (1-\frac{1}{9}\varrho)(C-D)_0}{\frac{3(1-\varrho)s}{4r}\sqrt{1-\frac{1}{9}\varrho s^2} + \frac{3(1-\varrho)s}{4r}\sqrt{1-\frac{1}{9}\varrho s^2}} \ldots$$

From $C_0 = 1 + \frac{1}{4}s^2$ and $D_0 = \frac{3}{4}\alpha \sin\alpha + \cos\alpha$ it follows that

$$(C-D)_0 = 1 + \tfrac{1}{4}\sin^2\alpha - \tfrac{3}{4}\alpha \sin\alpha - \cos\alpha$$

$$= \sin\alpha\left(\operatorname{tg}\frac{\alpha}{2} + \tfrac{1}{4}\sin\alpha - \tfrac{3}{4}\alpha\right).$$

Hence

$$|ra-x| < \frac{2(1-\varrho)^2(1-\frac{1}{9}\varrho)\, s\left(\operatorname{tg}\frac{\alpha}{2} + \frac{1}{4}\operatorname{tg}\alpha - \frac{3}{4}\alpha\right)}{\frac{2.3(1-\varrho)s}{4r}\sqrt{1-\frac{1}{9}\varrho s^2}}.$$

Consequently

$$|ra-x| < \tfrac{4}{3}\, r(1-\varrho)\left(\operatorname{tg}\tfrac{1}{2}\alpha + \tfrac{1}{4}\sin\alpha - \tfrac{3}{4}\alpha\right).$$

This establishes the proof of the first theorem. For the proof of the second theorem we put

$$p = \frac{P}{r} + \frac{Q}{r}\, s^2 \quad . \quad . \quad . \quad . \quad . \quad . \quad . \quad . \quad (18)$$

Then

$$C = 1 + \tfrac{1}{2}(p^2-q^2-1)\, s^2 = 1 + K s^2 + L s^4, \quad , \quad . \quad . \quad (19)$$

where P, Q, K and L are properly chosen functions of r. Formula (8) gives

$$D = \left(\frac{P}{r} + \frac{Q}{r}\, s^2\right) s \sin ra + \cos\alpha \cos ra,$$

hence

$$D=(Ps^2+Qs^4)\sum_{h=0}^{\infty}\frac{a_h s^{2h}}{(2h+1)!}+(1-s^2)\sum_{h=0}^{\infty}\frac{a_h}{(2h)!}s^{2h},$$

where

$a_h=(1^2-\varrho)(3^2-\varrho)\ldots((2h-1)^2-\varrho)$ and $a_0=1$, so $a_h=\{(2h-1)^2-\varrho\}\,a_{h-1}$,

consequently

$$D=\sum_0^{\infty}s^{2h}\left\{\frac{a_h}{(2h)!}-\frac{a_{h-1}}{(2h-2)!}+\frac{P\,a_{h-1}}{(2h-1)!}+\frac{Q\,a_{h-2}}{(2h-3)!}\right\}$$

$$=\sum_0^{\infty}s^{2h}\,a_{h-2}\left\{\frac{(2h-1)^2-\varrho}{(2h)!}((2h-3)^2-\varrho)-\frac{(2h-3)^2-\varrho}{(2h-2)!}+\right.$$

$$\left.+\frac{(2h-3)^2-\varrho}{(2h-1)!}P+\frac{Q}{(2h-3)!}\right\}.$$

This gives

$$D=\sum_0^{\infty}\frac{s^{2h}\,a_{h-2}}{(2h)!}\varphi(h)$$

where

$$\varphi(h)=-\{(2h-1)+\varrho\}\{(2h-3)^2-\varrho\}+2h\{(2h-3)^2-\varrho\}P+$$

$$+2h(2h-1)(2h-2)Q.$$

The functions P, Q, K and L are chosen such that the expansion of $C-D$ begins with s^8. By virtue of

$$D=1+\frac{s^2}{2!}(-1-\varrho+2P)+\frac{s^4}{4!}\{-(3+\varrho)(1-\varrho)+4(1-\varrho)P+4.3.2.Q\}+$$

$$+\frac{s^6(1-\varrho)}{6!}\{-(5+\varrho)(9-\varrho)+6(9-\varrho)P+6.5.4Q\}+\ldots$$

we get in connection with (19)

$$2K=-1-\varrho+2P; \quad\ldots\ldots\ldots \quad (20)$$

$$24L=-(3+\varrho)(1-\varrho)+4(1-\varrho)P+4.3.2.Q; \quad\ldots \quad (21)$$

$$-(5+\varrho)(9-\varrho)+6(9-\varrho)P+6.5.4.Q=0. \quad\ldots \quad (22)$$

Substitution in (19) of the values of p and $2K$, found respectively in (18) and (20) furnishes

$$q^2\varrho=(P-\varrho)^2+2s^2(PQ-L\varrho)+s^4Q^2. \quad\ldots\ldots \quad (23)$$

To simplify we put the right hand side of this equation equal to a perfect square, by choosing

$$PQ-L\varrho=(P-\varrho)Q, \text{ hence } L=Q.$$

From (21) follows

$$4(1-\varrho)P=(3+\varrho)(1-\varrho), \text{ hence } P=\frac{3+\varrho}{4}\ldots\ldots \quad (24)$$

Formula (22) gives

$$120\,Q=(5+\varrho)(9-\varrho)-6(9-\varrho)\,.\,\frac{3+\varrho}{4},$$

hence

$$Q=L=\frac{(1-\varrho)(9-\varrho)}{240}.$$

By (20) and (24) we obtain

$$K=\frac{1-\varrho}{4}.$$

Now (23) becomes

$$\varrho q^2=(P-\varrho+Qs^2)^2 \text{ and } rq=\pm(P-\varrho+Qs^2).$$

The left hand side of the last relation and also both $P-\varrho$ and Qs^2 are positive, so that the plus sign holds good. This gives

$$rq=\frac{1-\varrho}{240}\{180+(9-\varrho)s^2\}$$

and by (18)

$$rp=\frac{3+\varrho}{4}+\frac{(1-\varrho)(9-\varrho)}{240}s^2. \quad . \quad . \quad . \quad . \quad . \quad . \quad (25)$$

In order to obtain an upper bound of the error, we deduce from our lemma that this error is

$$|ra-x|<\frac{2|C-D|}{\sqrt{A^2+B^2-C^2}+\sqrt{A^2+B^2-D^2}};$$

here

$$C-D=-\sum_{h=4}^{\infty}\frac{s^{2h}\,a_{h-2}}{(2h)!}\varphi(h)$$

and

$$\varphi(h)=-\{2h-1+\varrho\}\{(2h-3)^2-\varrho\}+$$
$$+2h\{(2h-3)^2-\varrho\}P+2h(2h-1)(2h-2)Q.$$

Consequently

$$\varphi(h)=-\{(2h-1)+\varrho\}\{(2h-3)^2-\varrho\}+$$
$$+2h\{(2h-3)^2-\varrho\}\frac{3+\varrho}{4}+2h(2h-1)(2h-2)\frac{(1-\varrho)(9-\varrho)}{240},$$

which gives after reduction

$$\varphi(h)=\frac{(1-\varrho)(h-3)}{60}\{-102h^2+267h-180-\varrho(2h^2+3h-20)\},$$

hence

$$C-D=\frac{1-\varrho}{60}\sum_{h=4}^{\infty}(h-3)\frac{s^{2h}\,a_{h-2}}{(2h)!}\{102h^2-267h+180+\varrho(2h^2+3h-20)\}.$$

In this relation we have for $h \geqq 4$

$$a_{h-2} = (1-\varrho)\,(1-\tfrac{1}{9}\,\varrho)\,b_{h-2}(\varrho),$$

where $b_{h-2}(\varrho)$ is a polynomial in ϱ, which has in the interval $0 \leqq \varrho \leqq 1$ its maximum value at the point $\varrho = 0$, therefore

$$0 \leqq a_{h-2} \leqq (1-\varrho)\,(1-\tfrac{1}{9}\,\varrho)\,b_{h-2}(0) = (1-\varrho)\,(1-\tfrac{1}{9}\,\varrho)\,a_{h-2}(0).$$

Further

$$102\,h^2-267\,h+180+\varrho\,(2h^2+3h-20) \leqq (1+\tfrac{1}{81}\,\varrho)\,(102\,h^2-267\,h+180);$$

for this relation is equivalent to the inequality

$$62\,h^2+93\,h-620 \leqq 102\,h^2-267\,h+180,$$

which is evident in virtue of $h^2-9\,h+20 \geqq 0$. Hence

$$C-D \leqq$$

$$\leqq \frac{(1-\varrho)^2}{60}\,(1-\tfrac{1}{9}\,\varrho)\sum_{h=4}^{\infty}(h-3)\,\frac{s^{2h}}{(2h)!}\,a_{h-2}(0)\,(1+\tfrac{1}{81}\,\varrho)\,(102\,h^2-267\,h+180).$$

This furnishes

$$C-D \leqq (1-\varrho)\,(1-\tfrac{1}{9}\,\varrho)\,(1+\tfrac{1}{81}\,\varrho)\,(C-D)_0. \quad . \quad . \quad . \quad (26)$$

From (7), (8) and (25) we deduce

$$D = \frac{3+\varrho}{4r}\sin\alpha\sin r\alpha + \frac{(1-\varrho)\,(9-\varrho)}{240\,r}\sin^3\alpha\sin r\alpha + \cos\alpha\cos r\alpha,$$

hence

$$D_0 = \tfrac{3}{4}\,\alpha\sin\alpha + \tfrac{3}{80}\,\alpha\sin^3\alpha + \cos\alpha.$$

Further

$$C_0 = 1 + \tfrac{1}{4}\,s^2 + \tfrac{3}{80}\,s^4,$$

hence

$$(C-D)_0 = 1 + \tfrac{1}{4}\,s^2 + \tfrac{3}{80}\,s^4 - \tfrac{3}{4}\,\alpha\,s - \tfrac{3}{80}\,\alpha\,s^3 - \cos\alpha,$$

consequently

$$(C-D)_0 = \sin\alpha\,(\operatorname{tg}\tfrac{1}{2}\,\alpha + \tfrac{1}{4}\sin\alpha + \tfrac{3}{80}\sin^3\alpha - \tfrac{3}{80}\,\alpha\sin^2\alpha - \tfrac{3}{4}\,\alpha). \quad (27)$$

Further

$$A^2+B^2-C^2 = p^2\sin^2\alpha + \cos^2\alpha - (1+K\sin^2\alpha+L\sin^4\alpha)^2$$

$$= \left(\frac{P}{r}+\frac{Qs^2}{r}\right)^2 s^2 + 1 - s^2 - (1+K^2s^4+L^2s^8+2Ks^2+2Ls^4+2KLs^6),$$

where $Q = L$, hence

$$A^2+B^2-C^2 = \frac{P^2}{\varrho}\,s^2 + \frac{2PQ}{\varrho}\,s^4 + \frac{Q^2}{\varrho}\,s^6 +$$

$$+ 1 - s^2 - 1 - K^2s^4 - Q^2s^8 - 2Ks^2 - 2Qs^4 - 2KQs^6$$

$$= s^2\left\{\frac{P^2}{\varrho} - 1 - 2K + s^2\left(\frac{2PQ}{\varrho} - K^2 - 2Q\right) + s^4\left(\frac{Q^2}{\varrho} - 2QK\right) - Q^2s^6\right\}.$$

Substitution of the values of P, Q and K gives

$$\sqrt{A^2+B^2-C^2} = \frac{1-\varrho}{4}\, s \sqrt{\left\{ \frac{9}{\varrho} + \frac{9-11\varrho}{10\varrho}\, s^2 + \right.}$$

$$\left. + \frac{(9-\varrho)(9-121\varrho)}{3600\varrho}\, s^4 - \frac{(9-\varrho)^2}{3600}\, s^6 \right\}.$$

In order to deduce from this relation the inequality

$$\sqrt{A^2+B^2-C^2} \geqq \frac{1-\varrho}{4} \frac{3s}{\sqrt{\varrho}} (1-\tfrac{1}{9}\varrho)(1+\tfrac{1}{81}\varrho), \quad . \quad . \quad . \quad (28)$$

we remark that this inequality is equivalent to

$$\frac{9}{\varrho} + \frac{9-11\varrho}{10\varrho} \cdot s^2 + \frac{(9-\varrho)(9-121\varrho)}{3600\varrho}\, s^4 - \frac{(9-\varrho)^2}{3600}\, s^6$$

$$\geqq \frac{9}{\varrho} (1-\tfrac{2}{9}\varrho+\tfrac{1}{81}\varrho^2) \left(1+\frac{2}{31}\varrho+\frac{1}{31^2}\varrho^2\right)$$

and therefore equivalent to

$$\left(\frac{81}{3600}\, s^4 + \frac{9}{10}\, s^2\right) \frac{1}{\varrho} + \left(\frac{44}{31} - \frac{11}{10}\, s^2 - \frac{1098}{3600}\, s^4 - \frac{81}{3600}\, s^6\right)$$

$$+ \left(\frac{121}{3600}\, s^4 + \frac{18}{3600}\, s^6 + \frac{74}{9.961}\right) \varrho - \left(\frac{1}{3600}\, s^6 + \frac{44}{9.961}\right) \varrho^2 - \frac{1}{9.961}\, \varrho^3 \geqq 0.$$

To prove this inequality it is sufficient to consider the most unfavourable case, viz. $s = 1$; in this case the inequality becomes

$$\frac{369}{400}\frac{1}{\varrho} - \frac{101}{12400} + \frac{163179}{961.3600}\,\varrho - \frac{18561}{961.3600}\,\varrho^2 - \frac{1}{9.961}\,\varrho^3 \geqq 0,$$

which is true for every value of ϱ between 0 and 1.

By substituting in (16) the value of p found in (25) we get

$$\sqrt{A^2+B^2-D^2} = \frac{3(1-\varrho)}{4r}\, s + \frac{(9-11\varrho)(1-\varrho)}{240r}\, s^3 - \frac{r(1-\varrho)}{4.4!}\, s^5 \ldots$$

$$+ \sum_{n=4}^{\infty} \frac{r(2^2-\varrho)\ldots((2n-6)^2-\varrho)(1-\varrho)(2n-7)\{102n^2-369n+339+(n-3)(2n+7)\varrho\}\, s^{2n-1}}{120\,(2n-1)!}.$$

This gives

$$\left.\sqrt{A^2+B^2-D^2} \geqq \frac{3(1-\varrho)}{4r}\, s + \frac{(9-11\varrho)(1-\varrho)}{240r}\, s^3 - \right.$$

$$\left. - \frac{r(1-\varrho)}{4.4!}\, s^5 \geqq \frac{1-\varrho}{4} \frac{3s}{\sqrt{\varrho}} (1-\tfrac{1}{9}\varrho)(1+\tfrac{1}{81}\varrho). \right\} \quad (29)$$

In fact this relation becomes after reduction

$$\tfrac{1}{20}\, s^2 + \tfrac{22}{279}\,\varrho - \tfrac{11}{1810}\,\varrho\, s^2 + \tfrac{1}{2719}\,\varrho^2 - \tfrac{1}{72}\,\varrho\, s^4 \geqq 0,$$

that is

$$\tfrac{1}{20}\, s^2 + \varrho\,(\tfrac{22}{279} - \tfrac{11}{180}\, s^2 - \tfrac{1}{72}\, s^4) + \tfrac{1}{2}\tfrac{1}{79}\,\varrho^2 \geqq 0$$

and this inequality holds because for $0 \leqq s \leqq 1$ the factor of ϱ is at least equal to

$$\tfrac{22}{279} - \tfrac{11}{180} - \tfrac{1}{72} > 0.$$

Now by virtue of (26), (27), (28) and (29) the relation (9) becomes

$$|ra - x| <$$

$$< \frac{2(1-\varrho)(1-\frac{1}{9}\varrho)(1+\frac{1}{31}\varrho)\sin\alpha\,(\operatorname{tg}\frac{1}{2}\alpha + \frac{1}{4}\sin\alpha + \frac{3}{80}\sin^3\alpha - \frac{3}{80}\alpha\sin^2\alpha - \frac{3}{4}\alpha)}{2\,\frac{1-\varrho}{4}\,\frac{3s}{\sqrt{\varrho}}\,(1-\frac{1}{9}\varrho)(1+\frac{1}{31}\varrho)}$$

which gives after reduction

$$|ra - x| < \tfrac{4}{3}\, r\,(\operatorname{tg}\tfrac{1}{2}\alpha + \tfrac{1}{4}\sin\alpha + \tfrac{3}{80}\sin^3\alpha - \tfrac{3}{80}\,\alpha\sin^2\alpha - \tfrac{3}{4}\,\alpha).$$

This becomes in the special case $r = \frac{1}{3}$

$$|ra - x| < \tfrac{4}{9}\,(\operatorname{tg}\tfrac{1}{2}\alpha + \tfrac{1}{4}\sin\alpha + \tfrac{3}{80}\sin^3\alpha - \tfrac{3}{80}\,\alpha\sin^2\alpha - \tfrac{3}{4}\,\alpha).$$

This establishes the proof of the second theorem.

Mathematics. — *Een iteratieproces voor de oplossing van een randwaardeprobleem bij een lineaire partiële differentiaalvergelijking van de tweede orde.* I. By J. J. DRONKERS. (Communicated by Prof. W. VAN DER WOUDE.)

(Communicated at the meeting of February 26, 1949.)

§ 1.

In dit artikel wordt een iteratieproces behandeld, ter verkrijging van een oplossing $z(x, y)$ van een lineaire partiële differentiaalvergelijking van de tweede orde:

$$\frac{\partial^2 z}{\partial x^2} + a\frac{\partial^2 z}{\partial y^2} + b\frac{\partial^2 z}{\partial x \partial y} + c\frac{\partial z}{\partial x} + d\frac{\partial z}{\partial y} + ez + f = 0 \quad . \quad . \quad (1)$$

waarbij de randwaarden gegeven zijn voor $x = 0$:

$$\left(\frac{\partial z}{\partial x}\right)_{x=0} \text{ en } z(0, y). \quad . \quad . \quad . \quad . \quad . \quad . \quad . \quad . \quad (2)$$

Hierbij zijn a, b, c, d, e en f functies van x en y, waarbij in het vervolg die waarden van x en y beschouwd worden, die gelegen zijn in de intervallen $0 \leq x \leq A$ en $0 \leq y \leq B$.

Nu wordt het volgende verondersteld:

Van de functies b en c bestaan haar afgeleiden naar x van de eerste orde. Deze zijn tevens continu in x, hetgeen ook het geval is met de overige functies a, d, e en f.

In het bijzonder zijn alle functies a t.m. f, de genoemde afgeleide functies van b en c naar x van de eerste orde, benevens de randwaarden $\left(\frac{\partial z}{\partial x}\right)_{x=0}$ en $z(0, y)$ analytisch in y en begrensd.

Voor de afgeleide naar y van de k^e orde van ieder der genoemde functies geldt dan analoog als voor de functie a:

$$\left|\frac{\partial^k a}{\partial y^k}\right| < M_1 \varrho^k k! \quad (k = 1, 2 \ldots n, \ldots)$$

waarbij M_1 en ϱ onafhankelijk zijn van x, y en k, terwijl M_1 zo gekozen kan worden, dat ze ook voor alle andere functies toegepast kan worden.

Voor alle functies geldt dus, dat de afgeleiden naar y van de k^e orde na deling door $k!$ en ϱ^k begrensd zijn.

De iteratiemethode, die in dit artikel wordt behandeld, is verschillend van die, welke PICARD [1]) toepast om een integraal te verkrijgen van de hyperbolische partiële differentiaalvergelijking van de tweede orde, indien

---

[1]) E. PICARD: Mémoire sur la théorie des équations aux dérivées partielles et la

deze — eventueel na een coördinatentransformatie — van de vorm is:

$$\frac{\partial^2 z}{\partial x \partial y} = p\frac{\partial z}{\partial x} + q\frac{dz}{dy} + rz + s.$$

Een differentiaalvergelijking van deze vorm wordt zelfs in het vervolg uitgezonderd.

Ook is van PICARD een iteratiemethode afkomstig om een oplossing te verkrijgen van de elliptische partiële differentiaalvergelijking van de tweede orde.

In dit artikel wordt de partiële differentiaalvergelijking van de tweede orde (1), die van het hyperbolische, elliptische of parabolische type kan zijn, vervangen door 2 lineaire partiële differentiaalvergelijkingen van de eerste orde. Daarna wordt een iteratiemethode aangegeven om een oplossing te verkrijgen van deze twee vergelijkingen met randwaarden, die afhankelijk zijn van de randwaarden, welke in (2) zijn aangegeven. Dan wordt tevens de integraal $z(x, y)$ verkregen, die aan (1) en de gestelde randwaarden voldoet.

Alle iteratiemethoden betreffende partiële differentiaalvergelijkingen vertonen veel overeenkomst. De in dit artikel weergegeven oplossing onderscheidt zich door de voorwaarden, die aan de verschillende functies van (1) en (2) zijn opgelegd in verband met het convergentiebewijs van de iteratiemethode. Dit bewijs is van een andere structuur, dan gewoonlijk bij overeenkomstige iteratiemethoden voorkomt.

Om de convergentie van de iteratiemethoden van PICARD te bewijzen moet o.a. verondersteld worden, dat het gebied waarvoor de oplossing geldt, zo klein is, dat hiervoor de te bepalen functie $|z(x, y)|$, benevens $\left|\frac{\partial z}{\partial x}\right|$ en $\left|\frac{\partial z}{\partial y}\right|$ kleiner zijn dan een constante c.

Een dergelijke veronderstelling wordt in dit artikel niet gemaakt, zoals uit de hiervoren aangegeven voorwaarden blijkt. Er worden alleen voorwaarden opgelegd aan de bekende functies a, b, enz. van (1) en aan de randwaarden.

Betreffende de variabele x wordt alleen continuïteit verondersteld, terwijl de functies in y analytisch aangenomen worden.

Bij vele in de literatuur der toegepaste wiskunde voorkomende verhandelingen betreffende de convergentie van iteratiemethoden, is het o.a. nodig te veronderstellen, dat alle afgeleiden naar x of y van de bekende functies bestaan en tevens begrensd zijn. In verband hiermede moet vaak voor x of y of beiden een bepaalde lengte-eenheid gekozen worden (bv. sin $2x$ voldoet niet aan deze voorwaarden, sin x wel).

---

méthode des approximations successives. Journal de mathématiques pures et appliquées. Paris 1890.

E. GOURSAT: Cours d'analyse mathématique, troisième édition, tome III, pages 133 et 229 etc. Paris 1923.

COURANT und HILBERT: Mathemathische Physik II, pag. 317 e.v.

Doordat nu echter aangenomen wordt, dat de bekende functies analytisch in y moeten zijn, worden de mogelijkheden aanzienlijk uitgebreid, zo kan nu bijv. ook de functie $\frac{1}{y+h}$ beschouwd worden. Eveneens is het niet meer nodig om een bepaalde lengte-eenheid te kiezen.

Betreffende de gemaakte veronderstellingen worden nog enkele opmerkingen gemaakt:

1e. In (1) is de coëfficiënt van $\frac{\partial^2 z}{\partial x^2}$ gelijk aan één genomen. Indien deze term ontbreekt en dit niet het geval is met $\frac{\partial^2 z}{\partial y^2}$, wordt de coëfficiënt hiervan gelijk aan één gesteld. In de randgegevens (2) moeten dan x en y verwisseld worden, terwijl ook, hiermede corresponderend, hetgeen van de functies a t.m. f gegeven is, gewijzigd zal moeten worden.

Wij zullen echter wel veronderstellen, dat zeker één der coëfficiënten van $\frac{\partial^2 z}{\partial x^2}$ en $\frac{\partial^2 z}{\partial y^2}$ gelijk aan één gemaakt kan worden. Zoals reeds gezegd, beschouwde PICARD speciaal de gevallen, waarbij òf de beide coëfficiënten nul zijn, òf aan elkaar gelijk en dus gelijk aan één gemaakt kunnen worden.

2e. In het voorgaande is als randwaarde $z(0, y)$ aangenomen. Laat een dergelijke kromme algemeen voorgesteld worden door:

$$x = \varphi_1(u); \quad y = \varphi_2(u); \quad z = \varphi_3(u) \quad . \quad . \quad . \quad . \quad . \quad (3)$$

terwijl verder $\frac{\partial z}{\partial x} = \varphi_4(u)$ en $\frac{\partial z}{\partial y} = \varphi_5(u)$ bekende functies zijn, mits het verband bestaat:

$$\varphi_4(u)\,\varphi_1^{(1)}(u) + \varphi_5(u)\,\varphi_2^{(1)}(u) = \varphi_3^{(1)}(u).$$

Wordt in plaats van x, de coördinaat x_1 ingevoerd, zodat $x = \varphi_1(u) + x_1$, dan is de kromme (3) weer in het vlak $x_1 = 0$ gelegen.

3e. Zoals bekend volgen de karakeristieke krommen van de partiële differentiaalvergelijking (1), die in het xy vlak gelegen zijn, uit de vergelijking:

$$dy^2 - b\,dx\,dy + a\,dx^2 = 0.$$

Wordt nu een kromme volgens (3) gegeven, dan mogen de functies φ_1 en φ_2 voor geen enkele waarde van u voldoen aan de betrekking:

$$\varphi_2^{(1)2} - b\,\varphi_1^{(1)}\,\varphi_2^{(1)} + a\,\varphi_1^{(1)2} = 0$$

dat wil zeggen de raaklijn in een punt P van de projectie van de kromme (3) op het xy vlak mag niet samenvallen met de raaklijn in P aan een karakteristieke kromme, die door het punt P gaat.

Daar de coëfficiënt van $\frac{\partial^2 z}{\partial x^2}$ in (1) ongelijk aan nul is, zal de projectie van de kromme $z(0, y)$ op het xy vlak nimmer samenvallen met een

karakteristieke kromme of een deel daarvan. Wel kan in één of meer punten P de raaklijn aan de projectie samenvallen met de raaklijn aan de karakteristieke kromme in P.

Zoals bekend, worden in verband met het al of niet reëel zijn van de karakteristieke krommen, de partiële differentiaalvergelijkingen van de tweede orde onderscheiden in hyperbolische, parabolische en elliptische differentiaalvergelijkingen. Alleen in het laatst genoemde geval zijn de karakteristieke krommen imaginair. Dan zal dus een gesloten kromme in het xy vlak in geen enkel punt aangeraakt kunnen worden door een karakteristieke kromme, hetgeen wel het geval kan zijn bij de hyperbolische en parabolische differentiaalvergelijkingen. Deze raakpunten zullen dan uitgezonderd moeten worden.

In het vervolg wordt niet verondersteld dat de differentiaalvergelijking noodzakelijk elliptisch moet zijn. Voor dit geval is de in dit artikel behandelde iteratiemethode uit praktisch oogpunt wel het meest aangewezen.

4e. In vele praktische vraagstukken betreffende de elliptische partiële differentiaalvergelijkingen is de kromme $x = 0$, waarop $z(0, y)$ gegeven is, gesloten.

Laten wij weer aannemen, dat binnen het gebied G door $x = 0$ omsloten, de functies a, b, c, d, e en f voldoen aan de eisen in het voorgaande genoemd.

Als de integraal $z(x, y)$ op G bepaald is door haar waarden voor $x = 0$ en de eis dat zij en haar partiële afgeleiden tot de tweede orde binnen G doorlopend moeten zijn, kan de functie $\left(\frac{\partial z}{\partial x}\right)_{x=0}$ niet willekeurig gegeven zijn, maar moet ze zo bepaald worden, dat een dergelijke integraal $z(x, y)$ kan worden verkregen.

§ 2.

In plaats van (1) beschouwen wij de twee partiële differentiaalvergelijkingen van de eerste orde:

$$\left.\begin{aligned} &(a)\quad \frac{\delta z}{\delta x} = \alpha \frac{\delta u}{\delta y} + \beta_1 \frac{\delta z}{\delta y} + \gamma_1 z + \delta \\ &(b)\quad \frac{\delta u}{\delta x} = \beta_2 \frac{\delta z}{\delta y} + \gamma_2 z. \end{aligned}\right\} \quad \ldots\ldots \quad (4)$$

Ook nu zijn α, β_1, γ_1, δ, β_2 en γ_2 functies van x en y.

Elimineren wij u uit (4), dan wordt gevonden:

$$\left.\begin{aligned} \frac{\delta^2 z}{\delta x^2} = \beta_1 \frac{\delta^2 z}{\delta y\, \delta x} + \alpha\beta_2 \frac{\delta^2 z}{\delta y^2} + \left(\gamma_1 + \frac{1}{\alpha}\frac{\delta \alpha}{\delta x}\right)\frac{\delta z}{\delta x} + \left(\frac{\delta \beta_1}{\delta x} + \alpha\gamma_2 - \frac{\beta_1}{\alpha}\frac{\delta \alpha}{\delta x} + \right. \\ \left. + \alpha \frac{\delta \beta_2}{\delta y}\right)\frac{\delta z}{\delta y} + \left(\frac{\delta \gamma_1}{\delta x} + \alpha \frac{\delta \gamma_2}{\delta y} - \frac{\gamma_1}{\alpha}\frac{\delta \alpha}{\delta x}\right) z + \left(\frac{\delta \delta}{\delta x} - \frac{\delta}{\alpha}\frac{\delta \alpha}{\delta x}\right). \end{aligned}\right\} \quad (5)$$

Nu zullen (1) en (5) identiek zijn, indien de zes functies α, β_1, γ_1, δ, β_2 en γ_2 voldoen aan de zes vergelijkingen:

$$\left.\begin{array}{l} \beta_1 = -b\,; \quad \alpha\beta_2 = -a\,; \quad \gamma_1 + \dfrac{1}{\alpha}\dfrac{\delta\alpha}{\delta x} = -c\,; \\ \dfrac{\delta\beta_1}{\delta x} + \alpha\gamma_2 - \dfrac{\beta_1}{\alpha}\dfrac{\delta\alpha}{\delta x} + \alpha\dfrac{\delta\beta_2}{\delta y} = -d\,; \quad \dfrac{\delta\gamma_1}{\delta x} - \dfrac{\gamma_1}{\alpha}\dfrac{\delta\alpha}{\delta x} + \alpha\dfrac{\delta\gamma_2}{\delta y} = -e\,; \\ \dfrac{\delta\delta}{\delta x} - \dfrac{\delta}{\alpha}\dfrac{\delta\alpha}{\delta x} = -f. \end{array}\right\} \quad (6)$$

Wij bepalen hiervan een particulier stelsel oplossingen.

De functie β_1 is onmiddellijk bekend, terwijl volgens de tweede en derde betrekking γ_1 en β_2 in α zijn uit te drukken. Elimineren wij daarna γ_1, β_2 en γ_2 uit de vierde en vijfde vergelijking, dan wordt een ingewikkelde partiële differentiaalvergelijking gevonden voor α, namelijk:

$$\left.\begin{array}{l} \dfrac{\delta^2\alpha}{\delta x^2} + a\dfrac{\delta^2\alpha}{\delta y^2} + b\dfrac{\delta^2\alpha}{\delta x\,\delta y} - \dfrac{2}{\alpha}\left(\dfrac{\delta\alpha}{\delta x}\right)^2 - \dfrac{2a}{\alpha}\left(\dfrac{\delta\alpha}{\delta y}\right)^2 - \dfrac{2b}{\alpha}\dfrac{\delta\alpha}{\delta x}\dfrac{\delta\alpha}{\delta y} - \\ -\dfrac{\delta\alpha}{\delta x}\left(c - \dfrac{\delta b}{\delta y}\right) - \dfrac{\delta\alpha}{\delta y}\left(d - \dfrac{\delta b}{\delta x} - \dfrac{2\delta a}{\delta y}\right) + \alpha\left(\dfrac{\delta d}{\delta y} + \dfrac{\delta c}{\delta x} - e - \dfrac{\delta^2 b}{\delta x\,\delta y} - \dfrac{\delta^2 a}{\delta y^2}\right) = 0. \end{array}\right\} \quad (7)$$

Volgens de gegevens (zie § 1) bestaan alle coëfficiënten voor $0 \leq x \leq A$; $0 \leq y \leq B$ en zijn in ieder geval in x continu. Ten opzichte van y zijn alle coëfficiënten analytisch.

Deze partiële differentiaalvergelijking is ingewikkelder dan de partiële differentiaalvergelijking (1). Nu is het echter alleen nodig om een particuliere oplossing voor α te bepalen, zodanig dat $\alpha(x, y)$ en $\dfrac{\delta\alpha}{\delta x}$ in y analytisch zijn en ten opzichte van x continu. Dan behoeft niet aan bepaalde randwaarden voldaan te zijn. Daarna kunnen de overige functies β_1, γ_1 enz. direct bepaald worden en ook hun partiële afgeleiden naar y van de k^{de} orde.

Zodra α bepaald is, is δ volgens de laatste betrekking van (6) onmiddellijk te bepalen als een oplossing van een gewone lineaire differentiaalvergelijking.

Wij kunnen uit (6), in verband met hetgeen in § 1 is verondersteld, α, β_1, γ_1, δ, β_2 en γ_2 steeds zo bepalen, dat haar partiële afgeleiden naar y aan de voorwaarden voldoen, dat de afgeleiden naar y van de k^e orde na deling door $k!$ en een factor ϱ^k begrensd zijn en dus ook analytische functies in y zijn.

In het bijzondere geval dat:

$$\frac{\delta d}{\delta y} + \frac{\delta c}{\delta x} - e - \frac{\delta^2 b}{\delta x\,\delta y} - \frac{\delta^2 a}{\delta y^2} = 0 \quad . \quad . \quad . \quad . \quad . \quad . \quad (8)$$

zal $\alpha =$ constant $= k$ een particuliere oplossing zijn.

Dan is volgens (6):

$$\beta_1 = -b;\ \beta_2 = -\frac{a}{k};\ \gamma_1 = -c;\ \gamma_2 = -\frac{d}{k} + \frac{1}{k}\frac{\delta b}{\delta x} + \frac{1}{k}\frac{\delta a}{\delta y};\ \frac{\delta \delta}{\delta x} = -f.$$

Ook zal er vereenvoudiging optreden, als de functies a, b, c, d, e en f alleen van x of y afhankelijk zijn.

Het stelsel (6) kan dan vereenvoudigd worden door bijv. te veronderstellen, dat bij afhankelijkheid van x ook de functies α, β_1, γ_1, δ, β_2 en γ_2 slechts van x afhankelijk zijn, zodat

$$\frac{\delta \beta_2}{\delta y} = \frac{\delta \gamma_2}{\delta y} = 0.$$

Dan zal α een particuliere oplossing moeten zijn van de gewone differentiaalvergelijking:

$$\alpha \frac{d^2\alpha}{dx^2} - 2\left(\frac{d\alpha}{dx}\right)^2 - c\alpha\frac{d\alpha}{dx} + \left(\frac{dc}{dx} - e\right)\alpha^2 = 0.$$

Ten slotte nog een opmerking over het geval, dat in (1) de functie a gelijk is aan nul. Dan kan het mogelijk zijn om (1) door één partiële lineaire differentiaalvergelijking van de eerste orde, nl. van de vorm (4a) te vervangen, waarbij dan $\alpha = 0$. Volgens de tweede betrekking van (6) is nl. $\alpha\beta_2 = 0$, dus of $\beta_2 = 0$ of $\alpha = 0$.

Als $\beta_2 = 0$ en $\alpha \neq 0$, is (1) weder door twee lineaire partiële differentiaalvergelijkingen van de eerste orde te vervangen. Zodra echter $\alpha = 0$ kan zijn, kan (1) worden vereenvoudigd tot één lineaire partiële diff.verg. van de eerste orde, waarin een willekeurige functie van y voorkomt, die met behulp van de randwaarden (2) nader kan worden bepaald.

Dan moet verder nog deze lineaire partiële differentiaalvergelijking van de eerste orde worden opgelost.

In plaats van de partiële differentiaalvergelijking (1) en de gegeven randwaarden te beschouwen, trachten wij deze te vervangen door het stelsel vergelijkingen (4) met daarbij behorende randwaarden, op de wijze die in het voorgaande beschreven is.

Deze randwaarden worden dan als volgt bepaald:

Daar $z(0, y)$ en $\left(\frac{\partial z}{\partial x}\right)_{x=0}$ gegeven zijn, volgt uit (4a):

$$u^{(1)}(0, y) = \frac{1}{\alpha(0, y)}\left(\frac{\partial z}{\partial x}\right)_{x=0} - \frac{\beta_1(0, y)}{\alpha(0, y)} z^{(1)}(0, y) - \frac{\gamma_1(0, y)}{\alpha(0, y)} z(0, y) - \delta(0, y). \quad (9)$$

Alle termen van het rechterlid zijn bekend, zodat dit ook het geval is met $u^{(1)}(0, y)$ en dus $u(0, y)$, waarbij aan de integratieconstante een willekeurige getallenwaarde gegeven kan worden. Tevens zijn alle afgeleiden naar y van $u(0, y)$ te berekenen.

Wij bepalen nu eerst de functies $z(x, y)$ en $u(x, y)$ zodanig, dat zij aan (4) voldoen, terwijl deze functies voor $x = 0$ overgaan in de bekende functies $z(0, y)$ en $u(0, y)$.

De functie $z(x, y)$ zal dan tevens aan (1) en de gestelde randwaarden voldoen.

§ 3.

In deze paragraaf wordt aangegeven hoe de functies $z(x, y)$ en $u(x, y)$, die aan (4) en gegeven randwaarden moeten voldoen, volgens een iteratiemethode kunnen worden bepaald.

De randwaarden $z(0, y)$ en $u(0, y)$ geven wij dan kortweg aan met z_0 en u_0 en beschouwen deze als gegeven functies.

Verder wordt onder $z_0^{(k)}$ de afgeleide naar y van de k^e orde verstaan enz.

Van al deze k^e afgeleiden naar y ($k = 1, \ldots\ldots, n, \ldots\ldots$) wordt weer verondersteld, dat zij na deling door $k!$ en ϱ^k begrensd zijn en dan kleiner zijn dan een bepaald getal M. Het verband met een bepaalde lineaire partiële differentiaalvergelijking van de 2^e orde, dat in de vorige paragraaf is aangenomen, wordt echter voorlopig buiten beschouwing gelaten.

Als eerste benadering van $z(x, y)$ en $u(x, y)$, $\bar{z}_1$ en $\bar{u}_1$ genaamd, wordt gesteld:

$$\left.\begin{aligned} \bar{z}_1 &= z_0 + z_1 = z_0 + u_0^{(1)} \int_0^x \alpha\, dx + z_0^{(1)} \int_0^x \beta_1\, dx + z_0 \int_0^x \gamma_1\, dx + \int_0^x \delta\, dx \\ \bar{u}_1 &= u_0 + u_1 = u_0 + z_0^{(1)} \int_0^x \beta_2\, dx + z_0 \int_0^x \gamma_2\, dx. \end{aligned}\right\} \quad (10)$$

Zij geldt voor $0 \leq x \leq A$; $0 \leq y \leq B$.

Voor $x = 0$ is $\bar{z}_1 = z_0$, zodat $\bar{z}_1$ aan de gegeven randwaarden voldoet.

In het vervolg zullen wij in de formules de integratiegrenzen 0 en x niet meer aangeven.

Laat in het algemeen:

$$\bar{z}_{n-1} = z_0 + \ldots + z_{n-1} \quad \text{en} \quad \bar{u}_{n-1} = u_0 + u_1 + \ldots + u_{n-1}$$

berekend zijn. Dan worden z_n en u_n als volgt gevonden:

Voor $\frac{\delta \bar{z}_n}{\delta x}$ en $\frac{\delta \bar{u}_n}{\delta x}$ wordt gesteld:

$$\frac{\delta \bar{z}_n}{\delta x} = \alpha \sum_{k=0}^{n-1} u_k^{(1)} + \beta_1 \sum_{k=0}^{n-1} z_k^{(1)} + \gamma_1 \sum_{k=0}^{n-1} z_k + \delta.$$

$$\frac{\delta \bar{u}_n}{\delta x} = \beta_2 \sum_{k=0}^{n-1} z_k^{(1)} + \gamma_2 \sum_{k=0}^{n-1} z_k.$$

Hieruit volgt:

$$\bar{z}_n = z_0 + \int \alpha \left(\sum_{k=0}^{n-1} u_k^{(1)} \right) dx + \int \beta_1 \left(\sum_{k=0}^{n-1} z_k^{(1)} \right) dx + \int \gamma_1 \left(\sum_{k=0}^{n-1} z_k \right) dx + \int \delta\, dx,$$

$$\bar{u}_n = u_0 + \int \beta_2 \left(\sum_{k=0}^{n-1} z_k^{(1)} \right) dx + \int \gamma_2 \left(\sum_{k=0}^{n-1} z_k \right) dx.$$

Dus is:

$$\left.\begin{aligned} z_1 &= \int (\alpha u_0^{(1)} + \beta_1 z_0^{(1)} + \gamma_1 z_0 + \delta)\, dx, \\ z_2 &= \int (\alpha u_1^{(1)} + \beta_1 z_1^{(1)} + \gamma_1 z_1)\, dx, \\ &\vdots \\ z_n &= \int (\alpha u_{n-1}^{(1)} + \beta_1 z_{n-1}^{(1)} + \gamma_1 z_{n-1})\, dx \end{aligned}\right\} \quad \ldots \quad (11)$$

en:

$$\left.\begin{aligned} u_1 &= \int (\beta_2 z_0^{(1)} + \gamma_2 z_0)\, dx \\ u_2 &= \int (\beta_2 z_1^{(1)} + \gamma_2 z_1)\, dx \\ &\vdots \\ u_n &= \int (\beta_2 z_{n-1}^{(1)} + \gamma_2 z_{n-1})\, dx. \end{aligned}\right\} \quad \ldots \quad (12)$$

In het bijzondere geval, dat z_{n-1} en u_{n-1} identiek gelijk aan nul zijn, is dat eveneens het geval met z_n en u_n enz.

In § 6 wordt aangetoond, dat als de functies a, b, enz. voldoen aan de voorwaarden in § 1 genoemd, voor de variabelen x en y intervallen bestaan, waarvoor de genoemde reeksen gelijkmatig convergeren en z en u oplossingen zijn van de differentiaalvergelijkingen (4), die tevens aan de gestelde randwaarden voldoen. Worden daarna in de formule voor z, de functies u_0, u_1 enz. uitgedrukt in $\left(\frac{\partial z}{\partial x}\right)_{x=0}$ en $z(0, y)$ en haar afgeleiden naar y, dan wordt de functie gevonden, die aan (1) en de gegeven randwaarden voldoet.

Elimineren wij $u_{n-1}^{(1)}$ met behulp van (12) uit de uitdrukking voor z_n (zie (11)), dan wordt gevonden:

$$\left.\begin{aligned} z_n = \int \alpha \int \beta_2^{(1)} z_{n-2}^{(1)} dx^2 + \int \alpha \int \beta_2 z_{n-2}^{(2)} dx^2 + \int \alpha \int \gamma_2 z_{n-2}^{(1)} dx^2 + \\ + \int \alpha \int \gamma_2^{(1)} z_{n-2}\, dx^2 + \int \beta_1 z_{n-1}^{(1)} dx + \int \gamma_1 z_{n-1}\, dx. \end{aligned}\right\} \quad (13)$$

In verband met de gegevens is het nl. geoorloofd om de differentiatie naar y en de integratie naar x te verwisselen.

Door tweemaal achtereenvolgens naar x te differentiëren, blijkt:

$$\left.\begin{aligned} \frac{\delta^2 z_n}{\delta x^2} = \beta_1 \frac{\delta^2 z_{n-1}}{\delta y \delta x} + \alpha \beta_2 \frac{\delta^2 z_{n-2}}{\delta y^2} + \frac{1}{\alpha} \frac{\delta \alpha}{\delta x} \frac{\delta z_n}{\delta x} + \gamma_1 \frac{\delta z_{n-1}}{\delta x} + \\ + \left(-\frac{\beta_1}{\alpha} \frac{\delta \alpha}{\delta x} + \frac{\delta \beta_1}{\delta x}\right) \frac{\delta z_{n-1}}{\delta y} + \left(\alpha \frac{\delta \beta_2}{\delta y} + \alpha \gamma_2\right) \frac{\delta z_{n-2}}{\delta y} + \\ + \left(\frac{\delta \gamma_1}{\delta x} - \frac{\gamma_1}{\alpha} \frac{\delta \alpha}{\delta x}\right) z_{n-1} + \alpha \frac{\delta \gamma_2}{\delta y} z_{n-2}. \end{aligned}\right\} \quad (14)$$

Volgens het gegeven is ook:

$$\frac{\delta^2 z_{n-1}}{\delta y \delta x} = \frac{\delta^2 z_{n-1}}{\partial x \partial y}.$$

Wordt ten slotte toch weer aangenomen, dat er tussen de vergelijkingen

(1) en (4) het verband bestaat, dat in § 2 is verondersteld, dan kan voor (14) geschreven worden:

$$\left.\begin{aligned}\frac{\delta^2 z_n}{\delta x^2} = &-b\frac{\delta^2 z_{n-1}}{\delta x \delta y} - a\frac{\delta^2 z_{n-2}}{\delta y^2} - (c+\gamma_1)\frac{\delta z_n}{\delta x} + \gamma_1 \frac{\delta z_{n-1}}{\delta x} + \\ &+ \left(\alpha\frac{\delta \beta_2}{\delta y} + \alpha\gamma_2\right)\frac{\delta z_{n-2}}{\delta y} - \left(d + \alpha\gamma_2 + \alpha\frac{\delta\beta_2}{\delta y}\right)\frac{\delta z_{n-1}}{\delta y} - \\ &- \left(e + \alpha\frac{\delta\gamma_2}{\delta y}\right) z_{n-1} + \alpha\frac{\delta\gamma_2}{\delta y} z_{n-2}.\end{aligned}\right\} \quad (15)$$

Deze formule geldt voor $n \geq 2$.
Voor $n = 1$ luidt zij als volgt:

$$\frac{\delta^2 z_1}{\delta x^2} = -(c+\gamma_1)\frac{\delta z_1}{\delta x} - \left(d + \alpha\gamma_2 + \alpha\frac{\delta\beta_2}{\delta y}\right)\frac{\delta z_0}{\delta y} - \left(e + \alpha\frac{\delta\gamma_2}{\delta y}\right) z_0 - f. \quad (15a)$$

Mathematics. — *A non-homogeneous inequality for integers in a special cubic field.* By A. V. PRASAD. (Second communication.) (Communicated by Prof. J. G. VAN DER CORPUT.)

(Communicated at the meeting of March 26, 1949).

Lemma 9.

$$\alpha < \theta^4 - \theta^{-5}. \quad . \quad . \quad . \quad . \quad . \quad . \quad . \quad . \quad (48)$$

Proof. Suppose, if possible, that $\alpha \geq \theta^4 - \theta^{-5}$. Now by (16), (19) and (12)

$$\alpha \leqslant \gamma\{\alpha\,|\beta|^2\,\theta^2\} \leqslant \theta\,\gamma\{(5+\delta)\,(1-\varepsilon)\} < 3 < \theta^4,$$

so

$$|\alpha - \theta^4| < \theta^{-5}.$$

Hence, using (18) with $\xi = \theta^{-4}$,

$$|(\beta - \phi^4)\,(\bar{\beta} - \bar{\phi}^4)| \geqslant (1-\varepsilon)\,\theta^5,$$

so that

$$|\beta - \phi^4| \geqslant \theta^{\frac{5}{2}}\,\gamma(1-\varepsilon) > 2\cdot 019,$$

if ε is sufficiently small. Thus

$$|\beta| \geqslant |\beta - \phi^4| - |\phi^4| > 2\cdot 019 - \theta^{-2} > 2\cdot 019 - 0\cdot 570 = 1\cdot 449. \quad (49)$$

But, by (16) and (12) and our supposition about α,

$$|\beta| = \gamma\left\{\frac{\alpha\,|\beta|^2}{\alpha}\right\} \leqslant \gamma\left\{\frac{(5+\delta)\,(1-\varepsilon)}{\alpha}\right\} \leqslant \gamma\left\{\frac{5+\delta}{\theta^4 - \theta^{-5}}\right\}$$

$$< \gamma\left\{\frac{5\cdot 001}{2\,\theta^2 + \theta - 2}\right\} < \gamma\left\{\frac{5\cdot 001}{2\cdot 834}\right\} < 1\cdot 4,$$

contrary to (49). This contradiction proves the lemma.

6. The object of the next eight lemmas is to prove that α must be close to $\theta^2 + 1$ and that β must be close to $\phi^2 + 1$.

For this purpose it is convenient to work in polar coordinates. We write

$$\phi = r e^{i\psi} \quad . \quad . \quad . \quad . \quad . \quad . \quad . \quad . \quad . \quad (50)$$

$$\beta = d e^{i\chi} \quad . \quad . \quad . \quad . \quad . \quad . \quad . \quad . \quad . \quad (51)$$

where $r > 0$, $d > 0$ and ψ and χ are real.

We suppose that ψ is chosen so that $0 \leq \psi < 2\pi$, and that χ is chosen so that

$$3\psi - 2\pi \leqslant \chi < 3\psi \quad . \quad . \quad . \quad . \quad . \quad . \quad . \quad . \quad (52)$$

Then, as $\theta\,\phi\,\bar{\phi} = 1$ and $\theta + \phi + \bar{\phi} = 0$, we have

$$r = |\phi| = \theta^{-\frac{1}{2}},$$

and

$$\cos\psi = \frac{\phi + \bar{\phi}}{2|\phi|} = -\tfrac{1}{2}\,\theta^{\frac{3}{2}} = -\,0\cdot 7623\,512\ldots,$$

so that

$$\psi = 139^\circ\ 40' \cdot 31\ldots \quad \ldots\ldots\ldots \quad (53)$$

We note that

$$\left.\begin{aligned} 2\psi &= 279^\circ\ 20' \cdot 6\ldots, \\ 3\psi &= 419^\circ\ \ 0' \cdot 9\ldots, \\ 4\psi &= 558^\circ\ 41' \cdot 2\ldots, \\ 5\psi &= 698^\circ\ 21' \cdot 6\ldots. \end{aligned}\right\} \quad \ldots\ldots\ldots \quad (54)$$

We also write

$$\phi^2 + 1 = Re^{i\omega} \quad \ldots\ldots\ldots \quad (55)$$

where $R > 0$ and $0 \leq \omega < 2\pi$. Taking $x = 1$, $y = 0$, $z = 1$ in (31) and (33) we have

$$(1+\theta^2)(1+\phi^2)(1+\bar{\phi}^2) = 5. \quad \ldots\ldots\ldots \quad (56)$$

Hence

$$R = \mathfrak{f}\{(1+\phi^2)(1+\bar{\phi}^2)\} = \sqrt{\left\{\frac{5}{\theta^2+1}\right\}} = 1 \cdot 3472\,054\ldots$$

and

$$\cos\omega = \frac{2+\phi^2+\bar{\phi}^2}{2R} = \frac{2+(\theta^2+\phi^2+\bar{\phi}^2)-\theta^2}{2R}$$
$$= \frac{4-\theta^2}{2R} = 0 \cdot 8332\,51\ldots.$$

Thus

$$\omega = 326^\circ\ 26' \cdot 0\ldots. \quad \ldots\ldots\ldots \quad (57)$$

Lemma 10. *For $n = 2, 3, 4$ or 5,*

$$\left.\begin{aligned} \cos(\chi - n\psi) \leqslant {} & \tfrac{1}{2}\left(\frac{\alpha\theta^n}{5+\delta}\right)^{\frac{1}{2}}\left\{\frac{5+\delta}{\alpha} + \frac{1}{\theta^n} - \frac{1-\varepsilon}{|\alpha-\theta^n|}\right\} \\ & - \tfrac{1}{2}\theta^{n/2}\left\{\left(\frac{5+\delta}{\alpha}\right)^{\frac{1}{2}} - d\right\}. \end{aligned}\right\} \quad \ldots \quad (58)$$

Proof. For any rational integer n, we have

$$(\beta-\phi^n)(\bar{\beta}-\bar{\phi}^n) = (de^{i\chi} - r^n e^{in\psi})(de^{-i\chi} - r^n e^{-in\psi})$$
$$= d^2 + r^{2n} - 2r^n d\cos(\chi - n\psi),$$

so that

$$\cos(\chi - n\psi) = \{d^2 + r^{2n} - (\beta-\phi^n)(\bar{\beta}-\bar{\phi}^n)\}/2r^n d.$$

Using (18) with $\xi = \theta^{-n}$ we obtain, for all rational integers n,

$$\left.\begin{aligned} \cos(\chi - n\psi) &\leqslant \frac{1}{2r^n d}\left\{d^2 + r^{2n} - \frac{1-\varepsilon}{|\alpha-\theta^n|}\right\} \\ &= \frac{\theta^{n/2}}{2d}\left\{d^2 + \frac{1}{\theta^n} - \frac{1-\varepsilon}{|\alpha-\theta^n|}\right\}. \end{aligned}\right\} \quad \ldots \quad (59)$$

Since, by Lemma 9,

$$\alpha < \theta^4 - \theta^{-5} = 2\theta^2 + \theta - 2 < 2\theta^2$$

we have

$$|\alpha - \theta^n| < \theta^n$$

for $n = 2, 3, 4$ or 5. Thus if ε is sufficiently small

$$\frac{1}{\theta^n} - \frac{1-\varepsilon}{|\alpha - \theta^n|} < 0, \quad \text{for } n = 2, 3, 4, \text{ or } 5. \quad . \quad . \quad . \quad (60)$$

But by (51) and (16)

$$d^2 = \beta\bar{\beta} \leqq \frac{5+\delta}{\alpha}.$$

Now (58) follows from this result together with (59) and (60).

Lemma 11. *If* $\alpha \leq \theta^2 + 1$, *then*

$$322^\circ < \chi < 333^\circ. \quad . \quad . \quad . \quad . \quad . \quad . \quad . \quad . \quad . \quad (61)$$

Proof. By Lemma 8,

$$\alpha > \theta^3 + \theta^{-6} = 2\theta^2 - 1. \quad . \quad . \quad . \quad . \quad . \quad . \quad (62)$$

Thus

$$d^2 \leqq \frac{5+\delta}{\alpha} < \frac{5 \cdot 0001}{2\theta^2 - 1},$$

and by Lemma 10 and (60)

$$\cos(\chi - n\psi) < \theta^{n/2} \frac{1}{2} \left(\frac{2\theta^2 - 1}{5 \cdot 0001} \right)^{\frac{1}{2}} \left\{ \frac{5 \cdot 0001}{2\theta^2 - 1} + \frac{1}{\theta^n} - \frac{1-\varepsilon}{|\alpha - \theta^n|} \right\},$$

for $n = 2, 3$ or 4. Now numerically

$$\frac{1}{2} \left(\frac{2\theta^2 - 1}{5 \cdot 0001} \right)^{\frac{1}{2}} = \frac{1}{2} \left(\frac{2 \cdot 50975 \ldots}{5 \cdot 0001} \right)^{\frac{1}{2}} < \tfrac{1}{2} (0 \cdot 50194)^{\frac{1}{2}} < 0 \cdot 35424,$$

and

$$\frac{5 \cdot 0001}{2\theta^2 - 1} = \frac{5 \cdot 0001}{2 \cdot 50975 \ldots} < 1 \cdot 99263.$$

Also we have

$$|\alpha - \theta^2| \leqq 1,$$
$$|\alpha - \theta^3| \leqq \theta^2 + 1 - \theta^3 = \theta^{-3},$$
$$|\alpha - \theta^4| \leqq \theta^4 - 2\theta^2 + 1 = \theta^{-2}.$$

Thus, if ε is sufficiently small,

$$\begin{aligned} \cos(\chi - 2\psi) &< (1 \cdot 32472)(0 \cdot 35424)\{1 \cdot 99263 + 0 \cdot 56985 - 1\} \\ &< 0 \cdot 73323 < \cos 42^\circ\, 50', \\ \cos(\chi - 3\psi) &< (1 \cdot 52471)(0 \cdot 35424)\{1 \cdot 99263 + 0 \cdot 43016 - 2 \cdot 32471\} \\ &< 0 \cdot 05298 < \cos 86^\circ\, 57', \\ \cos(\chi - 4\psi) &< (1 \cdot 75488)(0 \cdot 35424)\{1 \cdot 99263 + 0 \cdot 32472 - 1 \cdot 75487\} \\ &< 0 \cdot 34967 < \cos 69^\circ\, 31'. \end{aligned}$$

Using the numerical values for 2ψ, 3ψ and 4ψ we see that it is not possible for χ to satisfy any of the inequalities

$$|\chi - 279^\circ\ 20'\cdot 6| \leqq 42^\circ\ 49'\cdot 9,$$
$$|\chi - 59^\circ\ \ 0'\cdot 9| \leqq 86^\circ\ 56'\cdot 9,$$
$$|\chi - 419^\circ\ \ 0'\cdot 9| \leqq 86^\circ\ 56'\cdot 9,$$
$$|\chi - 198^\circ\ 41'\cdot 2| \leqq 69^\circ\ 30'\cdot 9.$$

Hence, by (52),

$$322^\circ < \chi < 333^\circ.$$

Lemma 12. *If* $\alpha \geq \theta^2 + 1$, *then*

$$326^\circ < \chi < 327^\circ. \quad . \quad . \quad . \quad . \quad . \quad . \quad . \quad . \quad , \quad (63)$$

Proof. If $\alpha \geq \theta^2 + 1$ we have

$$d^2 \leqq \frac{5+\delta}{\alpha} < \frac{5\cdot 0001}{\theta^2+1}.$$

Thus by Lemma 10 and (60),

$$\cos(\chi - n\psi) < \theta^{n/2}\,\frac{1}{2}\left(\frac{\theta^2+1}{5\cdot 0001}\right)^{\frac{1}{2}}\left\{\frac{5\cdot 0001}{\theta^2+1} + \frac{1}{\theta^n} - \frac{1-\varepsilon}{|\alpha-\theta^n|}\right\},$$

for $n = 3$, 4 or 5. Now, numerically

$$\frac{1}{2}\left\{\frac{\theta^2+1}{5\cdot 0001}\right\}^{\frac{1}{2}} = \frac{1}{2}\left\{\frac{2\cdot 75487\ldots}{5\cdot 0001}\right\}^{\frac{1}{2}} < \tfrac{1}{2}\{0\cdot 55097\}^{\frac{1}{2}} < 0\cdot 37114,$$

$$\frac{1}{2}\left\{\frac{\theta^2+1}{5\cdot 0001}\right\}^{\frac{1}{2}} = \frac{1}{2}\left\{\frac{2\cdot 75487\ldots}{5\cdot 0001}\right\}^{\frac{1}{2}} > \tfrac{1}{2}\{0\cdot 55096\}^{\frac{1}{2}} > 0\cdot 37113,$$

and

$$\frac{5\cdot 0001}{\theta^2+1} = \frac{5\cdot 0001}{2\cdot 75487\ldots} < 1\cdot 81534.$$

Also, since $\theta^2 + 1 \leq \alpha < \theta^4 - \theta^{-5}$,

$$|\alpha - \theta^3| < \theta^4 - \theta^{-5} - \theta^3 = 2\theta^2 - 3 < 0\cdot 50976 < (1\cdot 96170)^{-1},$$
$$|\alpha - \theta^4| \leqq \theta^4 - \theta^2 - 1 = \theta^{-4},$$
$$|\alpha - \theta^5| \leqq \theta^5 - \theta^2 - 1 = \theta.$$

Thus, if ε is sufficiently small,

$$\cos(\chi - 3\psi) < (1\cdot 52471)(0\cdot 37114)\{1\cdot 81534 + 0\cdot 43016 - 1\cdot 96170\}$$
$$< 0\cdot 16060 < \cos 80^\circ\ 45',$$
$$\cos(\chi - 4\psi) < (1\cdot 75487)(0\cdot 37113)\{1\cdot 81534 + 0\cdot 32472 - 3\cdot 07959\}$$
$$< -0\cdot 61190 < \cos 127^\circ\ 43',$$
$$\cos(\chi - 5\psi) < (2\cdot 01981)(0\cdot 37114)\{1\cdot 81534 + 0\cdot 24513 - 0\cdot 75487\}$$
$$< 0\cdot 97872 < \cos 11^\circ\ 50'.$$

Using the numerical values for 3ψ, 4ψ and 5ψ, we see that it is not possible χ to satisfy any of the inequalities

$$\begin{aligned}
|\chi - 59^\circ\ 0'\cdot 9| &\leqslant 80^\circ\ 44'\cdot 9,\\
|\chi - 419^\circ\ 0'\cdot 9| &\leqslant 80^\circ\ 44'\cdot 9,\\
|\chi - 198^\circ\ 41'\cdot 2| &\leqslant 127^\circ\ 42'\cdot 9,\\
|\chi - 338^\circ\ 21'\cdot 6| &\leqslant 11^\circ\ 49'\cdot 9.
\end{aligned}$$

Hence, by (52)

$$326^\circ < \chi < 327^\circ.$$

Lemma 13. *For $n = 2, 3, 4$ or 5,*

$$\left.\begin{aligned}\cos(\chi - n\psi) < \frac{1}{2}\left(\frac{\alpha\theta^n}{5}\right)^{\frac{1}{2}}\left\{\frac{5}{\alpha} + \frac{1}{\theta^n} - \frac{1}{|\alpha-\theta^n|}\right\}\\ + 1\cdot 3\delta - \frac{1}{2}\left\{\left(\frac{5+\delta}{\alpha}\right)^{\frac{1}{2}} - d\right\}.\end{aligned}\right\} \quad . \quad . \quad (64)$$

Proof. It is clear from (12) that

$$\left(\frac{5+\delta}{\alpha}\right)^{\frac{1}{2}} < \left(\frac{5}{\alpha}\right)^{\frac{1}{2}}(1 + \tfrac{1}{5}\delta),$$

$$\left(\frac{\alpha}{5+\delta}\right)^{\frac{1}{2}} > \left(\frac{\alpha}{5}\right)^{\frac{1}{2}}(1 - \tfrac{1}{5}\delta).$$

Using these inequalities together with (60) in (58) we obtain

$$\left.\begin{aligned}\cos(\chi - n\psi) < \frac{1}{2}\left(\frac{\alpha\theta^n}{5}\right)^{\frac{1}{2}}\left\{\frac{5}{\alpha} + \frac{1}{\theta^n} - \frac{1}{|\alpha-\theta^n|}\right\}\\ + \frac{1}{10}\left(\frac{\alpha\theta^n}{5}\right)^{\frac{1}{2}}\left\{\frac{5}{\alpha} - \frac{1}{\theta^n} + \frac{1-\varepsilon}{|\alpha-\theta^n|}\right\}\delta\\ + \frac{1}{2}\left(\frac{\alpha\theta^n}{5}\right)^{\frac{1}{2}}\frac{\varepsilon}{|\alpha-\theta^n|} - \tfrac{1}{2}\theta^{n/2}\left\{\left(\frac{5+\delta}{\alpha}\right)^{\frac{1}{2}} - d\right\},\end{aligned}\right\} \quad (65)$$

for $n = 2, 3, 4$ or 5. Now since

$$\theta^3 + \theta^{-6} < \alpha < \theta^4 - \theta^{-5},$$

we have

$$\left.\begin{aligned}\left(\frac{\alpha\theta^n}{5}\right)^{\frac{1}{2}}\left\{\frac{5}{\alpha} - \frac{1}{\theta^n} + \frac{1-\varepsilon}{|\alpha-\theta^n|}\right\}\\ < \left(\frac{\theta^4\cdot\theta^5}{5}\right)^{\frac{1}{2}}\left\{\frac{5}{\theta^3+\theta^{-6}} - \frac{1}{\theta^5} + \theta^6\right\}\\ < \left(\frac{3\cdot 1\times 4\cdot 1}{5}\right)^{\frac{1}{2}}\left\{\frac{5}{2\cdot 5} - 0\cdot 2 + 5\cdot 5\right\}\\ = (2\cdot 542)^{\frac{1}{2}}(7\cdot 3) < (1\cdot 6)(7\cdot 3) < 12.\end{aligned}\right\} \quad . \quad . \quad . \quad (66)$$

Now provided ε is sufficiently small (65) and (66) prove (64).

Lemma 14. *If $\alpha \leq \theta^2 + 1$ and $n = 2$ or 3, or if $\alpha \geq \theta^2 + 1$ and $n = 4$ or 5, then*

$$\left.\begin{aligned}\cos(\chi - n\psi) < \cos(\omega - n\psi) + 1\cdot 3\delta \\ - \tfrac{1}{6}|\alpha - \theta^2 - 1| - \tfrac{1}{2}\left\{\left(\frac{5+\delta}{\alpha}\right)^{\frac{1}{2}} - d\right\}.\end{aligned}\right\} \quad . \quad . \quad (67)$$

Proof. We suppose that $n = 2$, 3, 4 or 5 and write

$$f_n(x) = \tfrac{1}{2}\left(\frac{x\theta^n}{5}\right)^{\frac{1}{2}}\left\{\frac{5}{x} + \frac{1}{\theta^n} - \frac{1}{|x-\theta^n|}\right\}, \quad . \quad . \quad . \quad . \quad (68)$$

for x satisfying

$$\theta^3 + \theta^{-6} < x < \theta^4 - \theta^{-5}. \quad . \quad . \quad . \quad . \quad . \quad . \quad (69)$$

Then

$$\left.\begin{aligned}\frac{d}{dx}f_n(x) = \tfrac{1}{2}\theta^{n/2}\left[-\frac{1}{2x}\left(\frac{5}{x}\right)^{\frac{1}{2}} + \frac{1}{2x}\left(\frac{x}{5}\right)^{\frac{1}{2}}\left\{\frac{1}{\theta^n} - \frac{1}{|x-\theta^n|}\right\}\right. \\ \left. + \left(\frac{x}{5}\right)^{\frac{1}{2}}\frac{1}{(x-\theta^n)|x-\theta^n|}\right] \\ = \tfrac{1}{4}\theta^{n/2}\left(\frac{x}{5}\right)^{\frac{1}{2}}\frac{1}{x(x-\theta^n)} \times \left[\frac{2x}{x-\theta^n} - \left(\frac{5}{x} - \frac{1}{\theta^n} + \frac{1}{|x-\theta^n|}\right)(x-\theta^n)\right]\end{aligned}\right\} \quad (70)$$

We consider two cases. First suppose that $n = 2$ or 3 and

$$2\theta^2 - 1 = \theta^3 + \theta^{-6} < x \leqslant \theta^2 + 1. \quad . \quad . \quad . \quad . \quad . \quad (71)$$

Then

$$\theta^{-6} < x - \theta^n \leqslant 1,$$

and by (70)

$$\begin{aligned}\frac{d}{dx}f_n(x) &> \tfrac{1}{4}\theta\left(\tfrac{1}{5}\right)^{\frac{1}{2}}\frac{1}{(\theta^2+1)} \times \left[2(2\theta^2-1) - \left|\frac{5}{2\theta^2-1} - \frac{1}{\theta^3}\right| - 1\right] \\ &> \frac{1}{4}\Big/\left\{\frac{\theta^2}{5(\theta^2+1)}\right\}\left[2(2\cdot 5) - \frac{5}{2\cdot 5} - 1\right] \\ &> \frac{1}{4}\Big/\left\{\frac{1}{5(1+0\cdot 6)}\right\} \times [2] = \frac{1}{2\cdot 8} > \tfrac{1}{6}.\end{aligned}$$

Consequently

$$f_n(x) \leqslant f_n(\theta^2+1) - \tfrac{1}{6}|x - \theta^2 - 1| \quad . \quad . \quad . \quad . \quad . \quad (72)$$

if x satisfies (71). Thus, if $n = 2$ or 3 and $\alpha \leq \theta^2 + 1$, it follows from (64), (68) and (72) that

$$\left.\begin{aligned}\cos(\chi - n\psi) < \tfrac{1}{2}\theta^{n/2}\left(\frac{\theta^2+1}{5}\right)^{\frac{1}{2}}\left\{\frac{5}{\theta^2+1} + \frac{1}{\theta^n} - \frac{1}{\theta^2+1-\theta^n|}\right\} \\ + 1\cdot 3\delta - \tfrac{1}{6}|\alpha - \theta^2 - 1| \\ - \tfrac{1}{2}\left\{\left(\frac{5+\delta}{\alpha}\right)^{\frac{1}{2}} - d\right\}.\end{aligned}\right\} \quad . \quad (73)$$

Now suppose that $n = 4$ or 5 and

$$\theta^2 + 1 \leqslant x < \theta^4 - \theta^{-5} = 2\theta^2 + \theta - 2. \quad . \quad . \quad . \quad . \quad . \quad (74)$$

Then

$$\theta^{-5} < \theta^n - x \leqslant \theta^5 - \theta^2 - 1 = \theta,$$

and, by (70)

$$\begin{aligned} \frac{d}{dx} f_n(x) &< -\tfrac{1}{4}\theta^2 (\tfrac{1}{5})^{\frac{1}{4}} \frac{1}{\sqrt{\{\theta^4 - \theta^{-5}\}}} \frac{1}{\theta} \\ &\quad \times \left[\frac{2(\theta^2+1)}{\theta} + \left(\frac{5}{\theta^4 - \theta^{-5}} - \frac{1}{\theta^4} \right) (\theta^{-5}) + 1 \right] \\ &< -\tfrac{1}{4}(\tfrac{1}{5})^{\frac{1}{4}} \frac{1}{\theta} [2(\theta + \theta^{-1}) + 1] \\ &< -\frac{2(1\cdot 3 + 0\cdot 7) + 1}{4(2\cdot 3)(1\cdot 4)} = -\frac{5}{12\cdot 88} < -\tfrac{1}{3}. \end{aligned}$$

Consequently

$$f_n(x) \leqslant f_n(\theta^2 + 1) - \tfrac{1}{3}|x - \theta^2 - 1| \quad . \quad . \quad . \quad . \quad . \quad (75)$$

if x satisfies (74). Thus, if $n = 4$ or 5 and $\alpha \geqslant \theta^2 + 1$, it follows from (64), (68) and (75) that (73) is satisfied.

We now show that (67) follows from (73) in the required cases by proving that

$$\cos(\omega - n\psi) = \tfrac{1}{2}\theta^{n/2} \left(\frac{\theta^2+1}{5} \right)^{\frac{1}{2}} \left\{ \frac{5}{\theta^2+1} + \frac{1}{\theta^n} - \frac{1}{|\theta^2 + 1 - \theta^n|} \right\}, \quad (76)$$

for $n = 2, 3, 4$ or 5. Since

$$\Phi = re^{i\psi} \text{ and } \Phi^2 + 1 = Re^{i\omega}$$

where

$$r = \frac{1}{\sqrt{\theta}} \text{ and } R = \sqrt{\left\{ \frac{1}{\theta^2+1} \right\}},$$

we have, as in the proof of Lemma 10,

$$\begin{aligned} \cos(\omega - n\psi) &= \{R^2 + r^{2n} - |\Phi^2 + 1 - \Phi^n|^2\}/2r^n R \\ &= \tfrac{1}{2}\theta^{n/2} \left(\frac{\theta^2+1}{5} \right)^{\frac{1}{2}} \left\{ \frac{5}{\theta^2+1} + \frac{1}{\theta^n} - |\Phi^2 + 1 - \Phi^n|^2 \right\} \cdot \left\{ \right. \quad (77) \end{aligned}$$

Now

$$\begin{aligned} \theta^2 + 1 - \theta^2 &= 1, \\ \theta^2 + 1 - \theta^3 &= \theta^{-3}, \\ \theta^2 + 1 - \theta^4 &= -\theta^{-4}, \\ \theta^2 + 1 - \theta^5 &= -\theta, \end{aligned}$$

and Φ and $\overline{\Phi}$ satisfy similar identities. Thus

$$|\theta^2 + 1 - \theta^n| \cdot |\Phi^2 + 1 - \Phi^n|^2 = 1,$$

for $n = 2, 3, 4$ and 5. Consequently when n has one of these values the

expression on the right hand side of (77) reduces to that on the right hand side of (76). This proves (76) and completes the proof of the lemma.

Lemma 15. *If* $\alpha \leq \theta^2 + 1$, *then*

$$|\sin \tfrac{1}{2}(\chi - \omega)| < \delta, \quad . \quad . \quad . \quad . \quad . \quad . \quad . \quad . \quad (78)$$

$$|\alpha - \theta^2 - 1| < 7 \cdot 8\,\delta, \quad . \quad . \quad . \quad . \quad . \quad . \quad . \quad . \quad (79)$$

and

$$\left(\frac{5+\delta}{\alpha}\right)^{\frac{1}{2}} - d < 2 \cdot 6\,\delta. \quad . \quad . \quad . \quad . \quad . \quad . \quad . \quad . \quad (80)$$

Proof. If $\alpha \leq \theta^2 + 1$, it follows by Lemma 14, that

$$\cos(\chi - n\psi) < \cos(\omega - n\psi) + 1 \cdot 3\,\delta - \tfrac{1}{6}|\alpha - \theta^2 - 1| - \tfrac{1}{2}\left\{\left(\frac{5+\delta}{\alpha}\right)^{\frac{1}{2}} - d\right\},$$

for $n = 2$ and 3. Thus

$$-2\sin\{\tfrac{1}{2}(\chi + \omega) - n\psi\}\sin\tfrac{1}{2}(\chi - \omega)$$

$$< 1 \cdot 3\,\delta - \tfrac{1}{6}|\alpha - \theta^2 - 1| - \tfrac{1}{2}\left\{\left(\frac{5+\delta}{\alpha}\right)^{\frac{1}{2}} - d\right\}, \quad . \quad (81)$$

for $n = 2$ and 3.

By Lemma 11 and the numerical values of ω and ψ we have

$$324^\circ < \tfrac{1}{2}(\chi + \omega) < 330^\circ,$$

so that

$$44^\circ < \tfrac{1}{2}(\chi + \omega) - 2\psi < 51^\circ,$$
$$-96^\circ < \tfrac{1}{2}(\chi + \omega) - 3\psi < -89^\circ.$$

Thus

$$2\sin\{\tfrac{1}{2}(\chi + \omega) - 2\psi\} > 2\sin 44^\circ > 1 \cdot 3,$$
$$2\sin\{\tfrac{1}{2}(\chi + \omega) - 3\psi\} < -2\sin 96^\circ < -1 \cdot 9.$$

These results together with (81) imply that

$$1 \cdot 3|\sin\tfrac{1}{2}(\chi - \omega)| < 1 \cdot 3\,\delta - \tfrac{1}{6}|\alpha - \theta^2 - 1| - \tfrac{1}{2}\left\{\left(\frac{5+\delta}{\alpha}\right)^{\frac{1}{2}} - d\right\},$$

so that

$$1 \cdot 3|\sin\tfrac{1}{2}(\chi - \omega)| + \tfrac{1}{6}|\alpha - \theta^2 - 1| + \tfrac{1}{2}\left\{\left(\frac{5+\delta}{\alpha}\right)^{\frac{1}{2}} - d\right\} < 1 \cdot 3\,\delta.$$

As the three terms on the left are non-negative, this inequality implies the inequalities (78), (79) and (80).

Lemma 16. *If* $\alpha \geq \theta^2 + 1$ *then*

$$|\sin \tfrac{1}{2}(\chi - \omega)| < 3 \cdot 7\,\delta, \quad . \quad . \quad . \quad . \quad . \quad . \quad . \quad . \quad (82)$$

$$|\alpha - \theta^2 - 1| < 7 \cdot 8\,\delta, \quad . \quad . \quad . \quad . \quad . \quad . \quad . \quad . \quad (83)$$

and

$$\left(\frac{5+\delta}{\alpha}\right)^{\frac{1}{2}} - d < 2 \cdot 6\,\delta. \quad . \quad . \quad . \quad . \quad . \quad . \quad . \quad . \quad (84)$$

Proof. If $\alpha \geq \theta^2 + 1$, it follows from Lemma 14 that

$$\begin{aligned} &-2\sin\{\tfrac{1}{2}(\chi+\omega)-n\psi\}\sin\tfrac{1}{2}(\chi-\omega) \\ &\qquad < 1\cdot 3\delta - \tfrac{1}{6}|\alpha-\theta^2-1| - \tfrac{1}{2}\left\{\left(\frac{5+\delta}{\alpha}\right)^{\frac{1}{2}}-d\right\}, \end{aligned} \quad \left.\right\} \quad (85)$$

for $n = 4$ and 5.

By Lemma 12 and the numerical values of ω and ψ we have

$$326^\circ < \tfrac{1}{2}(\chi+\omega) < 327^\circ,$$

so that

$$\begin{aligned} 127^\circ < \tfrac{1}{2}(\chi+\omega) - 4\psi + 2\pi < 129^\circ, \\ -13^\circ < \tfrac{1}{2}(\chi+\omega) - 5\psi + 2\pi < -11^\circ. \end{aligned}$$

Thus

$$\begin{aligned} 2\sin\{\tfrac{1}{2}(\chi+\omega)-4\psi\} > 2\sin 129^\circ > 1\cdot 5, \\ 2\sin\{\tfrac{1}{2}(\chi+\omega)-5\psi\} < -2\sin 11^\circ < -0\cdot 38. \end{aligned}$$

These inequalities together with (85) imply that

$$0\cdot 38\,|\sin\tfrac{1}{2}(\chi-\omega)| < 1\cdot 3\delta - \tfrac{1}{6}|\alpha-\theta^2-1| - \tfrac{1}{2}\left\{\left(\frac{5+\delta}{\alpha}\right)^{\frac{1}{2}}-d\right\},$$

so that

$$0\cdot 38\,|\sin\tfrac{1}{2}(\chi-\omega)| + \tfrac{1}{6}|\alpha-\theta^2-1| + \tfrac{1}{2}\left\{\left(\frac{5+\delta}{\alpha}\right)^{\frac{1}{2}}-d\right\} < 1\cdot 3\delta.$$

As the three terms on the left are non-negative, this inequality implies the inequalities (82), (83) and (84).

Lemma 17.

$$|\theta^2 + 1 - \alpha| < 7\cdot 8\,\delta, \quad \ldots\ldots\ldots \quad (86)$$

and

$$|\phi^2 + 1 - \beta| < 13\,\delta, \quad \ldots\ldots\ldots \quad (87)$$

Proof. The inequality (86) follows immediately from Lemmas 15 and 16. By those lemmas we also have

$$|\sin\tfrac{1}{2}(\chi-\omega)| < 3\cdot 7\,\delta, \quad \ldots\ldots\ldots \quad (88)$$

and

$$\left(\frac{5+\delta}{\alpha}\right)^{\frac{1}{2}} - d < 2\cdot 6\,\delta. \quad \ldots\ldots\ldots \quad (89)$$

Thus

$$\begin{aligned} |d-R| &= \left|d - \left(\frac{5}{\theta^2+1}\right)^{\frac{1}{2}}\right| \\ &\leqq \left|d - \left(\frac{5+\delta}{\alpha}\right)^{\frac{1}{2}}\right| + \left|\left(\frac{5+\delta}{\alpha}\right)^{\frac{1}{2}} - \left(\frac{5}{\theta^2+1}\right)^{\frac{1}{2}}\right| \\ &< 2\cdot 6\,\delta + \left|\left(\frac{5+\delta}{\theta^2+1-7\cdot 8\,\delta}\right)^{\frac{1}{2}} - \left(\frac{5}{\theta^2+1}\right)^{\frac{1}{2}}\right| \\ &< 2.6\,\delta + \left(\frac{5}{\theta^2+1}\right)^{\frac{1}{2}}\left\{(1+\tfrac{1}{5}\delta)\left(1+\frac{7\cdot 8\,\delta}{\theta^2+1}\right)-1\right\} \\ &< 2\cdot 6\,\delta + 1\cdot 35\left(\tfrac{1}{5}+\frac{8}{\theta^2+1}\right)\delta \\ &< 7\,\delta. \end{aligned}$$

Now, as in Lemma 10,

$$\begin{aligned}|\beta-\Phi^2-1|^2 &= |d e^{i\chi}-R e^{i\omega}|^2 \\ &= \{d^2+R^2-2dR\cos(\omega-\chi)\} \\ &= (d-R)^2+4dR\sin^2\tfrac{1}{2}(\omega-\chi) \\ &< 49\delta^2+4dR(3\cdot 7)^2\delta^2 \\ &< 49\delta^2+4R(R+7\delta)(3\cdot 7)^2\delta^2 \\ &< 169\delta^2.\end{aligned}$$

Consequently

$$|\beta-\Phi^2-1|<13\delta.$$

7. In this section we prove that $\alpha=\Theta^2+1$ and $\beta=\Phi^2+1$. We write

$$\alpha=\frac{\Theta^2+1}{1-\alpha'}\quad,\quad \beta=\frac{\Phi^2+1}{1-\beta'}, \qquad (90)$$

and if $|\beta'|>0$ we write

$$\beta'=\varrho e^{i\lambda} \qquad (91)$$

where $\varrho>0$ and λ is real.

Lemma 18. *For every rational integer n, we have*

$$|(\alpha'(-\Theta^2)^n-1)(\beta'(-\Phi^2)^n-1)(\bar\beta'(-\bar\Phi^2)^n-1)|>1-\tfrac{1}{5}\delta. \qquad (92)$$

Proof. It is clear that the number

$$\xi_n=\frac{1-(-\Theta^2)^n}{\Theta^2+1}=\frac{1-\{1-(\Theta^2+1)\}^n}{\Theta^2+1}=(-\Theta^2)^n\frac{\{1-(\Theta^2+1)\}^{-n}-1}{\Theta^2+1} \qquad (93)$$

is an integer of $k(\theta)$ for all rational integers n. So, by (17) with $\xi=\xi_n$,

$$\left|\left(\alpha\frac{1-(-\Theta^2)^n}{\Theta^2+1}-1\right)\left(\beta\frac{1-(-\Phi^2)^n}{\Phi^2+1}-1\right)\left(\bar\beta\frac{1-(-\bar\Phi^2)^n}{\bar\Phi^2+1}-1\right)\right|\geqq 1-\varepsilon,$$

for all rational integers n. Thus, by (90)

$$\left|\left(\frac{1-(-\Theta^2)^n}{1-\alpha'}-1\right)\left(\frac{1-(-\Phi^2)^n}{1-\beta'}-1\right)\left(\frac{1-(-\bar\Phi^2)^n}{1-\bar\beta'}-1\right)\right|\geqq 1-\varepsilon,$$

so that, using (16) and (56),

$$\left.\begin{aligned}&|(\alpha'-(-\Theta^2)^n)(\beta'-(-\Phi^2)^n)(\bar\beta'-(-\bar\Phi^2)^n)| \\ &\geqq(1-\varepsilon)|(1-\alpha')(1-\beta')(1-\bar\beta')| \\ &=(1-\varepsilon)\frac{|(\Theta^2+1)(\Phi^2+1)(\bar\Phi^2+1)|}{|\alpha\beta\bar\beta|} \\ &\geqq\frac{5}{5+\delta}>1-\tfrac{1}{5}\delta,\end{aligned}\right\} \qquad (94)$$

for all rational integers n. Replacing n by $-n$ and using the identity $\theta\phi\bar\phi=1$ we obtain (92) from (94).

Lemma 19.

$$\alpha = \theta^2 + 1. \quad . \quad . \quad . \quad . \quad . \quad . \quad . \quad . \quad . \quad . \quad (95)$$

Proof. We have, by (90)

$$\alpha' = 1 - \frac{\theta^2 + 1}{\alpha} \quad , \quad \beta' = 1 - \frac{\phi^2 + 1}{\beta}.$$

So, by Lemma 17,

$$|\alpha'| < \frac{7 \cdot 8\,\delta}{\theta^2 + 1 - 7 \cdot 8\,\delta} < \frac{7 \cdot 8\,\delta}{2 \cdot 6} = 3\delta, \quad . \quad . \quad . \quad . \quad (96)$$

and

$$|\beta'| < \frac{13\,\delta}{|\phi^2 + 1| - 13\,\delta} = \frac{13\,\delta}{R - 13\,\delta} < \frac{13\,\delta}{1 \cdot 3} = 10\,\delta. \quad . \quad . \quad (97)$$

Suppose, if possible, that $|\alpha'| > 0$. Then since

$$3\delta < \theta^{-2},$$

it is clear that there will be two consecutive non-negative rational integral values of n satisfying

$$\theta^{-4} \leqslant |\alpha' (-\theta^2)^n| < 1.$$

So we can choose a non-negative rational integer n satisfying

$$\theta^{-4} \leqslant \alpha' (-\theta^2)^n < 1.$$

For this integer we have

$$|\alpha' (-\theta^2)^n - 1| \leqslant 1 - \theta^{-4},$$

and

$$|(\beta' (-\phi^2)^n - 1)(\bar{\beta}' (-\bar{\phi}^2)^n - 1)| \leqslant (1 + |\beta'|)^2 < (1 + 10\,\delta)^2.$$

Thus

$$\left.\begin{aligned} |(\alpha' (-\theta^2)^n - 1)(\beta' (-\phi^2)^n - 1)(\bar{\beta}' (-\bar{\phi}^2)^n - 1)| & \\ < (1 - \theta^{-4})(1 + 10\,\delta)^2 & \\ < 1 - \theta^{-4} + 21\,\delta. & \end{aligned}\right\} \quad . \quad . \quad . \quad (98)$$

Since

$$22\,\delta < \theta^{-4},$$

the inequalities (92) and (98) are incompatible for this rational integer n. This contradiction proves that $\alpha' = 0$. Now (95) follows from (90).

Lemma 20.

$$\beta = \phi^2 + 1. \quad . \quad . \quad . \quad . \quad . \quad . \quad . \quad . \quad . \quad . \quad (99)$$

Proof. Suppose, if possible, that $\beta' \neq 0$. Write

$$\mu = 2\psi - \pi = 99^\circ\, 20' \cdot 6 \ldots, \quad . \quad . \quad . \quad . \quad . \quad . \quad (100)$$

so that

$$-\phi^2 = \theta^{-1} e^{i\mu}.$$

Then it follows from Lemmas 18 and 19 and (91) that for every rational integer n,

$$\left.\begin{aligned} 1-\tfrac{1}{5}\delta &< |(\beta'(-\Phi^2)^{-n}-1)(\bar{\beta}'(-\bar{\Phi}^2)^{-n}-1)| \\ &= |(\varrho\,\Theta^n e^{i(\lambda-n\mu)}-1)(\varrho\,\Theta^n e^{-i(\lambda-n\mu)}-1)| \\ &= 1+\varrho^2\Theta^{2n}-2\varrho\,\Theta^n\cos(\lambda-n\mu). \end{aligned}\right\} \quad . \quad . \quad . \quad (101)$$

Now, since $\varrho > 0$, there will be three consecutive rational integers n satisfying

$$\Theta^{-3}\cos 86^\circ < \varrho\,\Theta^n \leqq \cos 86^\circ.$$

Further, it follows, from (100), that for at least one of these three consecutive integers

$$\cos(\lambda-n\mu) > \cos 86^\circ.$$

For this integer n,

$$\begin{aligned} &2\varrho\,\Theta^n\cos(\lambda-n\mu)-\varrho^2\Theta^{2n} \\ &\quad = \varrho\,\Theta^n\{2\cos(\lambda-n\mu)-\varrho\,\Theta^n\} \\ &\quad > \Theta^{-3}\cos 86^\circ\{2\cos 86^\circ-\cos 86^\circ\} \\ &\quad = \Theta^{-3}\cos^2 86^\circ > 0\cdot 001 > \tfrac{1}{5}\delta, \end{aligned}$$

contrary to (101). This contradiction proves that $\beta' = 0$. Now (99) follows from (90).

8. **Lemma 21.** *If a, b, $\bar{b}$ are of the form (9), where ξ_1, η_1, $\bar{\eta}_1$ are conjugate integers and σ, τ, $\bar{\tau}$ are conjugate units of the fields $k(\theta)$, $k(\Phi)$, $k(\bar{\Phi})$ then there is no integer ξ of $k(\theta)$ with conjugates η, $\bar{\eta}$ satisfying*

$$|(\xi-a)(\eta-b)(\bar{\eta}-\bar{b})| < \tfrac{1}{5},$$

but there are an infinite number of integers ξ of $k(\theta)$, with conjugates η, $\bar{\eta}$ satisfying

$$|(\xi-a)(\eta-b)(\bar{\eta}-\bar{b})| = \tfrac{1}{5}. \quad . \quad . \quad . \quad . \quad . \quad . \quad (102)$$

Proof. It is clearly sufficient to prove this lemma in the special case when

$$a = \frac{1}{\theta^2+1} \quad , \quad b = \frac{1}{\Phi^2+1} \quad , \quad \bar{b} = \frac{1}{\bar{\Phi}^2+1},$$

Then

$$\begin{aligned} |(\xi-a)(\eta-b)(\bar{\eta}-\bar{b})| &= \left|\left(\xi-\frac{1}{\theta^2+1}\right)\left(\eta-\frac{1}{\Phi^2+1}\right)\left(\bar{\eta}-\frac{1}{\bar{\Phi}^2+1}\right)\right| \\ &= \left|\frac{N(\xi(\theta^2+1)-1)}{N(\theta^2+1)}\right| \\ &= \tfrac{1}{5}|N(\xi(\theta^2+1)-1)|. \end{aligned}$$

Now for any integer ξ of $k(\theta)$,

$$N(\xi(\theta^2+1)) = N(\theta^2+1)\,N(\xi) = 5\,N(\xi),$$

so that either

$$N(\xi(\theta^2+1)) = 0, \quad \text{or} \quad |N(\xi(\theta^2+1))| \geqslant 5.$$

So there is no integer ξ of $k(\theta)$ satisfying

$$\xi(\theta^2+1) = 1.$$

Consequently

$$|(\xi-a)(\eta-b)(\bar{\eta}-\bar{b}_j| = \tfrac{1}{5}\,|N(\xi(\theta^2+1)-1)| \geqslant \tfrac{1}{5}$$

for every integer ξ of $k(\theta)$. This proves the first part of the lemma.

But, when $\xi = \xi_n$, where n is any rational integer and ξ_n is the corresponding integer of $k(\theta)$ given by (93),

$$\begin{aligned} &|(\xi_n-a)(\eta_n-b)(\bar{\eta}_n-\bar{b})| \\ &\quad = \left|\left(\frac{-(-\theta^2)^n}{\theta^2+1}\right)\left(\frac{-(-\phi^2)^n}{\phi^2+1}\right)\left(\frac{-(-\bar{\phi}^2)^n}{\bar{\phi}^2+1}\right)\right| \\ &\quad = \frac{1}{|N(\theta^2+1)|} = \tfrac{1}{5}. \end{aligned}$$

This completes the proof of the lemma and the theorem.

University College, London.

Mathematics. — SOMMERFELD's *Polynomial Method in the Quantum Theory*. By A. RUBINOWICZ. (Communicated by Prof. H. A. KRAMERS.)

(Communicated at the meeting of February 26, 1949.)

§ 1. *Scope of the paper.* A. SOMMERFELD [1]) has devised a method which enables us to treat many of the most simple but also most important eigenvalue problems in a very easy manner. His polynomial method starts with a splitting of the eigenfunction f of the originally given differential equation into two factors E and P

$$f = EP. \quad . \quad . \quad . \quad . \quad . \quad . \quad . \quad . \quad . \quad (1)$$

The factor E takes care of the convergence of the normalization integral and of the fulfilment of the boundary conditions. The factor P however is assumed to be a polynomial, so that it does not disturb these properties of E. We suppose moreover that P is a solution of a differential equation of the second order with a recurrence formula containing only two terms, that is one of the form

$$(A_2 + B_2 x^h) x^2 \frac{d^2 P}{dx^2} + 2 (A_1 + B_1 x^h) x \frac{dP}{dx} + (A_0 + B_0 x^h) P = 0. \quad . \quad (2)$$

A_l and B_l [2]) are constants and h is a positive integer.

In the present paper we will indicate the eigenvalue problems which can be treated by SOMMERFELDs polynomial method. In § 2 we suppose that the polynomial P in (1) is a solution of (2). Then a relation connecting the coefficients of the differential equation (2) and the original one determines the general form of the potential V which appears in the original differential equation. But the function V obtained in such a way contains the eigenvalue parameter λ and the coefficients A_l and B_l which depend generally on λ. If V has a real physical meaning it can however not depend on λ. That means that there are some relations between λ and the coefficients A_l and B_l. Further relations follow if we require that E guarantees the fulfilment of boundary conditions. All these equations determine not only uniquely the potential function V but settle also the eigenvalues.

From this point of view we treat in the following sections some special problems completely. In § 3 we deal with the radial functions of the spherical symmetric case. In § 4 we discuss the differential equation of associated Legendre functions. In § 5 we start from the same differential equation as in § 4, but apply the polynomial method after a linear transformation of the independent variable. In this way we obtain the differential equation of JACOBI polynomials.

§ 2. *The connection between the original and the polynomial differential equations.* Going over from the "original" differential equation

$$f'' + 2af' + bf = 0 \quad . \quad . \quad . \quad . \quad . \quad . \quad . \quad . \quad (1)$$

with the aid of (1.1) [3]) to the differential equation of the polynomials

$$P'' + 2\alpha P' + \beta P = 0 \quad . \quad . \quad . \quad . \quad . \quad . \quad . \quad . \quad (2)$$

we get between the coefficients of both the differential equations the relations

$$\alpha = \frac{E'}{E} + a, \quad . \quad . \quad . \quad . \quad . \quad . \quad . \quad . \quad . \quad . \quad (3a)$$

$$\beta = \frac{E''}{E} + 2a\frac{E'}{E} + b. \quad . \quad . \quad . \quad . \quad . \quad . \quad . \quad (3b)$$

Eliminating E we obtain a relation between the coefficients of both the differential equations (1) and (2)

$$a^2 + a' - b = \alpha^2 + \alpha' - \beta. \quad . \quad . \quad . \quad . \quad . \quad . \quad . \quad (4)$$

We denote this expression in the following considerations by S.

We assume that the coefficients of (1) are real numbers and that (1) is the differential equation of an eigenvalue problem. (1) is then selfadjoint and has the form

$$\frac{d}{dx}\left(p\frac{df}{dx}\right) - qf + \lambda\varrho f = 0. \quad . \quad . \quad . \quad . \quad . \quad . \quad . \quad (5)$$

λ denotes the eigenvalue parameter and $\varrho(x)$ the density function. It appears in the integral

$$\int_{x_1}^{x_2} f_2^* f_1 \varrho \, dx \quad . \quad . \quad . \quad . \quad . \quad . \quad . \quad . \quad . \quad (6)$$

which decides in case of discrete eigenvalues about normalization and orthogonality of eigenfunctions. x_1 and x_2 are the boundaries of the fundamental interval.

Comparing (1) and (5) we obtain

$$a = \frac{1}{2}\frac{p'}{p}. \quad . \quad . \quad . \quad . \quad . \quad . \quad . \quad . \quad . \quad . \quad (7a)$$

$$b = -\frac{q - \lambda\varrho}{p}. \quad . \quad . \quad . \quad . \quad . \quad . \quad . \quad . \quad . \quad (7b)$$

According to (4) and (7) we can represent S in the form

$$S = \frac{1}{p}\left(\frac{1}{2}p'' - \frac{1}{4}\frac{p'^2}{p} + q - \lambda\varrho\right). \quad . \quad . \quad . \quad . \quad . \quad . \quad (8)$$

so that q becomes

$$q = pS + \lambda\varrho + \frac{1}{4}\frac{p'^2}{p} - \frac{1}{2}p''. \quad . \quad . \quad . \quad . \quad . \quad . \quad (9)$$

The form of the expression S which appears in (9) is known because we suppose that the differential equation for P is given by (1.2) and therefore

$$\alpha = \frac{1}{x}\frac{A_1 + B_1 x^h}{A_2 + B_2 x^h} \qquad \beta = \frac{1}{x^2}\frac{A_0 + B_0 x^h}{A_2 + B_2 x^h} \quad . \quad . \quad . \quad (10)$$

so that according to (4)

$$S = \alpha^2 + \alpha' - \beta = \left.\begin{aligned} &\frac{(A_1 + B_1 x^h)\,[A_1 - A_2 + (B_1 - (h+1)\,B_2,\, x^h]}{x^2\,(A_2 + B_2 x^h)^2} - \\ &- \frac{A_0 + (B_0 - h\,B_1)\,x^h}{x^2\,(A_2 + B_2 x^h)}. \end{aligned}\right\} \quad (11)$$

Our final result is: If the differential equation (5) with given p and q is solvable by $f = E\,P$, P being a solution of (1.2), q must be of the form (9) where S has the form (11).

We apply this proposition in cases where we can split the SCHROEDINGER equation

$$\triangle \psi + \varkappa\,(\mathcal{E} - V)\,\psi = 0. \qquad \varkappa = \frac{2m}{\hbar^2}. \quad . \quad . \quad . \quad . \quad . \quad (12)$$

into a number of differential equations of the form (5). Both p and ϱ are then completely determined by the coordinates used for the separation of the variables and q contains generally an expression given by the potential function V. By (9) and (11) are settled the forms of the q's of all these differential equations therefore also the form of the potential function V.

A more exact determination of V we obtain by the demand that the coefficients of V can not depend on the eigenvalue parameter λ, if V has a real physical meaning. This takes place if the expressions (9) for q do not depend on λ [4]). But this can be fulfiled only if the coefficients B_i which appear in S are functions of λ. To find out this dependence we can expand the expression

$$pS + \lambda\varrho \quad . \quad . \quad . \quad . \quad . \quad . \quad . \quad . \quad . \quad . \quad (13)$$

contained in (9) in a power series in powers of $x - x_0$ (x_0 arbitrary) eventually after multiplication with a function of x. On this occasion we also find, that only for distinct values of h the expression (13) can be made independent of λ.

Further conclusions as to the A_i and B_i and so as to the potential V we can draw from the boundary conditions for the eigenfunctions. As a rule the fundamental interval in the quantum theory in bounded by two singular points of the equation (5). In such points the solution has a tendency towards becoming infinite. From the mathematical point of view it is the task of the boundary conditions to suppress this tendency.

If we confine ourselves to the discrete eigenvalue spectrum we must claim that the integral (6) is convergent for any two eigenfunctions f_1 and f_2, since otherwise we can not speak of their normalization or orthogonality.

Also in case of singular boundary points x_1 and x_2 we prove the orthogonality of two eigenfunctions f_1 and f_2 with the eigenvalues λ_1 and λ_2 by the aid of the well known relation

$$(\lambda_2-\lambda_1)\int_{x_1}^{x_2} f_2^* f_1 \varrho\, dx = \lim_{x\to x_2} \Phi(x) - \lim_{x\to x_1} \Phi(x) \quad . \quad . \quad . \quad (14)$$

where

$$\Phi(x) = p(x)\left[f_2^*(x)\frac{df_1(x)}{dx} - f_1(x)\frac{df_2^*(x)}{dx}\right]. \quad . \quad . \quad . \quad (15)$$

To apply (14) in this case in the usual manner we have to claim not only the convergence of the integral (6) appearing in (14) but also the existence and equality of both the limits

$$\lim_{x\to x_1} \Phi(x) = \lim_{x\to x_2} \Phi(x). \quad . \quad . \quad . \quad . \quad . \quad . \quad . \quad (16)$$

Physical arguments can stipulate to claim more, e.g. that (16) is zero or the eigenfunctions are periodic. But also mathematical motives can do it if e.g. the eigenfunctions have to form a complete set of orthogonal functions.

Both factors E and P which form f can facilitate or make more difficult the fulfilment of the boundary conditions. P is a product of x^σ with a "genuine" polynomial, beginning with a constant and consisting of integer powers of x^h. The exponent σ is given here by the determining fundamental equation

$$\sigma(\sigma-1)A_2 + 2\sigma A_1 + A_0 = 0. \quad . \quad . \quad . \quad . \quad . \quad (17)$$

But also the form of E is determined. According to (3a) we get

$$E = \exp\left(\int (\alpha - a)\, dx\right).$$

From (7a) we find

$$\exp -\int a\, dx = \frac{\text{const}}{p^{1/2}}$$

whereas $\exp \int \alpha\, dx$ may be evaluated by the use of (10). Carrying out this calculation we have to distinguish three cases, according to the disappereance or non-disappereance of the constants A_2 and B_2. We get without an insignificant constant

(I) in case of $A_2 \neq 0$, $B_2 \neq 0$

$$E = p^{-1/2} x^{A_1/A_2} (A_2 + B_2 x^h)^{\frac{1}{h}\left(\frac{B_1}{B_2} - \frac{A_1}{A_2}\right)} \quad . \quad . \quad . \quad . \quad (18a)$$

(II) in case of $A_2 = 0$, $B_2 \neq 0$

$$E = p^{-1/2} x^{B_1/B_2} e^{-\frac{1}{h}\frac{A_1}{B_2}\frac{1}{x^h}}, \quad . \quad . \quad . \quad . \quad . \quad . \quad . \quad (18b)$$

(III) in case of $A_2 \neq 0$, $B_2 = 0$

$$E = p^{-1/2} x^{A_1/A_2} e^{\frac{1}{h}\frac{B_1}{A_2}x^h} \quad . \quad . \quad . \quad . \quad . \quad . \quad . \quad . \quad (18c)$$

The role played by the singular and zero points of ϱ, p, P and E in the fulfilment of the boundary conditions we shall discuss when considering the different special cases.

To these relations we have to add SOMMERFELDs condition of breaking off the power series

$$(\sigma+n)(\sigma+n-1)B_2+2(\sigma+n)B_1+B_0=0 \quad . \quad . \quad . \quad (19)$$

which makes of P a polynomial and determines the eigenvalues of λ in their dependence of an integer n, divisible by h.

Finally we indicate a very useful property of the polynomial equation (2). It does not change its form, if we multiply the polynomial P with a given power of x. Putting $E=x^\nu$ we get from (3)

$$a=\alpha-\frac{\nu}{x}, \quad b=\beta-2\alpha\frac{\nu}{x}+\frac{\nu(\nu+1)}{x^2}.$$

We obtain therefore for $f=x^\nu P$ the differential equation (1), in which the coefficients a, b are of the form (10) of the coefficients α, β.

In both the cases (I) and (III) in which $A_2\neq 0$ we shall use the abbreviations

$$a_i=\frac{A_i}{A_2}, \quad b_i=\frac{B_i}{A_2}.$$

§ 3. *Spheric symmetric field of force.* Splitting off from a Schrödinger eigenfunction a spherical harmonic we obtain for the radial function $R(x)$ the differential equation

$$\frac{d}{dx}x^2\frac{dR}{dx}+\varkappa\left[\mathcal{E}x^2-Vx^2-\frac{1}{\varkappa}l(l+1)\right]R=0 \quad . \quad . \quad . \quad (1)$$

i.e. the differential equation (2.5) with

$$p=\varrho=x^2, \ \lambda=\varkappa\mathcal{E}, \ q=\varkappa V x^2+l(l+1) \quad . \quad . \quad . \quad . \quad (2)$$

V is here the potential function and l the azimuthal quantum number.

From (2) and (2.11) we obtain V in the form

$$V=\frac{S}{\varkappa}-\frac{l(l+1)}{\varkappa x^2}+\mathcal{E}. \quad . \quad . \quad . \quad . \quad . \quad . \quad . \quad . \quad (3)$$

We assume that the fundamental interval is given by $0<x<+\infty$ and use for our considerations the factor E first.

To make the normalizing integral (cp. (2.6))

$$\int_0^\infty x^2 R^* R\,dx \quad . \quad . \quad . \quad . \quad . \quad . \quad . \quad . \quad . \quad (4)$$

convergent at its upper limit we have to assume case III i.e.

$$A_2\neq 0, \quad B_2=0. \quad . \quad . \quad . \quad . \quad . \quad . \quad . \quad . \quad (5)$$

According to (2.18c) and (2) E becomes

$$E=x^{\frac{A_1}{A_2}-1}e^{\frac{1}{h}\frac{B_1}{A_2}x^h} \quad . \quad . \quad . \quad . \quad . \quad . \quad . \quad . \quad (6)$$

and the convergence for $x \to +\infty$ requires $B_1/A_2 < 0$. Finally we assume

$$A_1 = A_2 \quad . \quad . \quad . \quad . \quad . \quad . \quad . \quad . \quad . \quad . \quad (7)$$

to unite the x-power from E with the polynomial P.

For further considerations we use V. According to (2.11), (5) and (7) the expression S is given here by

$$S = \frac{1}{x^2}\left[-a_0 + ((h+1)\,b_1 - b_0)\,x^h + b_1^2\,x^{2h}\right].$$

To free V, Eq. (3), from $\mathfrak{E}$ we have here only both the possibilities $h = 1$ or $= 2$. For $h = 1$ the potential becomes

$$V = \frac{c_{-2}}{x^2} + \frac{c_{-1}}{x} + c_0, \quad . \quad . \quad . \quad . \quad . \quad . \quad . \quad . \quad (8)$$

where the constants

$$c_{-2} = -\frac{1}{\varkappa}(a_0 + l(l+1)), \quad . \quad . \quad . \quad . \quad . \quad . \quad . \quad (9a)$$

$$c_{-1} = \frac{1}{\varkappa}(2\,b_1 - b_0) \quad . \quad . \quad (9b), \qquad c_0 = \mathfrak{E} + \frac{b_1^2}{\varkappa} \quad . \quad . \quad . \quad (9c)$$

are independent of $\mathfrak{E}$. Therefore we obtain for V a Coulomb potential superposed by a potential inversely proportional to the square of the distance. The coefficients c_i in (8) are arbitrary because their dependence on A_i, B_i does not imply any connection between them.

To the potential (8) belongs the RYDBERG formula. From (2.19) and (5) follows

$$b_0 = -2\,b_1\,(n+\sigma) \quad . \quad . \quad . \quad . \quad . \quad . \quad . \quad . \quad . \quad (10)$$

and hence, in accordance with (9b), $c_{-1} = \frac{b_1}{2}\,(n+\sigma+1)$ so that we obtain from (9c) in fact the RYDBERG formula

$$\mathfrak{E} = -\frac{\varkappa}{4}\,\frac{(c_{-1})^2}{(n+\sigma+1)^2} + c_0. \quad . \quad . \quad . \quad . \quad . \quad . \quad . \quad (11)$$

Supposing further, that the Coulomb potential has the right constant $c_{-1} = -e^2 Z$ we obtain in (11) the RYDBERG constant. Eq. (9a) not yet used determines σ and hence the RYDBERG correction. From (2.17), (7) and (9a) we obtain

$$\sigma(\sigma+1) = -a_0 = l(l+1) + \varkappa c_{-2}. \quad . \quad . \quad . \quad . \quad . \quad . \quad (12)$$

In a pure Coulomb field, there is $c_{-2} = 0$ and therefore $\sigma = l$ (for $\sigma = -l-1$ the normalizing integral (4) is not convergent) so that we obtain the BALMER formula.

In case $h = 2$ we have

$$V = \frac{c_{-2}}{x^2} + c_2\,x^2 + c_0$$

where

$$c_{-2} = -\frac{1}{\varkappa}(a_0 + l(l+1)) \quad . \quad . \quad . \quad . \quad . \quad . \quad . \quad . \quad . \quad (13a)$$

$$c_2 = \frac{1}{\varkappa} b_1^2 \quad . \quad . \quad . \quad (13b), \qquad c_0 = \mathcal{E} + \frac{1}{\varkappa}(3b_1 - b_0) \quad . \quad . \quad (13c)$$

The potential V is consequently given by a superposition of an elastic potential and of a potential inversely proportional to the square of the distance.

The dependence of $\mathcal{E}$ upon the quantum numbers we obtain from (10), (13*b*) and (13*c*)

$$\mathcal{E} = -2\frac{b_1}{\varkappa}(n+\sigma+\tfrac{3}{4}) + c_0 = 2\sqrt{\frac{c_2}{\varkappa}}(n+\sigma+\tfrac{3}{2}) + c_0 . \quad . \quad (14)$$

The positive sign of the square root is determined by (6).

If to the pure elastic field of force corresponds a frequency ω (in 2π sec), we have to put $c_2 = \frac{m}{2}\omega^2$. Like in case $h = 1$ the constant σ is given by (12).

In case of a pure elastic potential there is $c_{-2} = 0$ and therefore $\sigma = l$. For the eigenvalues of the spatial harmonic oscillator we obtain then

$$\mathcal{E} = (n+l+\tfrac{3}{2})\hbar\omega + c_0 . \quad . \quad . \quad . \quad . \quad . \quad . \quad (15)$$

The general case (14) we can conceive now as (15) with a RYDBERG correction σ. The constant c_0 is in all the formulae of Legendre functions arbitrary and we can put $c_0 = 0$, if V is normalized as usual.

§ 4. *The differential equation for associated Legendre functions.* To have an example of an eigenvalue problem in a finite fundamental interval we generalize the equation for associated Legendre functions

$$\frac{d}{dx}\left((1-x^2)\frac{dK}{dx}\right) + \left(\lambda - \frac{m^2}{1-x^2}\right)K = 0$$

putting $V(x)$ for $m^2/(1-x^2)$

$$\frac{d}{dx}\left((1-x^2)\frac{dK}{dx}\right) + (\lambda - V(x))K = 0 . \quad . \quad . \quad . \quad . \quad (1)$$

We obtain hence the differential equation (2.5) with

$$p = 1-x^2, \quad \varrho = 1, \quad q = V . \quad . \quad . \quad . \quad . \quad . \quad . \quad (2)$$

From (2.9) and (2) we get therefore

$$V = \frac{1}{1-x^2} + S(1-x^2) + \lambda . \quad . \quad . \quad . \quad . \quad . \quad (3)$$

For the fundamental interval we choose $-1 < x < +1$ and use first for our considerations the factor E, given by one of the Eqs. (2.18).

The zero points of p, which according to (2) are situated in $x = \pm 1$, endanger the convergence of the normalizing integral given according to (2.6) and (2) by

$$\int_{-1}^{+1} K^* K \, dx \quad \ldots \ldots \ldots \quad (4)$$

because $p^{-\frac{1}{2}}$ appears in the factors E in all the cases (2.18). This danger can be eliminated only in case I, Eq. (2.18a), where

$$A_2 \neq 0, \quad B_2 \neq 0 \quad \ldots \ldots \ldots \quad (5)$$

and where according to (2.18a) and (2)

$$E = x^{\frac{A_1}{A_2}} \frac{(A_2 + B_2 x^h)^{\frac{1}{h}\left(\frac{B_1}{B_2} - \frac{A_1}{A_2}\right)}}{(1 - x^2)^{1/2}}.$$

To avoid E disturbing the convergence of the normalization integral (4) in the endpoints $x = \pm 1$ of the fundamental interval and to secure the finiteness of the expressions (2.15) the binomial $A_2 + B_2 x^h$ must be divisible by $1 - x^2$. Hence follows that

$$A_2 = -B_2 \quad \ldots \ldots \ldots \quad (6)$$

and

$$h = \text{even integer.} \quad \ldots \ldots \ldots \quad (7)$$

Both our demands restrict also the variability of the exponent of $A_2 + B_2 x^h$; the demand that the expressions (2.15) are finite goes further and claims in accordance with (6) that

$$\frac{A_1 + B_1}{A_2} + 1 \leqq 0. \quad \ldots \ldots \ldots \quad (8)$$

To transpose x^{A_1/A_2} from E to P we must put

$$A_1 = 0. \quad \ldots \ldots \ldots \quad (9)$$

Now let us use V. In accordance with (5), (6) and (9) we obtain from (2.11)

$$S = x^{h-2} b_1 \frac{-1 + (b_1 + h + 1) x^h}{(1 - x^h)^2} - \frac{a_0 + (b_0 - h b_1) x^h}{x^2 (1 - x^h)}. \quad (10)$$

Developing S in a power series we get from the expression Sp appearing in Eq. (3)

$$\left. \begin{aligned} Sp = S(1 - x^2) = -\frac{a_0}{x^2} + a_0 - M(x^{h-2} - x^h) - (M+N)(x^{2h-2} - x^{2h}) + \\ + (M + 2N)(x^{3h-2} - x^{3h}) + \ldots \end{aligned} \right\} \quad (11)$$

where $M = a_0 + b_0 - (h-1) b_1$, $N = -b_1 (b_1 + h)$.

If V is independent of λ the coefficients of a development of V in a power series can also not depend on λ. Hence in accordance with (3) the coefficients of a power series development of

$$S(1 - x^2) + \lambda \quad \ldots \ldots \ldots \quad (12)$$

must be independent of λ.

First we assume that $h \neq 2$, i.e. according to (7): $h = 4, 6, 8, \ldots$. In accordance with (11) and (12) then the values of a_0, $a_0 + \lambda$, M, N must be constant. But from the simultaneous constancy of a_0 and $a_0 + \lambda$ it follows that also the eigenvalue parameter λ is invariable. In such a case however our problem is not an eigenvalue problem.

For $h = 2$ we have to demand, that only the three quantities a_0, $a_0 - M + \lambda$ and N are constant. From this and the Eqs. (2.17) and (2.19) we could determine the dependence of the eigenvalues λ upon the quantum numbers. But we may come to this conclusion in an easier way.

For $h = 2$ we obtain from (3) and (10) for V the expression

$$V = \frac{A}{1-x^2} + \frac{B}{x^2} + C \quad \ldots\ldots\ldots \quad (13)$$

where the constants are given by

$$A = (b_1 + 1)^2 \ (14a), \quad B = -a_0 \ (14b), \quad C = \lambda - (b_1^2 + b_1 + b_0). \quad (14c)$$

If we put $b_1 + 1 = -m$ and remark that from (2.18) it follows $b_0 = (\sigma + n)(\sigma + n - 1) - 2b_1(\sigma + n)$ we finally obtain from (14c)

$$\lambda = (\sigma + m + n)(\sigma + m + n + 1) + C. \quad \ldots\ldots \quad (15)$$

In accordance with (8) and (9), m is here a positive constant.

From (2.17) and (9) we obtain for σ the relation

$$\sigma(\sigma - 1) = -a_0 = B. \quad \ldots\ldots\ldots \quad (16)$$

By SOMMERFELD's polynomial method we can therefore solve a slightly more general differential equation than the one for the associated Legendre functions. This last differential equation we obtain by putting $B = 0$. In this case is $\sigma = 0$ or $= 1$. Remembering that n is an even integer ($h = 2!$) and hence $n + \sigma$ an arbitrary positive integer we see that (15) represents the well known eigenvalues of the differential equation for the associated Legendre functions.

To demonstrate by an example the simplifications caused by the transposition of the x-power from E to P, we indicate the results arrived at without the supposition (8). Instead of (11) we obtain an expression in which is substituted

$$a_0 - a_1(a_1 - 1) \text{ for } a_0, \quad M - a_1(2a_1 + 2b_1 + h - 1) \text{ for } M,$$
$$N - a_1(a_1 + 2b_1 + h) \text{ for } N.$$

But this does not alter the conclusion that $h = 2$.

We obtain V in the same way from (13) but have to substitute

$$A' = (a_1 + b_1 + 1)^2, \quad B' = B + a_1(a_1 - 1), \quad C' = C$$

for A, B, C.

Putting $a_1 + b_1 + 1 = -m$ so that we have again $A = m^2$ we obtain for the eigenvalues the expression

$$\lambda = (\sigma + a_1 + m + n)(\sigma + a_1 + m + n + 1) + C' \quad \ldots \quad (15')$$

where $\sigma + a_1$ is given by the equation

$$(\sigma + a_1)(\sigma + a_1 - 1) = B. \quad . \quad . \quad . \quad . \quad . \quad . \quad (16')$$

The equations (15') and (16') we obtain from (15) and (16) if we write $\sigma + a_1$ instead of σ. But this changes only the notation.

§ 5. *The differential equation of* JACOBI *polynomials.* If SOMMERFELD's polynomial method is not applicable to a certain differential equation, we can try to give the latter a new form by a transformation of the independent variable and then to apply this method. We expect to succeed in this way from the fact, that in SOMMERFELD's polynomial equation (1.2) the zero point plays a distinguished role which is after a transformation taken over by another point of the fundamental interval. That means: If we replace in a "given" differential equation the independent variable by a new one and regard such an obtained equation as the "original" differential equation (2.1) or (2.5) we can generally solve the "given" differential equation by the polynomial method for other potentials V, as by direct application of this method to the "given" differential equation.

To verify this statement we use the differential equation of the associated Legendre functions (4.1) i.e.

$$\frac{d}{dx'}\left((1-x'^2)\frac{dK}{dx'}\right) + (\lambda - V(x'))K = 0 \quad . \quad . \quad . \quad . \quad (1)$$

where we have denoted the independent variable by x'. Substituting here by

$$x' = x - 1 \quad . \quad . \quad . \quad . \quad . \quad . \quad . \quad . \quad . \quad . \quad (2)$$

the new independent variable x, we obtain the differential equation

$$\frac{d}{dx}x(2-x)\frac{dK}{dx} + (\lambda - V(x))K = 0$$

which we will consider as the "original" equation of SOMMERFELD's polynomial method. It has the form (2.5) with

$$p = x(2-x), \quad \varrho = 1, \quad q = V \quad . \quad . \quad . \quad . \quad . \quad (3)$$

so that according to (2.9) and (3) the potential V has the form

$$V = \frac{1}{x(2-x)} + Sx(2-x) + \lambda \quad . \quad . \quad . \quad . \quad . \quad . \quad (4)$$

In the variable x' the fundamental interval is bounded by ± 1, in x it is therefore given by $0 < x < 2$.

For further conclusions we use first the factor E. We have to choose it in the form (2.18a) to guarantee finiteness of the normalizing integral

$$\int_0^2 K^* K \, dx \quad . \quad . \quad . \quad . \quad . \quad . \quad . \quad . \quad . \quad . \quad (5)$$

Otherwise $p = x(2-x)$ endangers the convergence of (5) at its upper limit. Therefore we have to put $A_2 \neq 0$, $B_2 \neq 0$ and obtain

$$E = x^{\frac{A_1}{A_2}-1} \frac{(A_2 + B_2 x^h)^{\frac{1}{h}\left(\frac{B_1}{B_2}-\frac{A_1}{A_2}\right)}}{(2-x)^{1/2}}.$$

To guarantee the convergence of (5) for $x = 2$ we must suppose that the expression $A_2 + B_2 x^h$ is divisible by $2-x$, i.e. that

$$B_2 = -\frac{1}{2^h} A_2. \quad \ldots\ldots\ldots \quad (6)$$

Further we have to assume according to the higher demands of (2.15) that

$$2\left[\frac{1}{h}\left(\frac{B_1}{B_2}-\frac{A_1}{A_2}\right)-\frac{1}{2}\right]+1 = \frac{2}{h}\left(\frac{B_1}{B_2}-\frac{A_1}{A_2}\right) > \frac{1}{2}. \quad \ldots \quad (7)$$

Finally the removal of the x-power from E to P gives

$$A_1 = \tfrac{1}{2} A_2. \quad \ldots\ldots\ldots \quad (8)$$

To use V for further considerations we remark that according to (6) and (8) the expression S is given by

$$S = -\frac{(1+m y^h)(1+n y^h)}{16 y^2 (1-y^h)^2} - \frac{a_0}{4}\frac{1+p y^h}{y^2(1-y^h)}$$

where $y = x/2$ and

$$m = 2^{h+1} b_1, \quad n = -2^{h+1} b_1 - 2(h+1), \quad p = \frac{2^h (b_0 - h b_1)}{a_0}.$$

Developing S in a power series in y we obtain for the expression $Sx(2-x)$ appearing in Eq. (4) for V

$$Sx(2-x) = 4 Sy(1-y) = -(a_0 + \tfrac{1}{4})\left(\frac{1}{y} - 1\right) + M(y^{h-1} - y^h) +$$
$$+ (M+N)(y^{2h-1} - y^{2h}) + (M+2N)(y^{3h-1} - y^{3h}) + \ldots$$

where

$$M = \frac{h}{2} - a_0 - 2^h (b_0 - h b_1), \quad N = \tfrac{1}{4}[2h - 1 + 2^{h+1} b_1 (2^{h+1} b_1 + 2h + 2)].$$

To fix the value of h we can now use the demand, that the coefficients of $Sx(2-x) + \lambda$ (cp. (2.13) and (4)) are independent of λ. For $h = 2, 3, 4 \ldots$ we have to claim that $a_0 + 1/4$, $a_0 + 1/4 + \lambda$, M, N are constant, so that λ would be constant.

For $h = 1$ the expressions

$$a_0 + \tfrac{1}{4}, \quad a_0 + \tfrac{1}{4} + M + \lambda, \quad N$$

only have to be constant. But this means that

$$a_0 = \text{const}, \; b_1 = \text{const} \quad (9a), \quad \lambda = -M + \text{const} = 2b_0 + \text{const} \quad (9b)$$

λ can now depend on quantum numbers because b_0 is not constant now.

To consider the case $h = 1$ in detail we remark that according to (2.11), (4), (6) and (8) the potential V has the form

$$V = \frac{A}{x-2} + \frac{B}{x} + C$$

where

$$A = -8b_1(b_1+1) - 2 \text{ (10a)}, \quad B = -2a_0 \text{ (10b)}, \quad C = \lambda - 2(b_0+b_1+2b_1^2). \text{ (10c)}$$

The relations (9a) follow also from (10a) and (10b) and the relation (9b) follows from (10c).

Reintroducing by (2) again the variable x', we obtain V in the form

$$V = \frac{A}{x'-1} + \frac{B}{x'+1} + C = \frac{x'(A+B) + A - B}{x'^2-1} + C.$$

But (1) represents with this V the differential equation of JACOBI polynomials. It is therefore situated at the limit of the applicability of SOMMERFELD's polynomial method.

In the quantum theory of a spinning symmetrical top we have to do with this equation with

$$A = -\tfrac{1}{2}(\tau-\tau')^2, \qquad B = \tfrac{1}{2}(\tau+\tau')^2 \quad . \quad . \quad . \quad . \quad (11)$$

where τ and τ' are positive or negative integers.

Using that we have according to (2.19) and (6)

$$(\sigma + n)(\sigma + n - 1) - 4(\sigma + n)b_1 - 2b_0 = 0,$$

we obtain from (10) the eigenvalues

$$\lambda = (\sigma + n - 2b_1)(\sigma + n - 2b_1 - 1) + C.$$

According to (2.17), (8) and (10) we have to calculate σ from

$$\sigma^2 = -a_0 = -\tfrac{1}{2}B. \quad . \quad . \quad . \quad . \quad . \quad . \quad . \quad (12)$$

Supposing especially the case (11) we get from (10) according to (7): $b_1 = -\frac{1}{2} + \frac{|\tau-\tau'|}{2}$ and from (12) in accordance with the fact that $\sigma > 0$ (otherwise we would obtain for $x' = -1$ an inadmissible singularity): $\sigma = \frac{|\tau-\tau'|}{2}$. Hence we get the well known result

$$\lambda = (n + \tau^*)(n + \tau^* + 1) + C$$

where $\tau^* = \frac{|\tau+\tau'|}{2} - \frac{|\tau-\tau'|}{2}$ is the larger of both the integers $|\tau|$ and $|\tau'|$.

REFERENCES.

1. A comprehensive treatment was given by A. SOMMERFELD in Atombau und Spektrallinien, Vol. II, Braunschweig 1939, cp. p. 716.
2. SOMMERFELD denotes our coefficients $2A_1$ and $2B_1$ by A_1 and B_1.
3. (a, b) means equation b of section a.
4. Compare however (3.1) where q depends on l.

Biochemistry. — *Elastic-viscous oleate systems containing KCl.* IV. *The flow properties as a function of the shearing stress at 15° and constant KCl concentration.* By H. G. BUNGENBERG DE JONG and H. J. VAN DEN BERG.

(Communicated at the meeting of February 26, 1949.)

1. *Introduction.*

An orientating investigation [1]) on the viscous behaviour of KCl containing oleate sols at 25° C, was performed with a viscometer which worked with constant hydrostatic head. The maximum shearing stress (at the wall of the capillary) was therefore nearly constant (of the order of 40 dynes/cm^2) [2]). As PHILIPPOFF [3]) has shown that under certain conditions Na oleate sols may show "structural viscosity", it seemed safe to adopt for a further investigation of the viscous behaviour of the KCl containing oleate systems methods which allow of a wide variation of the shearing stress. In Part I, II and III of this series [4]) the elastic properties of these systems have been studied at 15° C (at which temperature the damping of elastic oscillations is in general much smaller than at 25° C) and at a favourable KCl concentration (at or very near to the minimum damping at the given temperature). We chose therefore the same conditions for the present work and performed all experiments with "Na-oleinicum, medicinale pur.pulv. Merck", which is present in the KCl (+ KOH) medium in a relatively low concentration.

The first impression these systems make on the observer is that they are gels. The definition of gels often includes the presence of a yield value. Our first aim will therefore be to investigate if a yield value can be detected, which involves the study of the flow phenomena at low shearing stresses.

2. *Measurements at very low shearing stresses.*

The viscometer used (see fig. 1) is in principle that of MICHAUD [5]), whose characteristic feature is that slight level differences are obtained by immersion of a glass rod (in our case 0.55 cm diameter) into one of the

---

[1]) H. G. BUNGENBERG DE JONG and G. W. H. M. VAN ALPHEN, Proc. Kon. Ned. Akad. v. Wetensch., Amsterdam, **50**, 849, 1011 (1947).

[2]) Dimensions of the capillary: $R = 0.0425$ cm, $l = 24$ cm; constant hydrostatical head $h = 43.1$ cm.

[3]) W. PHILIPPOFF, Viskosität der Kolloide, Dresden (1942). Cf. p. 116, 122, 279—280 and fig. 61 (p. 128) and fig. 162 (p. 280).

[4]) H. G. BUNGENBERG DE JONG and H. J. VAN DEN BERG, Proc. Kon. Ned. Akad. v. Wetensch., Amsterdam, Part. I: **51**, 1197 (1948); Part II: **52**, 15 (1949); Part III: **52**, 99 (1949).

[5]) F. MICHAUD, Ann. de Phys. **19**, 63 (1923).

wide tubes (we used 3.6 cm diameter) and that the movement in the capillary of the system investigated, is observed in the microscope.

For the viscometer used a level difference of 0.0239 cm is obtained by screwing the glass rod downwards or upwards over a distance of one centimeter. With the aid of the formula $P = R.p/2.l$ we obtain from the dimensions of the capillary ($R = 0.0425$ cm; $l = 24$ cm) and from the

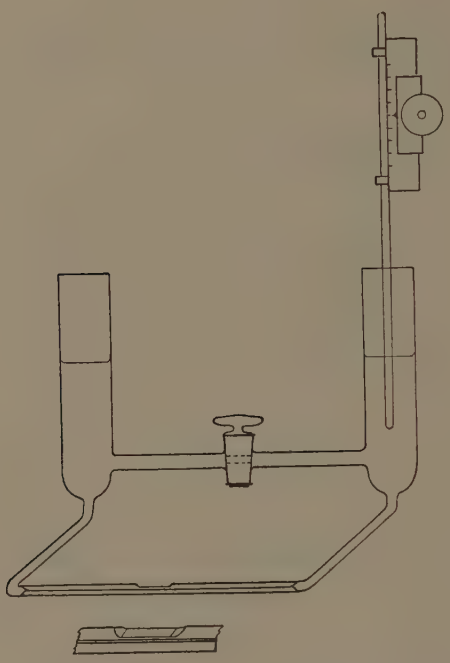

Fig. 1.

density of the soap system ($\varrho = 1.066$) a value of 0.0169 dynes/cm^2 for P, the shearing stress at the wall of the capillary for one centimeter immersion of the rod.

Before starting a series of measurements the stopcock in the horizontal tube connecting the wide vertical tubes is closed and a certain quantity of the oleate system is brought into the left hand wide tube. With the aid of suction the capillary and the horizontal tubes connected with it are next completely filled with the oleate system. The apparatus is then put into its definite position, the capillary plus attached horizontal tubes [6]) being immersed in a tray (standing on the stage of the microscope and provided with a glass window at the bottom) through which flows water of constant temperature [7]). Now the glass rod is moved into such a position that after

---

[6]) Only these parts of the apparatus need be at the desired temperature, because the very high viscosity of the oleate systems practically excludes all convection currents.

[7]) Running tapwater was used, which practically did not change in temperature during the measurements (constant within 0.2° C).

completely filling the apparatus it will be immersed some 5 cm into the oleate system. This original position of the glass rod will be called position "zero".

The levelling of the oleate system and the drainage of the walls of the wide tubes above the levels (which during the manipulations have become wetted by the oleate system) is then obtained by opening the stopcock (wide bore) for a sufficiently long time (we took 2—3 hours).

One is not sure, however, that after closing the stopcock exact levelling has really been accomplished (e.g. on account of very high viscosity of the system or on account of any presence of a yield value).

But the position of the glass rod which corresponds to real levelling follows from the measurements themselves [8]).

The latter consist in measuring the velocity of displacement (v) of suspended particles in the axis of the capillary at various positions (p) of the glass rod. These positions are varied into both directions (reckoned from position "zero"), so that a number of values p are obtained in which the system in the capillary flows to the left and another number in which it flows to the right. Providing these p and v values with + or — signs and putting them in a graph, a symmetrical figure must result, the symmetrical point of which lies on the abscis axis (position of the glass rod) and represents that position of the rod at which real levelling exists. Various forms of such symmetrical figures can be imagined, from which a few are given under *a*, *b*, *c* and *d* in fig. 2. The vertical, dotted line represents the

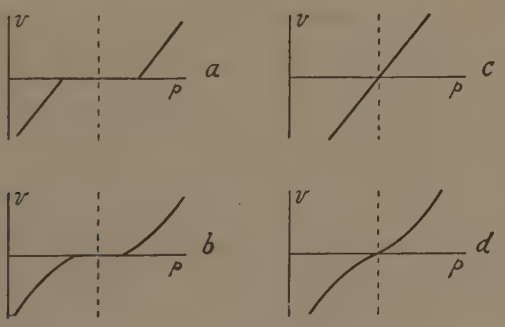

Fig. 2.

position of the rod at real levelling (which will in general differ slightly from position "zero").

In *a* and *b* a yield value is present, in *c* and *d* it is absent (or smaller than the experimental error). In *c* the velocity of flow is proportional to

---

8) This position must remain constant during a series of measurements. This will only reasonably be the case if the stopcock after filling the apparatus has been left open for a sufficiently long time to allow the drainage of the walls. Otherwise a gradual shift of this position will occur during a series of measurements.

the shearing stress, in *a* it is a linear function of the latter and in *b* and *d* this function is more complicated.

Two oleate systems were investigated with the technique described above. They were made by mixing 50 and 125 cc respectively of a stock solution (10 gr. Na oleate + 500 cc H_2O + 50 cc KOH 2 N) with 75 cc H_2O + 75 cc KCl 3.8 N and with 75 cc KCl 3.8 N respectively. Practically the systems differ only in the final concentration of the oleate (0.45 and 1.14 gr per 100 cc). The electrolyte concentration (1.43 N KCl + + 0.05 N KOH or 1.43 N KCl + 0.11 N KOH) is such that the damping of the elastic oscillations is near to its minimum value. The mixtures had now to be provided with particles, that would indicate the velocity of flow.

We will discuss this problem together with our experiments on the 0.45 % oleate system. In preparing the mixture it was thoroughly shaken and had to be left to itself for a considerable time to become approximately free from air, though some small bubbles still happened to be present. It was now tried if such entrapped air bubbles could be used as "indicators" of the velocity of flow in the axis of the capillary. An ideal indicator should have the following properties:

a. it shall not alter the properties of the oleate system;

b. the dimension of the particles (bubbles or drops) of the indicator shall be small in comparison with that of the capillary;

c. its particles, etc. shall neither rise nor sink during the measurement;

d. a sufficient number of particles should always be present in the microscopic image, so that one can select one in the axis of the capillary for each single measurement.

For entrapped air bubbles only a. is fulfilled. Very small bubbles are absent or relatively rare (contrary to b. and d.), so that one must select larger ones, which, however, are all rising upwards (contrary to c.). Soon after the beginning of a series of measurements no air bubbles are present any longer in the axis of the capillary and all lie now pressed at the upper part of the glasswall of the capillary.

The use of air bubbles is therefore not possible for indicating the velocity of flow in the axis of the capillary. Nevertheless it was decided to start a series of measurements on such an air bubble. There were no indications of the presence of a three-phase contact (air — soapsystem — glass), so that it was supposed that the air bubble could freely move along the glass boundary. If this assumption is correct, we would get information on the mean velocity of flow of the oleate system in a zone [9]) close to the wall as function of the shearing stress and the results could be compared

---

[9]) This zone of course depends on the relative diameter of bubble and radius of the capillary. It is further necessary that the bubble shall not alter its diameter during the whole series of experiments. In our case this requisite was nearly fulfilled.

with measurements in the axis of the capillary which were to be performed with a more appropriate indicator later on.

The results are given in fig. 3 in which v is expressed in scale-divisions of the eye piece micrometer per 100 seconds. The order in which the

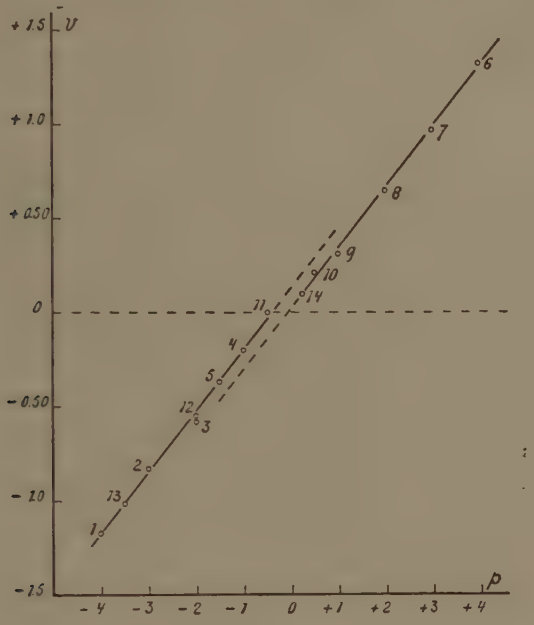

Fig. 3.

successive measurements have been taken is given by the numbers next to the experimental points. The figure obtained is of the type represented in fig. 2*a*, which would mean that there is a simple type of functional linear relation between rate of flow and shearing stress in the investigated range considered (0—0.07 dynes/cm^2) as well as a yield value. The latter expressed in dynes/cm^2 can be calculated from half the horizontal distance of the two parallel straight lines through the experimental points, bearing in mind that every cm change in the position of the glass-rod corresponds with 0.0169 dynes/cm^2. The horizontal distance being approximately 0.35 cm change in position of the rod, we obtain a yield value in the order of only 0.003 dynes/cm^2.

But it may be seriously doubted if a yield value of the oleate system itself is really indicated by fig. 3. It is very well conceivable, that the assumption of wholly free movability of the air bubble along the glasswall (as we did) is not true and that a certain difference in pressure between the two sides of the air drop must be exceeded before the air bubble itself "yields" from its original position (pressed against the glasswall).

The measurements of the velocity of flow in the axis of the capillary were performed by using paraffine oil as an indicator. We added two drops

of paraffine oil, which slowly dripped from a 5.5 mm diameter glass rod held vertically into 200 cc of the 0.45 % oleate system. This was shaken vigourously in order to emulsify the paraffine oil. The oleate system being full of entrapped air was then left standing till the next day, to become free from air bubbles.

The system was turbid in consequence of the paraffine oil having emulsified into very small drops, which were extremely useful for indicating the rate of flow in the axis of the capillary. Indeed, paraffine oil is the nearest approach to the ideal indicator, fulfilling the requirements mentioned sub b., c. and d. on page 366.

As to exigence a. (according to preliminary experiments) the influence on the period of the rotational oscillation was found to be very slight or negligeable. The velocity of flow was measured with a stopwatch by checking the time necessary for a very small drop (diameter $\pm$ 0.2 scale divisions) to move over a number of scale divisions of the micrometer, and by calculating from this the number of scale divisions per 100 sec. See table I (upper part) and fig. 4, from which it appears that:

a. There is no indication of the presence of a yield value;

b. the velocity of flow in the axis of the capillary is proportional to the shearing stress at the glasswall [10]).

Comparing fig. 4 with fig. 3 (in which the same arbitrary units for the velocity of flow have been used) we perceive from the far smaller inclination of the straight lines in the latter figure, that the mean velocity in a zone next to the wall (in which zone the air bubble moved) is much smaller than in the axis of the capillary. Unfortunately we did not measure the dimension of the air bubble and of the capillary (the diameter of the bubble may have been in the order of $^1/_5$ of the capillary diameter), so that no quantitative calculations can be made to examine whether this difference in rate of flow is compatible with laminar flow. Except for any future indications to the contrary it seems probable that in the range of small maximum shearing stresses (0 — approximately 0.07 dynes/cm^2) the oleate system, although it shows marked elastic properties, behaves as a Newtonian liquid.

We therefore conclude that our oleate systems, although they make the impression of being gels, can be described better by the term: "elastic fluids".

---

[10]) Fig. 4 deviates slightly from the simple scheme of fig. 1c, in as much the experimental points do not lie exactly on one straight line. Instead of it the points lie on two straight lines, with a slightly different inclination, meeting each another at the same point of the horizontal level at $v = 0$. In connection with the order of the measurements (alternatingly a point with a positive v and a point with a negative v, and further choosing these points in such a way that their absolute values become increasingly smaller) the shape of fig. 3 can be explained by a slight gradual shifting to the left as has been discussed in note 8. The conclusions a. and b. in the text are of course not endangered by this circumstance.

TABLE I.

Velocity of flow (v, in scale divisions per 100 sec) in the axis of the capillary.

System investigated	Immersion depth (p) of the glassrod in cm, relative to the original position									
	+4	+3	+2	1+	+0.5	−0.5	−1	−2	−3	−4
0.45% oleate	6.85	5.36	3.69	1.94	1.04	−0.65	−1.55	−3.32	−5.22	−6.96
system at	7.06	5.45	3.61	1.90	1.09	−0.69	−1.52	−3.27	−5.18	−6.96
15.4°			3.55	1.86	1.03	−0.61	−1.50	−3.27		
(see fig. 4)				1.88						
mean:	6.96	5.41	3.62	1.90	1.05	−0.65	−1.52	−3.29	−5.20	−6.96
1.14% oleate	0.357	0.248	0.164					−0.202	−0.276	−0.351
system at	0.350	0.241	0.158					−0.204	−0.259	−0.348
14.4°	0.351	0.242	0.161					−0.195	−0.277	−0.349
(see fig. 5)										
mean:	0.351	0.244	0.161					−0.200	−0.271	−0.349

The results obtained with the 1.14 % oleate system on the whole are the same. Because of the much higher viscosity of this more concentrated oleate system the drainage factor becomes of great importance now. (We waited 3 hours for levelling with open stopcock). The influence of this factor becomes plainly visible during the measurements, for after each displacement of the glassrod it will now take a long time until the new position of the levels is exactly reached in consequence of the slow drainage of the walls of the tubes and of the glassrod after the latter has been moved up, and of slowly renewed positions of the menisci against these

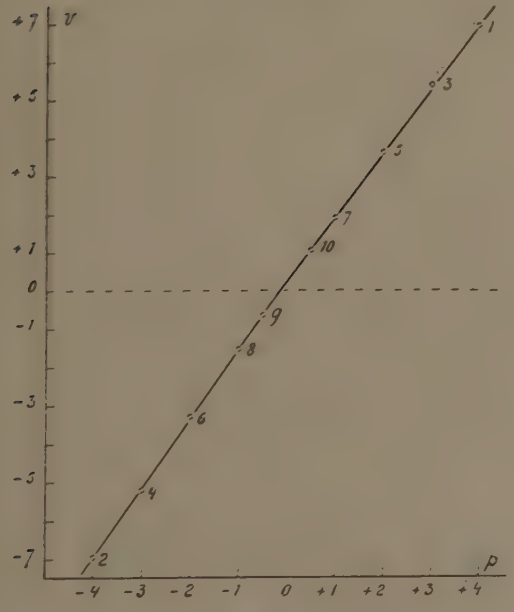

Fig. 4.

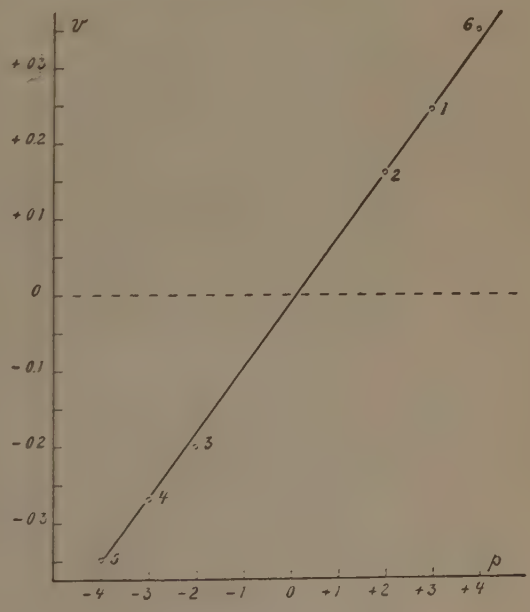

Fig. 5.

glass-surfaces aftere the glassrod has been lowered). The experimental results show this influence of the drainage factor (see table II and fig. 5). The apparently irregular positions of the experimental points around the straight line drawn can be accounted for from the above if we take the order of the separate measurements into consideration (indicated by the figure next to each experimental point).

We perceive, for instance, that the greatest deviation of a point from the straight line occurs if the glassrod has been displaced over a great distance just before the measurement. See point 3 and point 6, which both show too high a velocity (as can be expected from the above). Taking these disturbing influences of slow drainage and of slowly renewed wetting into consideration, we feel justified in concluding that also in the case of the 1.14 % oleate system no yield value is present and that the velocity of flow is proportional to the maximum shearing stress at the wall. In the domain of very low shearing stresses (0—0.07 dynes/cm^2) this oleate system, since it shows very marked elastic properties and at the same time behaves as a Newtonian liquid, should not be described as a gel but as an elastic fluid.

3. *Measurements at higher shearing stresses.*

An investigation of the flow behaviour in a large range of much higher shearing stresses (order of 1—1000 dynes/cm^2) showed that the simple flow behaviour we met at very low shearing stresses (section 2) is lost.

In principle we followed the method described by PHILIPPOFF [11]) and calculated from the experimental data the quantities V $(= 4\,Q/\pi R^3)$, the mean velocity of flow expressed in cc/sec., and P $(= R.p/2L)$, the shearing stress at the wall of the capillary expressed in dyne/cm^2.

A survey of the flow behaviour is then obtained by drawing a curve — the flow rate curve — through the experimental points in a diagram in which log V is represented as a function of log P.

But for the differences mentioned below, the same device was adopted for observing the velocity of displacement of a drop of petroleum in a calibrated tube placed horizontally. Differences: a. only one capillary was used, and as a consequence a number of tubes of different diameters for the drops of petroleum; b. the viscometer was calibrated with a Newtonian liquid of known viscosity, from which measurement the radius R of the capillary (its length being known = 11.8 cm) was calculated (which value $R = 0.0542$ cm was needed for the calculation of the quantities V and P mentioned above).

The use of only one capillary, though not in every respect a happy choice [12]), made it possible to exclude, that the peculiar shape of the flow

---

11) W. PHILIPPOFF, Kolloid Z., **75**, 155 (1936).

12) It is of course not to be expected that with one capillary it will be possible to measure the rate of flow accurately in the large tract of P-values used.

At very high P-values and low viscosity the rate of flow of the oleate system is so great

rate curve, obtained with oleate systems containing KCl, was somehow connected with the succesive use of capillaries of different diameters. The curves obtained in b. made it further possible to control that in our viscometer the Newtonian calibrating liquids showed, indeed, a quite normal behaviour.

Fig. 6 gives in a log V vs log P diagram the flow rate curves of the two calibration liquids used (60 % sucrose at 15° and a mineral oil purchased

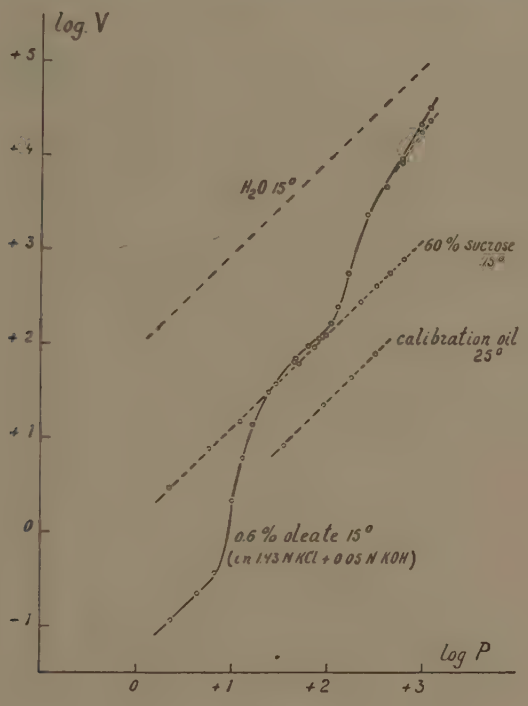

Fig. 6.

from and calibrated by the laboratory of the "Bataafsche Petroleum Maatschappij", Amsterdam [13]) and the flow rate curve of an approximately 0.6 % oleate system (containing 1.43 N KCl + 0.05 N KOH) at 15° C.

---

that the correction for the kinetic energy (HAGENBACH) had to be made (see note 14). At very low P-values the rate of flow of the oleate system is extremely small and a capillary tube had to be used for the drop of petroleum. The displacement of this latter drop (read off on the scale divisions of an eye piece micrometer) was observed in the telescope of a cathetometer. Certain difficulties, which seriously interfered with the accurate measurements of the rate of flow of very high viscous oleate systems, will be discussed in note 16.

[13]) The mineral oil had a kinematic viscosity of 4,424 Stokes at 25°. According to F. J. BATES and associates, Polarimetry, Saccharimetry and the Sugars, circular of the National Bureau of Standards, C 440, Washington 1942, see table p. 671, the 60 % sucrose solution must have a viscosity of 80,1 centipoises at 15°. The sucrose used was recrystallized and from the flow data obtained with the two calibration liquids, followed a viscosity of 79,6 ± 0.7 centipoises of the 60 % sucrose solution which agrees well with the value given above.

The curves (dotted ones) of the two calibration liquids, as is to be expected, are straight lines with a slope of practically 45°.

The curve for the oleate system, although presenting a similar course at low values of log P, considerably deviates with further increase of log P[14]). The shape of this curve, as we will see in the next communication of this series, is characteristic for the oleate systems containing KCl, which show marked elastic phenomena, although its position in the log V vs log P diagram still depends on a number of variables.

The typical flow behaviour is perhaps more conveniently represented by fig. 7, in which the abscissae are once more log P values, the ordinates, however, giving the values of log P—log V. The latter quantity has the meaning of the logarithm of a viscosity η (expressed in poises) at the given value of log P. These curves will therefore be called viscosity-shear stress curves.

We see from fig. 7 curve A that our 0.6 % oleate system behaves as a Newtonian liquid (log P—log V independent of log P) at low values of

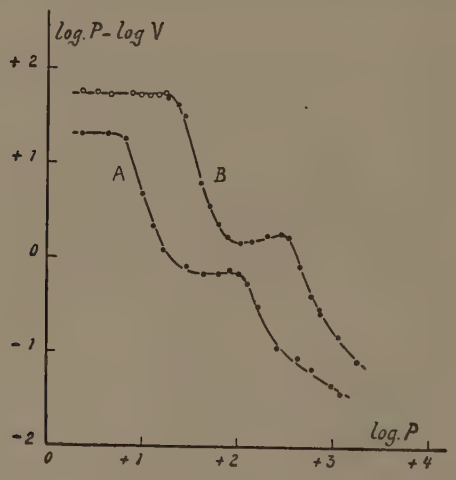

Fig. 7.

the shearing stress only. Obviously we have here the continuation of the simple flow behaviour we met in section 2, at much lower log P values.

The viscosity of the 0.6 % oleate system in fig. 7 in this range is of the order of 20 poises (log P—log $V = \pm 1.30$). However, with increasing log P values the viscosity decreases extremely strongly. At the highest P values investigated, its viscosity (of the order of 4 centipoises only) is still on its way downward.

It seems probable that at still higher log P values the viscosity-shear

---

14) Application of the correction of HAGENBACH had a visible influence on the course of the flow rate curve in fig. 6 at the three highest P-values used. These corrected values lie on the drawn curve, those that have not been corrected on the dotted curve.

stress curve will reach asymptotically an end value, which, according to PHILIPPOFF, may be denoted by η_∞. If we denote the highest horizontal level by η_0, the pecularity of our oleate systems containing KCl consists in the occurrence of an additional level [15]) situated between η_0 and η_∞. This level may be denoted by η_i (i = intermediate).

If it is permitted to interpret the viscosity-shear stress curve of the 0.6 % oleate system from the point of view of its structure, we obtain the following picture: At very low shearing stresses (0—0.07 dynes/cm^2, see section 2) there is a structure in the oleate fluid which allows a steady flow proportional to the shearing stress. This is still possible at slightly higher shearing stresses (the η_0 level in fig. 7) but above a certain value (in fig. 7 in the order of 8 dynes/cm^2) this structure breaks down in two steps. In the first step the "viscosity" decreases from approximately 20 poises to approximately 0.7 poises, in the second step, beginning in fig. 7 at approximately 100 dynes cm^2, it decreases to values which are only a few times larger than that of the corresponding KCl solution (order of 0.01 poise) without the oleate. It is further important to remark, that the two steep curve branches and the intermediate level of the viscosity curve are well defined. One may switch over to other P values situated far apart and into both directions without influencing the position of the flow rate curve. This means that if we spoke above of a structure in the oleate fluid, this structure is not one which breaks down irreversibly. On the contrary, the structure postulated is one which in accordance with the prevailing shearing stresses, practically immediately breaks down to or rebuilds itself to certain equilibrium states.

In this connection it seems of importance, that soaps belong to "Association Colloids" and it suggests that the very high viscosity at the η_0 level of rather diluted oleate systems is connected with large scale associations of the oleate molecules. Such associations in principle represent equilibria.

It might be supposed that these equilibria are influenced by sufficiently large shearing stresses and that the above mentioned "breaking down or rebuilding the structure" is connected with it.

Fig. 7, curve B, gives the results of measurements with an approximately 1.2 % oleate system at 15° C. The black dots represent measurements with the same viscometer used for the 0.6 % oleate system. At the low log P values the rate of flow of this far more viscous system becomes so small, that as a result of disturbances connected with the small radius of the capillary [16]), it became impossible to obtain reliable measurements.

---

[15]) A similar type of flow rate curve was found by PHILIPPOFF in 13,84 % Na-oleate solutions, containing NaOH and 1,62—7 % m-Kresol at 20°. See his book (quoted in note 2) on p. 279—280, fig. 162.

[16]) The entrapped air between the meniscus of the oleate system and the drop of petroleum in the capillary makes a sensitive air thermometer. Slight fluctuations in the temperature of the thermostate reflect themselves in an irregular displacement of the

That here too a η_0 level (analogous to that of the 0.6 % oleate system) is actually present [17]), follows from measurements (white dots) with a viscometer provided with a capillary of wider bore ($R = 0.1062$ cm).

Curve B shows the same general characteristics as curve A so that we need not discuss its form again. Increase of the oleate concentration has obviously two consequences, a. the values of the η levels become higher (for curve B $\eta_0 = \pm 52$ poises, $\eta_i = \pm 1.5$ poises, η_∞, not reached, lies below 0.08 poises), b. the values of the (max.) shearing stress at which "the structure breaks down" are greater (first step: order of 20 dynes/cm^2; second step: order of 300 dynes/cm^2) [18]).

Comparing the curves A and B more closely we perceive, however, a difference in the position of the intermediate η "level". In B the experimental points do not lie on a horizontal line, but on one that is slightly sloping upwards to the right.

We are here dealing with "shear rate thickening", the viscosity increasing ($\pm 1.3 \rightarrow 1.7$ poises) with increasing shearing stress. This might indicate, that the "residual structure" left after the first step downwards (from the η_0 niveau) is modified at further increase of the shearing stress in such a way that it offers more resistance to flow, before definitely breaking up (fall of the curve towards the η_∞ level).

This shear rate thickening at the intermediate "level" is obviously facilitated by an adequate concentration of the oleate, which point will be of importance for a theory on the internal state of our oleate systems.

In the next communication, in which another viscometer will be used, we will meet with more examples of this shear rate thickening and once

---

petroleum drop (standstills with time and occasional temporary changes in the direction of displacement occurred). This irregular movement of the drop does not reflect a property of the oleate system; indeed in section 2, where we used still lower shearing stresses, but observed the flow of the oleate system itself in the capillary, we always found completely steady flow. It is still possible to investigate highly viscous oleate systems with the petroleum drop method, but one must for that end follow the displacement of the drop for a long time. Yet such a determination may be wrong, if apart from the relatively fast fluctuations in temperature, there happens to occur a slow and slight displacement (e.g. a few 0.01°) of the mean temperature of the thermosatte during the single measurement. Therefore one ought to repeat such measurements many times, which would take many hours for the location of a single point on the η_0 level. It is easier to use a viscometer having a capillary of wider bore, which reduces the influence of the said disturbances on the measurements considerably (the quantity of fluid flowing through the capillary per second being proportional to the fourth power of the radius). The viscometer used to measure the η_0 level of the 1,2 % system is, however, not suited to measure the whole flow curve with it.

[17]) From the results of section 2 the occurrence of an η_0 level at low values of the shearing stresses was already certain (proportionality between rate of flow and shearing stress).

[18]) The approximately 0,6 and 1,2 % oleate systems used for these experiments are not wholly comparable in age and composition. It is therefore not allowed to compare them quantitatively, e.g. as regards the functional relation between η_0 and oleate concentration.

more we will find it clearly present at higher oleate concentrations (1.2 and 1.8 %) and absent at lower ones (0.6 and 0.3 %). This absence might of course be only apparent. as the method used is not accurate enough to detect a very slight shear rate thickening.

4. *Certain particularities of the oleate systems containing KCl explained by the shape of their flow curves.*

If we have a relatively large vessel (e.g. 1L) partially filled with an 1.2 % oleate system and try to pour out its contents, we have not the least difficulty in doing so. Certainly the fluid does not impress us as being extremely viscous. This is caused by sufficient shearing stresses being set up, so that the system does no longer behave as a fluid of $\pm$ 50 poises viscosity, but as one of materially lower viscosity. When the fluid is poured out, our working point is no longer on the η_0 level, but much lower.

In Part I (see section 12) we described the appearance of a dimple in the surface of the oleate system soon after excitation of the rotational oscillation. It is followed by a slight elevation of the surface, which may last some seconds (see fig. 6g and h in Part I). Now we can understand why this elevation may last several seconds. During the vigorous motion attending the formation of the dimple and its disappearance, the oleate fluid does not behave as a very high viscous system (too large shearing stresses).

A certain quantity of the oleate system is then brought above the horizontal level. As the large shearing stresses have meanwhile disappeared, a certain quantity of oleate system with the viscosity corresponding to the η_0 level, lies a fraction of a millimeter higher than the surrounding surface. So the shearing stresses which try to level out this elevation are very small, and therefore even its edge may remain visible for a couple of seconds, before it rounds off.

5. *Summary.*

1. The viscous behaviour of a few oleate systems containing KCl which showed marked elastic properties, has been investigated at 15°, with the techniques given by MICHAUD in the range of very small shearing stresses and by PHILIPPOFF in the range of larger shearing stresses.

2. In the domain of very small shearing stresses (shearing stresses at the wall of the capillary varying from 0—0.07 dynes/cm^2) the oleate system showed a steady rate of flow proportional to the shearing stress.

3. A yield value could not be demonstrated. Our elastic oleate systems, which at first sight may make the impression of gels, can for this reason be better characterised as elastic fluids.

4. In the domain of larger shearing stresses (order 1—1000 dynes/cm^2) flow rate curves were obtained, which show a very strong decrease in the viscosity (more than 500 times) in a two step process.

5. After the first step downwards (from the η_0 level) the viscosity retains over a certain range of shearing stresses, nearly the same value (the 0.6 % oleate system) or it increases slightly ("shear rate thickening; 1.2 % oleate system) before the second step downwards (towards the η_∞ level) sets in.

6. The sequence in which the shearing stress is varied does not change the position of the flow rate curve. If a structure is postulated in the original oleate system, which is broken down in a two step process, it must be one which, in accordance with the prevailing shearing stresses, allows a rapid and completely reversible rebuilding. In this connection some suggestions are made regarding the role of large scale associations of the oleate molecules.

7. A few particularities of the elastic oleate systems containing KCl described previously find an explanation from the shape of the flow rate curves.

Department of Medical Chemistry,
University of Leiden.

Biochemistry. — *Elastic viscous oleate systems containing KCl.* V [1]). *Viscous and elastic behaviour compared.* By H. G. BUNGENBERG DE JONG, H. J. VAN DEN BERG and L. J. DE HEER.

(Communicated at the meeting of March 26, 1949.)

Introduction.

According to MAXWELL's well known formula $\eta = G \times \lambda$, the product of the shear modulus G (in dynes/cm^2) and the relaxation time λ (in sec.) must have the meaning of a viscosity coefficient (in poises).

In this communication measurements of the elastic and of the viscous behaviour have been performed side by side at 15° to compare the product $G \times \lambda$ with the viscosity levels η_0, η_i and η_∞, which according to the results obtained in Part IV of this series, occur in the viscosity shearing stress diagram of markedly elastic fluids containing KCl.

2) *Methods used.*

Previous to measuring the flow behaviour each oleate system was investigated as to its elastic properties, for which purpose we used the rotational oscillation in completely filled spherical vessels of different radii. For particulars see Parts I, II and III of this series. The method used for obtaining a survey of the flow behaviour was in principle the same as in Part IV, in which only one capillary and a number of tubes of different diameters were used to observe the rate of displacement of a drop of petroleum.

In connection with this choice it was no longer necessary to keep the original shape of PHILIPPOFF's viscometer. The capillary and the other tubes, all of Jena glass, were therefore sealed together, and instead of the original spherical reservoirs of relatively small capacity, we used relatively wide cylindrical reservoirs (see fig. 1).

The difference in level of the oleate system (or of the calibration liquids) could be easily read off by means of a cathetometer at the beginning and the end of each separate measurement. This mean hydrostatic pressure added to or subtracted from the air pressure applied (read off on a H_2O or Hg-manometer) gave the pressure over the capillary. From this corrected pressure we calculated the value P, the (maximum) shearing stress at the wall of the capillary, for which purpose $\left(P = \frac{R \cdot p}{2L}\right)$ the length of the capillary ($L = 11{,}8$ cm) and its radius must be known. This

[1]) Part I has appeared in these Proceeding **51**, 1197 (1948), Parts II, III and IV in these Proceedings **52**, 15, 99, 363 (1949).

radius ($R = 0.0716$ cm) was calculated from the calibration of the viscometer with the same Newtonian liquids of known viscosity as were used in Part IV.

The other quantity necessary for the plotting of flow rate curves, V, the mean rate of flow, was calculated from the rate of displacement of the drop of petroleum by using the formula $V = 4Q/\pi R^3$.

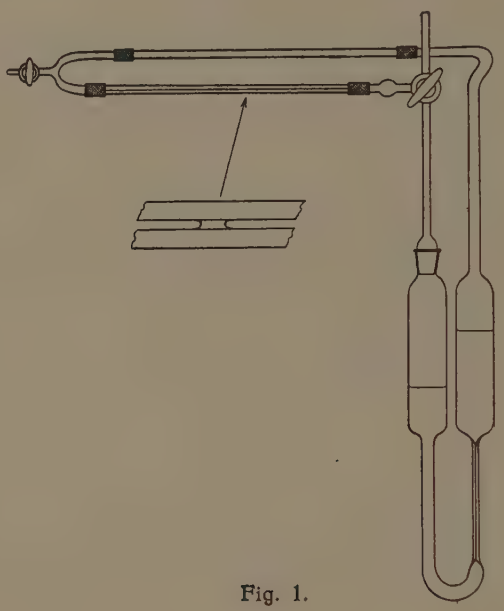

Fig. 1.

This time a wider radius of the capillary was chosen than in Part IV, as this diminishes the irregularities in the displacement of the drop of petroleum (cf. Part IV section 3, note 16), which do occur in the range of low shearing stresses with the very high viscous 1.2 and 1.8 % oleate systems. These irregularities could be further diminished by using in this range exclusively level differences between the oleate system in the cylindrical tubes and by closing the apparatus by a bent connecting tube as depicted in fig. 1. The drop of petroleum now separates two volumes of entrapped air (viz. between its own menisci and the menisci of the oleate system in the left and right reservoirs). Slight fluctuations in the temperature of the thermostate now effect slight variations in pressure on either side of the drop of petroleum which compensate one another partially. Although this device gave an improvement, nevertheless irregularities were still present, so that the measurements at low shearing stresses and very high viscosities showed a relatively bad reproducibility and the mean of a number of separate measurements may still embody a considerable error.

To check the conclusion in section 3, based on the results obtained with this viscometer, we will use in section 4 a technique by which the quantity of fluid flowing through the capillary is measured directly.

3) *Comparison of the values $G \cdot \lambda$ with η_0, η_i and η_∞.*

As in all the preceding parts of this series, we will also restrict ourselves in this section to a KCl (+ KOH) concentration, which at 15° C coincides or lies very near to the minimum damping of the elastic oscillations for the preparation of Na-oleate used (Na-oleinicum med. pur. pulver. Merck).

TABLE I.

Measurements of the rotational oscillation with 1.8, 1.2, 0.6 and 0.3 % oleate systems (containing 1.43 N KCl + 0.18 N KOH at 15° C).

Na oleate g/100 cc	R (cm)	n	$10 \times \frac{T}{2}$ (sec.)	Λ	$10 \times \frac{T}{2}$ corr.	λ (sec.)	G (dynes/cm²)	$G \times \lambda$ (poises)
1.8	7.46	50.0	5.41	0.193	5.41	2.80	99.8	263
	4.92	57.8	3.57	0.137	3.57	2.61 mean	99.7 mean	
	4.12	65.3	2.97	0.124	2.97	2.40 2.63	101.0 100.2	
	7.46	—	5.40	0.201	5.40	2.69	100.2	
1.2	7.46	35.3	8.44	0.348	8.43	2.42	41.1	97
	4.92	39.5	5.60	0.246	5.60	2.27 mean	40.6 mean	
	4.12	41.6	4.55	0.196	4.55	2.33 2.34	43.0 41.6	
0.6	7.46	18.8	18.09	0.755	17.96	—	9.06	—
	5.01	19.0	12.35	0.757	12.26	—	8.77 mean	
	4.12	19.1	10.03	0.763	9.96	—	8.98 8.94	
0.3	5.65	7.7	35.48	1.105	34.94	—	1.37	
	5.03	8.0	31.53	1.105	31.05	—	1.38 mean	
	4.12	8.4	24.48	1.112	24.11	—	1.53 1.42	
	3.18	9.0	20.75	1.105	20.44	—	1.27	
	1.70	9.4	10.03	1.109	9.88	—	1.55	

In a first series of measurements we investigated four oleate systems of different concentrations (1.8, 1.2, 0.6 and 0.3 g per 100 cc 1.43 N KCl + 0.18 N KOH). The results of the elastic measurements (rotational oscillation at 15° C) have been collected in Table I and represented in

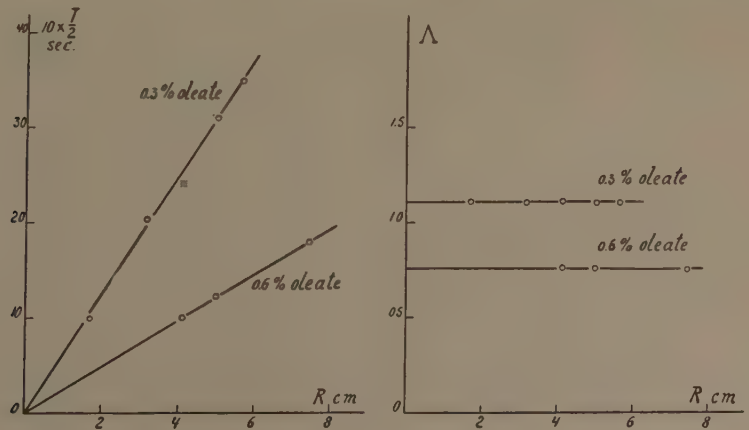

Fig. 2.

fig. 2 and 3. In accordance with the results obtained in Parts II and III of this series, we find that for oleate systems containing 0.3 and 0.6 g per 100 cc (see fig. 2 B) Λ is independent of the radius of the sphere and

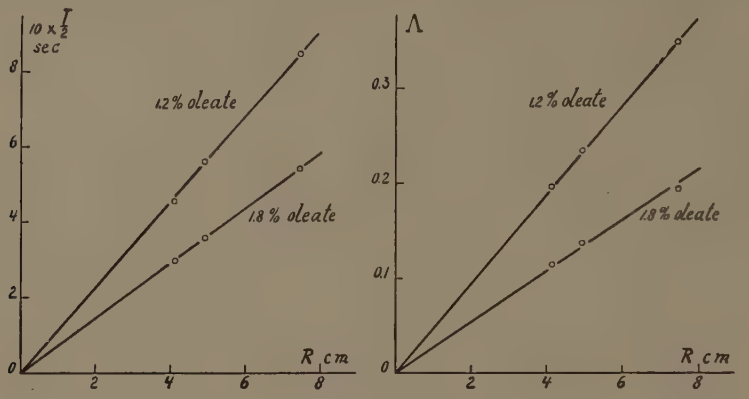

Fig. 3.

TABLE II.

Flow measurements at 15° C of the oleate systems of Table I.

1.8 g. oleate per 100 cc.			1.2 g. oleate per 100 cc.			0.6 g. oleate per 100 cc.			0.3 g. oleate per 100 cc.		
log V	log P	log P/V	log V	log P	log P/V	log V	log P	log P/V	log V	log P	log P/V
0.14—2	0.15	2.01	0.56 – 2	0.29	1.74	0.97—2	0.15	1.18	0.99—2	0.50—1	0.52
0.53—2	0.50	1.97	0.75—2	0.56	1.82	0.10—1	0.36	1.26	0.33—1	0.81—1	0.49
0.70—2	0.76	2.05	0.59—1	1.18	1.59	0.25—1	0.51	1.26	0.55—1	0.00	0.45
0.98—2	1.09	2.11	1.75	1.73	0.98—1	0.72—1	0.82	1.10	0.81—1	0.17	0.35
0.41—1	1.37	1.96	2.03	1.88	0.86—1	0.99	1.05	0.06	0.35	0.38	0.03
0.76—1	1.57	1.81	2.35	2.26	0.91—1	1.53	1.21	0.67—1	0.69	0.47	0.79—1
0.38	1.78	1.40	2.52	2.53	0.01	1.86	1.51	0.66—1	0.83	0.53	0.70—1
1.99	2.05	0.07	2.71	2.66	0.95—1	2.14	1.76	0.62—1	1.24	0.68	0.45—1
2.27	2.29	0.03	3.05	2.79	0.74—1	2.40	1.92	0.52—1	1.60	0.84	0.24—1
2.43	2.51	0.09	3.76	3.07	0.31—1*	2.53	2.06	0.53—1	1.88	1.00	0.12—1
2.51	2.65	0.15	4.24	3.31	0.07—1*	2.89	2.23	0.33—1	2.17	1.30	0.14—1
2.68	2.86	0.18				3.46	2.59	0.13—1*	2.62	1.67	0.05—1*
2.69	2.88	0.20				4.00	2.89	0.89—2*	3.15	1.96	0.81—2*
3.61	3.19	0.58—1*				4.66	3.36	0.70—2*	3.50	2.23	0.73—2*
4.18	3.43	0.25—1*							4.13	2.73	0.60—2*
$\log \eta_0 = 2.02$ (mean of first five values of log P/V)			$\log \eta_0 = 1.78$ (mean of first two values of log P/V)			$\log \eta_0 = 1.23$ (mean of first three values of log P/V)			$\log \eta_0 = 0.49$ (mean of first three values of log P/V)		
$\log \eta_i = 0.03 \rightarrow 0.20$ $\log \eta_\infty < 0.25—1$			$\log \eta_i = 0.86—1 \rightarrow 0.01$ $\log \eta_\infty < 0.07—1$			$\log \eta_i = 0.65—1$ (mean) $\log \eta_\infty < 0.70—2$			$\log \eta_i = 0.13—1$ (mean) $\log \eta_\infty < 0.60—2$		
$\eta_0 = 105$ poises $\eta_i = 1.1 \rightarrow 1.6$ poises $\eta_\infty < 0.18$ poises			$\eta_0 = 60$ poises $\eta_i = 0.7 \rightarrow 1.0$ poises $\eta_\infty < 0.12$ poises			$\eta_0 = 17$ poises $\eta_i = 0.45$ poises $\eta_\infty < 0.05$ poises			$\eta_0 = 3.1$ poises $\eta_i = 0.11$ poises $\eta_\infty < 0.04$ poises		

* After application of the correction of HAGENBACH.

that at higher oleate concentrations (1.2 and 1.8 g per 100 cc) Λ is proportional to this radius (see fig. 3 B).

In these two latter cases only the relaxation time λ and consequently a value $\eta = G \cdot \lambda$ can be calculated. Though for the purpose of comparing $G \cdot \lambda$ with η_0, η_i and η_∞ it would suffice to measure the viscous behaviour of the 1.2 and 1.8 % oleate systems only, we have investigated the 0.3 and 0.6 % systems as well, in order to gain some insight into the flow behaviour as a function of the oleate concentration. The results have been given in Table II and represented in fig. 4 A and 7 A.

Fig. 4 A.

Fig. 4 B.

A second series of measurements was started from the 1.2 % oleate system (which served as a blank) to which small amounts of n.hexylalcohol were added. The results of the elastic measurements (rotational oscillation at 15° C) have been collected in Table III and represented in fig. 5 and 6.

It was found that the addition of hexylalcohol in the two concentrations which still permitted elastic measurements, does not change the proportionality between Λ and the radius of the spherical vessel. Therefore λ values and consequently $\eta = G \cdot \lambda$ values could be calculated. For the third concentration of hexylalcohol elastic measurements were no longer possible. It was nevertheless interesting to include also this latter oleate

TABLE III.

Measurements of the rotational oscillation with 1.2 % oleate systems (1.43 N KCl + 0.18 N KOH) containing n. Hexylalcohol at 15° C. (For blank see Table I.)

n. Hexylalcohol mol/L	R (cm)	n	$10\times\frac{T}{2}$ (sec.)	Λ	$10\times\frac{T}{2}$ corr.	λ (sec.)		G (dynes/cm^2)		$G\times\lambda$ (poises)
0.00063	7.46	33.6	8.12	0.459	8.09	1.76	mean 1.64	44.6	mean 43.5	71.2
	5.04	34.7	5.45	0.337	5.44	1.61		45.1		
	4.12	38.1	4.44	0.288	4.44	1.54		45.2		
	3.18	39.4	3.70	0.224	3.70	1.65		38.9 (?)		
0.00188	7.46	10.2	7.68	1.528	7.46	0.49	mean 0.50	52.5	mean 5.21	25.9
	4.92	13.7	4.95	1.026	4.89	0.48		53.1		
	4.12	17.2	4.22	0.804	4.19	0.52		50.7		

system in our investigations of the viscous behaviour. The results of these measurements have been collected in Table IV and represented in fig. 4 B and 7 B.

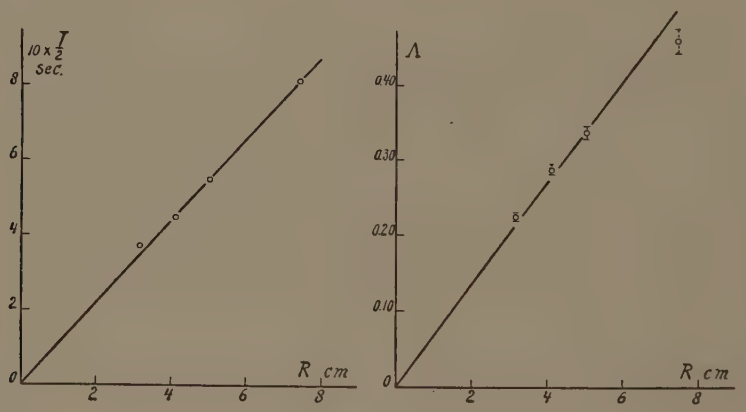

Fig. 5.

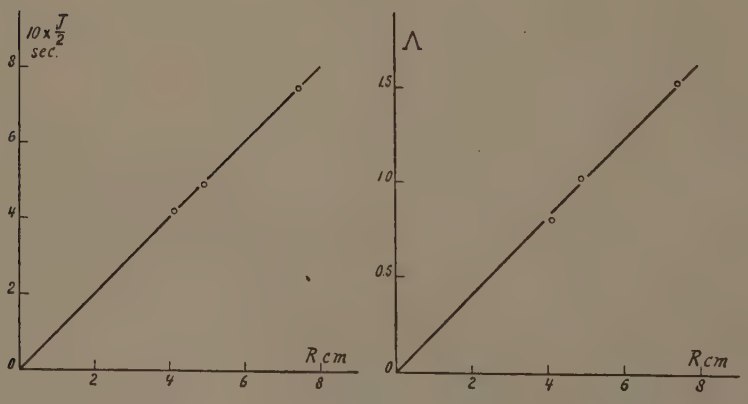

Fig. 6.

In discussing the results of the above two series of measurements we will first say a few words on the viscous behaviour. The flow rate curves of fig. 4 A and 4 B (log V as a function of log P) and the viscosity-

TABLE IV.

Flow measurements at 15° C of 1.2% oleate systems containing various concentrations of n Hexylalcohol..

0.00063 mol/L hexylalcohol			0.00188 mol/L hexylalcohol			0.00327 mol/L hexylalcohol		
log V	log P	log P/V	log V	log P	log P/V	log V	log P	log P/V
0.86—2	0.53	1.67	0.03—1	0.41	1.38	0.26—1	0.97—1	0.71
0.15—1	0.87	1.72	0.38—1	0.68	1.31	0.74—1	0.32	0.58
0.62—1	1.11	1.50	0.57—1	0.81	1.24	0.17	0.59	0.42
0.52	1.40	0.88	0.91—1	1.09	1.19	0.55	0.86	0.31
1.94	1.72	0.78—1	1.47	1.44	0.97—1	1.36	1.22	0.86—1
2.25	1.92	0.67—1	2.24	1.66	0.42—1	2.14	1.51	0.37—1
2.43	2.12	0.69—1	2.82	1.95	0.14—1	2.72	1.76	0.03—1
2.68	2.42	0.74—1	3.01	2.22	0.21—1	3.25	2.07	0.82—2*
2.97	2.71	0.75—1	3.35	2.58	0.22—1	3.65	2.39	0.74—2*
3.49	2.93	0.45—1*	3.69	2.89	0.20—1*	4.01	2.68	0.67—2*
4.19	3.26	0.07—1*	4.19	3.21	0.01—1*	4.46	3.06	0.61—2*
			4.60	3.38	0.78—2*			
$\log \eta_0 = 1.70$ (mean of first two values of log P/V)			$\log \eta_0 = 1.35$ (mean of first two values of log P/V)			$\log \eta_0 > 0.71$		
$\log \eta_i = 0.66—1 \rightarrow 0.75—1$			$\log \eta_i = 0.14—1 \rightarrow 0.22—1$			η_i level degenerated		
$\log \eta_\infty < 0.07—1$			$\log \eta_\infty < 0.78—2$			$\log \eta_\infty < 0.61—2$		
$\eta_0 = 50$ poises			$\eta_0 = 22$ poises			$\eta_0 > 5$ poises		
$\eta_i = 0.46 \rightarrow 0.56$ poises			$\eta_i = 0.14 \rightarrow 0.17$ poises			η_i = level degenerated		
$\eta_\infty < 0.12$ poises			$\eta_\infty < 0.06$ poises			$\eta_\infty < 0.04$ poises		

* After application of the correction of HAGENBACH.

shear stress curves of fig. 7 A and 7 B (log V—log P as a function of log P) show with one exception (the lowest curve in fig. 7 B) the same characteristics viz. η_0 level, a tendency to reach an η_∞ level and the presence of an intermediate "level", η_i, the experimental points on it lying either on a practically horizontal line or on lines that are sloping upwards to the right: shear rate thickening (as the corresponding curves in Part IV of this series, cf. fig. 7 in that publication). These characteristics were already discussed in Part IV, so that we need not discuss them again.

It is remarkable that the curve deviating from this typical curve form, (at its lowest in fig. 7 B) belongs to an oleate system, the elastic properties of which could not be measured on account of the exceedingly great damping of the oscillations (at most only two turning points were present). The viscosity-shear stress curve characteristic of the markedly elastic oleate systems (marked on account of smaller damping) has now degenerated to one in which an η_i level is no longer present and it already strongly resembles the curve form found in many cases of non Newtonian viscosity, in which there are only two levels (η_0 and η_∞).

We might further draw attention to a similarity on the one hand and a difference on the other between the influences of lowering the oleate concentration and of adding n. hexylalcohol at a constant oleate concentration. Comparing fig. 7 A with fig. 7 B we see in both cases that the viscosity-shear stress curve as a whole is displaced downwards. In lowering

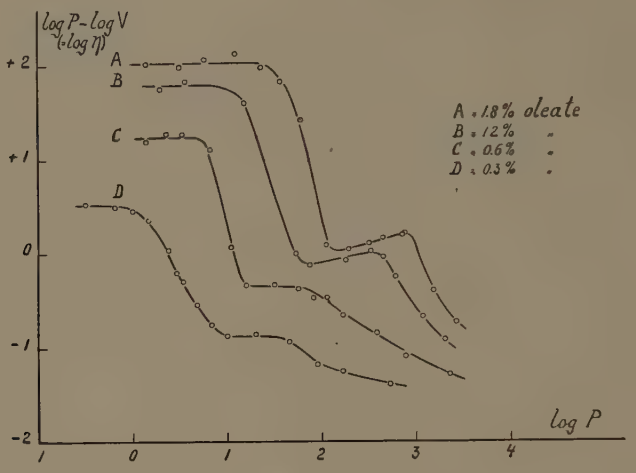

Fig. 7 A.

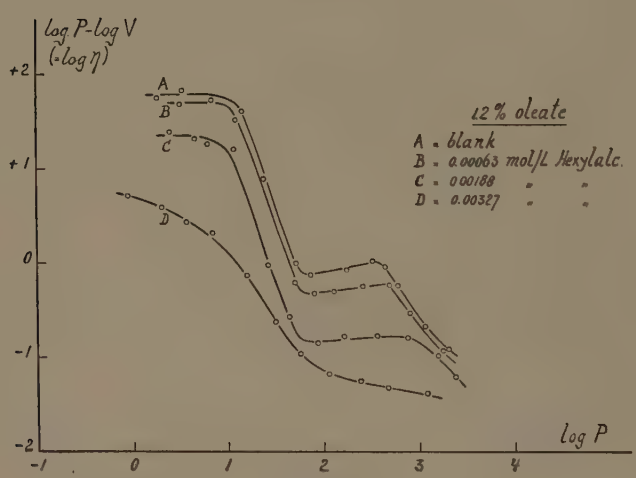

Fig. 7 B.

the oleate concentration, see fig. 7 A, the viscosity-shear stress curve is at the same time displaced to the left in a highly marked way. When adding hexylalcohol at a constant oleate concentration this displacement is absent, however.

We have now come to the comparison of the values $G \cdot \lambda$ with η_0, η_i and η_∞, and refer to Table V, in which we have collected the numerical values of these quantities for the four oleate systems in which this comparison is possible.

We perceive from this Table that the product $G \cdot \lambda$ does not coincide with any of the three η levels observed. The product is extremely different from η_∞, still very different from η_l, but it is of the same order of magnitude as η_0.

TABLE V.

Comparisson of $G \times \lambda$ with η_0, η_l and η_∞

Composition		$G \times \lambda$	η_0	η_l	η_∞
Oleate (g. per 100 cc)	Hexylalcohol (mol. L)	(poises)	(poises)	(poises)	(poises)
1.8	—	263	105	1.1 → 1.6	< 0.18
1.2	—	97	60	0.7 → 1.0	< 0.12
1.2	0.00063	71	50	0.46 → 0.56	< 0.12
1.2	0.00188	26	22	0.14 → 0.17	< 0.06

4) *The discrepancy between the values found for η_0 and for $G \cdot \lambda$.*

The same order of magnitude of the values found for η_0 and $G \cdot \lambda$ gives rise to the question if these values are really equal and if only experimental errors cause the discrepancy formed.

The difficulties we met with in measuring high η_0 values at low shearing stresses, and the discussion of these difficulties [2]) made us much more suspicious regarding the reliability of the average η_0 values than regarding that of the average G or λ values.

We decided therefore to compare a new $G \cdot \lambda$ with η_0, the η_0 value no longer being obtained with the aid of the petroleum drop method, but by directly measuring the quantity of the oleate fluid flown through the capillary of the viscometer. The latter was of the type as depicted in fig. 1 and the measurements consisted in reading at stated intervals the position of the levels of the oleate fluid in the equally wide reservoirs, (which were in direct communication with the air) with the aid of a cathetometer. A larger radius of the capillary [3]) ($R = 0.1062$ cm, $L = 12.1$ cm) was taken and a smaller diameter of the cylindrical reservoirs ($= 1.773$ cm) to reduce the time which the measurements still required (the series of seven given in the table below took two whole days).

From the effective hydrostatic height [4]) $\left(\triangle h / ln \frac{h_1}{h_2} \right)$, the density of the oleate fluid, the change in position of the levels during the time elapsed, the dimensions of the capillary and the diameter of the reservoirs the viscosity was calculated with the aid of POISEUILLE's formula.

This method gave satisfactory results only if, after filling the apparatus and bringing about an initial level difference one does not start with the

2) See section 2 and in Part IV section 3, note 16.

3) The radius of the capillary was calculated from flow measurements with the same calibration liquids as were used in Part IV.

4) See E. HATSCHEK, Die Viskosität der Flüssigkeiten, Dresden 1929.

measurements immediately, but checks the flow of the oleate fluid for several hours by means of a counter air pressure (to give the walls of the cylindrical reservoirs time to drain) [5]). The counter pressure is then removed and some hours later one begins with the measurements.

The apparatus functions well if after the intermission between two level readings, the level has risen in one reservoir quite as much as it has fallen in the other.

As we had no more Na oleinicum "Merck" in stock and it could not be purchased either, we used Na oleate, neutral powder, "Baker" [6]) for the renewed comparison of $G \cdot \lambda$ and η_0 at 15° C. The composition of the system investigated was 1.2 g oleate per 100 cc (1.25 N KCl + 0.05 N KOH) [7]). Table VI contains the η_0 values obtained by the above method

TABLE VI.

Measurements of the viscosity of 1.2% oleate system (oleate "Baker" in 1.25 N KCl + 0.05 N KOH) at 15° C.

Mean P (dynes/cm^2)	32.10	27.97	23.98	23.26	17.82	14.56
η (poises)	68.2	76.0	74.9	77.9	76.6	74.7

η_0 mean = 76.0 poises

at a number of (mean) shearing stresses at the wall of the capillary [8]). One perceives that compared with the large fluctuations of the log η_0 values in the Tables I and II the fluctuation of η_0 is small now, so that we may trust its mean value much better. Table VII gives the results

TABLE VII.

Measurements of the rotational oscillation of 1.2% oleate system (Oleate "Baker" in 1.25 N KCl + 0.05 N KOH) at 15° C.

R (cm)	n	$10 \times \frac{T}{2}$ (sec)	b_1/b_3	Λ	λ (sec)	G (dynes/cm^2)	$G \times \lambda$ (poises)
2.98	60.3	3.13	1.118	0.112	2.79	46.6	
4.99	63.5	5.21	1.198	0.181	2.88 mean	47.1 mean	
7.16	68.0	7.40	1.291	0.255	2.90 **2.87**	48.1 **46.6**	**134**
4.99*	61.2 ± 0.2	5.35 ± 0.03	1.202 ± 0.0034	0.184 ± 0.003	2.91	44.7	

* Measurement several days later during the flow experiments. From this single measurement would follow $G \cdot \lambda = 130$ poises. One is however not sure to conclude from a single measurement to a real decrease of $G \cdot \lambda$ with time.

[5]) Cf. in Part IV section 2, notes 8 and 10 from which follows the necessity of taking a long time for this drainage.

[6]) We are glad to express our profound gratitude to the Rockefeller Foundation, which kindly put at our disposal a large quantity of KCl and of the preparation mentioned in the text in order to enable us to continue our researches on oleate systems.

[7]) The KCl (+ KOH) concentration at which the damping of the elastic oscillations is a minimum lies lower than for the oleate preparation of MERCK. It was recently ascertained that it lay even a little lower than the concentration mentioned in the text, which lies still close to this minimum.

[8]) In the execution of these measurements we were assisted by W. W. H. WEIJZEN and W. A. LOEVEN, to whom we also wish to express our thanks here.

obtained in the investigation on the rotation oscillation (see also fig. 8). When we compare now the mean η_0 value ($=$ 76 poises) with the mean $G \cdot \lambda$ value ($=$ 134 poises) we still come to the same result as in the preceding section: η_0 is not equal to, but smaller than $G \cdot \lambda$, though both are of the same order of magnitude.

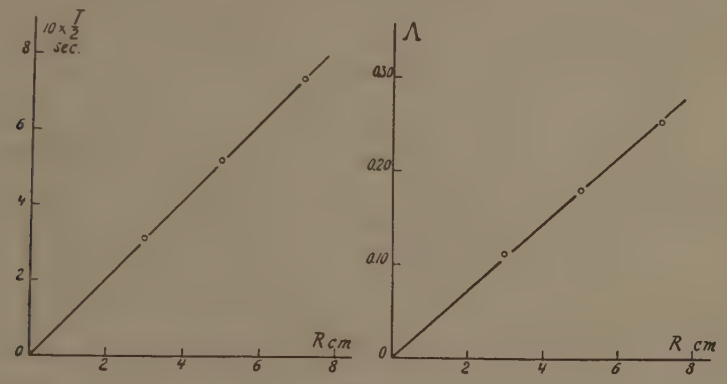

Fig. 8.

We could leave it at this general conclusion, but it is interesting that there appears to be a system in the disagreement between the two values. See the following survey. (Table VIII), giving the five cases in which η_0 and $G \cdot \lambda$ could be compared, arranged in the order of decreasing η_0.

TABLE VIII.

Concentration Oleate	n. Hexylalc. Mol/L	η_0 (mean) (poises)	$G \cdot \lambda$ (mean) (poises)	$\eta_0 / G \cdot \lambda$
1.8 % (MERCK)	—	105	263	0.40
1.2 % (BAKER)	—	76	134	0.57
1.2 % (MERCK)	—	60	97	0.62
1.2 % (MERCK)	0.0006	50	71	0.70
1.2 % (MERCK)	0.0018	22	25.9	0.85

We see from column 5 that the disagreement between η_0 and $G \cdot \lambda$ decreases with a decreasing value of η_0. Cf. fig. 9, which gives $\eta_0 / G \cdot \lambda$ as a function of η_0 and which shows that the experimental points fairly coincide with a curve drawn through $\eta_0 / G \cdot \lambda = 1$ at $\eta_0 =$ zero. This might mean that MAXWELL's relation $\text{L} = G \cdot \lambda$ in principle holds good, but that certain unknown systematic errors [9]) in the experimental methods we used for determining G or λ or η, distort this equality and the more so as the absolute values of these quantities are higher. But it might also mean that the equation representing the connection between η, G and λ for our

[9]) The fear of any occurence of a systematic error in the mean η_0 values obtained in section 3 has been considerably diminished by the fact that the experimental point obtained in this section with a quite different viscosimetric technique lies on the same curve as the other experimental points (see fig. 9).

systems is really of a more complicated nature and approximates to $\eta = G \cdot \lambda$ at low values of these quantities.

Be that as it may, the same order of magnitude found for $G \cdot \lambda$ and for η_0 seems to indicate that the mechanism of viscous flow in the range of small shearing stresses is mainly due to relaxation of elastic stresses.

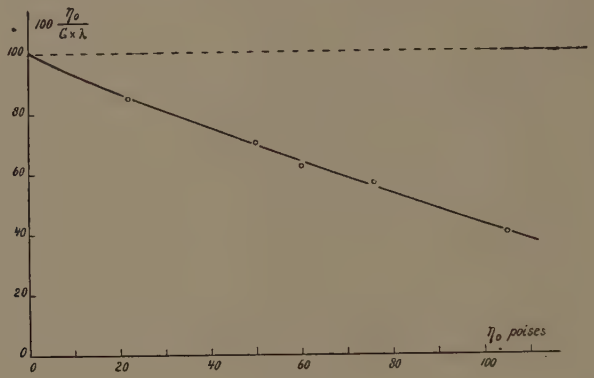

Fig. 9.

Summary.

1) The viscous and the elastic behaviour of a number of oleate systems containing KCl have been investigated at 15° C side by side to compare the viscosity coefficient calculated from elastic measurements ($\eta = G \cdot \lambda$, MAXWELL) with the viscosity coefficients η_0, η_i and η_∞ manifesting themselves as levels in the viscosity-shearing stress diagram of the oleate systems.

2) It has been found, that both η_∞ and η_i are far smaller and of a quite different order than $G \cdot \lambda$, that η_0, however, the viscosity coefficient at low shearing stresses, is of the same order of magnitude as $G \cdot \lambda$.

3) The percentual difference between η_0 and $G \cdot \lambda$ (η_0 has always turned out to be smaller than $G \cdot \lambda$) decreases in a marked way with decreasing absolute value of these quantities.

4) This suggests that either still unknown systematic errors, which increase percentually with increasing values of G, λ or η_0, bring about this difference; or that a more complicated relation between G, λ and η is operative for the oleate fluid, which at small values of these quantities may practically be simplified to $\eta = G \cdot \lambda$.

Department of Medical Chemistry,
University of Leyden.

Geology. — *Tectonics of the Mt. Aigoual pluton in the southeastern Cevennes, France.* Part I. By D. DE WAARD. (Communicated by Prof. H. A. BROUWER.)

(Communicated at the meeting of March 26, 1949.)

1. *Introduction.*

In the summer of 1947 detailed tectonic field-work was carried out in the southeastern Cevennes of France. The purpose of the investigation was to tackle structural problems in the little-known granite massif near the Mt. Aigoual. This massif is shown in the southwerstern corner of sheet Alais of the French geological map, 1 : 80,000, as a red dot of granite stretching away to the north in slates. Mapping has been done in and around this granite dot (fig. 1) in a purely structural sense. The well-exposed country in this part of the Cevennes facilitated detailed study, though mapping proved to be hampered sometimes by glacial deposits, hillside waste and afforestation. Excellent exposures are provided by a large number of small rivers.

During the survey, the area of the red dot of granite on the geological map appeared to comprise a small batholith surrounded by a complicated pattern of granitic, porphyritic and dark coloured dikes in the slaty country rock. The large scale map at the back shows the geological units of the mapped area.

The author's thanks are due to Professor W. NIEUWENKAMP for helpful discussions and criticism in field and laboratory, to Mr. R. C. HEIM for valuable data and good companionship during the field-work and to Miss D. E. WISDEN, M.Sc., Southampton for assistance with the English.

The writer acknowledges the receipt of a Z.W.O. grant (Dutch Organization of Pure Sciences) which made possible some comparative studies in adjacent granite massifs of the Cevennes.

2. *Synopsis of literature.*

The Central Plateau is situated in the middle of France as a large isle of mainly metamorphic and crystalline rocks with a local cover of young volcanic material on its peneplained surface, surrounded by Mesozoic and Tertiary sediments (fig. 1).

The age of the metamorphic rocks has long been uncertain. The "Archean age" theory has been rejected since the discovery of Cambrian and Ordovician fossils. Precambrian rocks are still mentioned however. According to most authors, folding and metamorphism of the Palaeozoic geosynclinal strata has taken place in the Sudetic phase of the variscan orogeny. The tectonic units with metamorphic imbricate and nappe struc-

tures have been analysed especially by the studies of DEMAY (e.g. 1931b, 1934), summarized by VON GAERTNER (1937).

Also from this part of France granitization phenomena are extensively

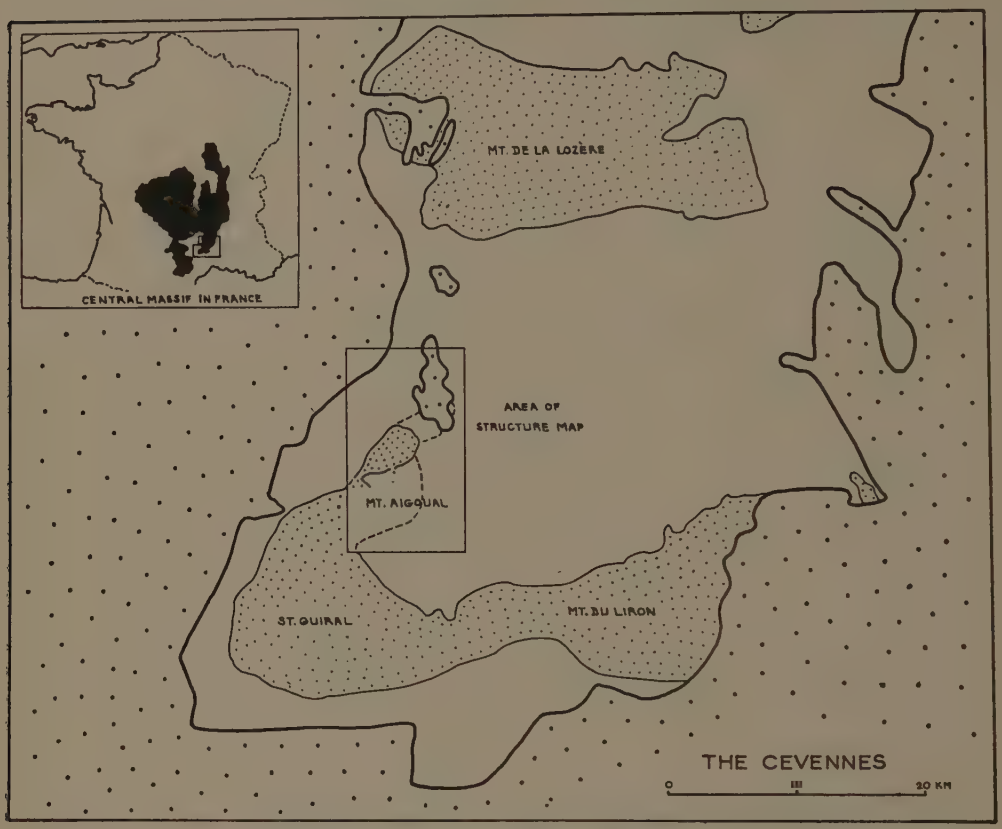

Fig. 1. Map of the southeastern part of the Central Massif showing the geographical position of the mapped area between slates (white) and adjoining granite massifs (dotted). The surrounding mesozoic strata are coarsely dotted.

described by French authors (e.g. DEMAY, 1935, 1942, RAGUIN, 1930, 1946, ROQUES, 1941). According to these publications the granite plutons in the Central Massif may be distinguished in 'pretectonic', 'syntectonic anatectic', 'synkinetic intrusive' and 'posttectonic intrusive' with respect to the Middle Carbonian orogeny. There seems to be no apparent relation between anatectic and intrusive granites. No rule could be laid down for the mode of occurrence, or for the texture of the posttectonic intrusive granites. Sometimes they are porphyritic, but syntectonic plutons too may have a similar texture (ROQUES, 1941, RAGUIN, 1946).

The Mt. Aigoual granite pluton, subject of this paper, is briefly mentioned in several French publications (e.g. BERGERON, 1889, 1904, DEMAY, 1931a). According to all authors it is a posttectonic intrusion, cutting the schistosity of the slates. A narrow metamorphic aureole is further evidence of its intrusive character. The texture of the granite is

described as homogeneous and porphyritic, with large crystals of orthoclase. Because of similarity in these properties, connections are postulated with the adjacent St. Guiral pluton. The Mt. Aigoual pluton is mentioned by DEMAY (1931a) as an apophyse of the much larger St. Guiral massif.

The first mapping of this area was achieved by FABRE and CAYEUX (1901) in sheet Alais of the geological map of France and for the second edition by THIÉRY (1923). Of the numerous granitic dikes north and south of the granite body only a few have been mapped separately in this sheet. Those nearer to the intrusive body are lumped together in one large granite outcrop extending southward as far as the St. Guiral massif.

The morphological study of BAULIG (1928) of the Central Plateau, as well as his maps, show many faults and fault-blocks. Two of these faults, continuing in one are drawn through the Mt. Aigoual granite. In the mapped area, however, little evidence for these faults could be found.

According to VON GAERTNER (1937) and based on DEMAY (1931a), the Mt. Aigoual region forms part of the Orthocevennes complex, a pennine nappe-like tectonic unit of the Central Massif. The granite of the Mt. Aigoual, together with the southern adjacent massif, is mentioned and drawn in section by VON GAERTNER as a late orogenic (posttectonic) intrusive sheet, flatlying in the cleavage plane of the slates.

3. *Geology.*

In the centre of the mapped area a small elliptical pluton of granite crops out surrounded by slates. The granite body, 5 km long and 2,5 km wide is very homogeneous; no endomorphism could be observed.

The granite is a light coloured, black and white rock of coarse grained texture with 10—15 cm long idiomorphic phenocrysts of orthoclase. Main components are quartz, orthoclase, plagioclase and biotite. Thanks to the granite-porphyritic texture, planar and linear flow structures could be measured nearly everywhere in the pluton. Joint systems occur usually in a variety of directions; only in few cases have slickensides been formed. Aplite, lamprophyre and quartz porphyry dikes have been observed inside the granite massif.

Nearly everywhere round the granite body results of contact metamorphism are visible. The contact plane is always sharp; its strike and dip vary locally.

The country rock farther away from the contact is in general slaty. According to DEMAY (1931a) a Cambrian age of the slates would be probable. The slates are not subdivided on sheet Alais of the geological map of France; on sheet Séverac, some kilometers west of the mapped area, a probable Potsdamian age is indicated.

Normally the slate is veined with white quartz. Though differing in quantity, usually numerous thin veins and lenses as well as small dikes to 40 cm wide occur. Intensely folded veins have been observed. They do not penetrate in joint systems or faults and very seldom in cleavage planes.

In several parts the slaty rock is a well-developed phyllite. Locally quartzite layers parallel to the schistosity of the slates are observed; elsewhere microscopical folds in bedded slates cross the cleavage planes. Spotted slates too are found in some places.

Usually the slates possess one or two systems of ribs on their cleavage planes. In the south of the mapped area they have minor folds with wave lengths between 10 and 100 cm. In this region they often pass into folded gneiss. Directions of ribs and fold axes as well as cleavage planes and joint systems in the country rock have been measured for structural purposes.

Dikes cut through the country rock round the pluton. Granitic dikes in large numbers present themselves as a fringe-like extension of the pluton. This edging has a limited extension at the northern and eastern side. Dikes are found much farther towards the south, but they are almost absent on the western pluton border.

Lamprophyre dikes occur in groups, mostly outside the edging of granitic dikes. They are often intruded along the cleavage planes of the slates. Their occurrence within the granite and in porphyry dikes prove them to be younger. More basic dike rocks have been observed.

Quartz porphyry dikes of light coloured material with phenocrysts of quartz and also of both quartz and orthoclase are observed between granite dikes and inside the granite pluton. They cross granitic dikes and are crossed by lamprophyre dikes.

Faults and faultzones, with and without drag, occur frequently in the mapped region. Faults cutting dikes have not been found. In one case drag is observed in the country rock at the contact with a granitic dike. Quartz veins always are disturbed by faulting; quartz does not occur within the fault fissures, only crushed in fault breccia.

The geological history in the mapped region according to the observed phenomena may be summarized in the following succession.

Sedimentation of strata probably in Cambrian time. Folding and metamorphism accompanied by exudation of quartz (according to most authors in the Middle Carbonian, Sudetic phase of the variscan orogeny). Development of schistosity and joint systems. Both segregation of quartz and jointing will be products of the same cause, the latter somewhat younger than the former. Intrusion of granite accompanied by contact metamorphism and intrusion of quartz porphyry, lamprophyre, aplite and pegmatite.

4. *Petrology and microtectonics.*

The microscopic compositions and microtectonic features of the mapped rocks will be mentioned here in brief. The petrology of the Mt. Aigoual area is discussed in a separate paper by HEIM (1949).

The granite of the pluton is a coarse-grained, light-coloured rock with up to 15 cm large twinned automorphic phenocrysts of white K-feldspar.

Main components are white K-feldspar, plagioclase, dark grey grains of quartz and many small black biotite crystals dispersed through the rock and in a dark rim around the large feldspars. Thin sections show Carlsbad-twinned orthoclase, much albite- and pericline-twinned oligoclase, brown biotite, quartz and occasionally hornblende. According to the mineralogical composition the rock may be classified in the granodioritic subdivision of the granites *sensu lato*. Quartz shows in general slight undulatory extinction.

In the field little difference could be observed between the granite in the pluton and in the dikes. The latter may show however some more variation in size of the smaller minerals between the large feldspars. Quartz too may thus have an automorphic habitus, giving the rock frequently a granite-porphyritic texture. In that case the quartz phenocrysts are corroded and rounded. Evidence of stronger dynamo metamorphism in the granite dikes is shown by wide-spread and strongly undulatory extinction of quartz and by bent and frayed biotite crystals. Sometimes recrystallised nonundulatory, suture-grained parts within quartz crystals do occur. The microscopic texture as a rule is lacking in orientation.

The quartz porphyry dikes contain a light-coloured, dense rock with many automorphic, dark-coloured quartz grains and irregularly distributed feldspar phenocrysts. The dikes are sharply jointed in small regular blocks. The rock is composed of quartz, orthoclase, biotite and albite phenocrysts in a dense, partly spherulitic or micrographic groundmass of mainly quartz and orthoclase. The quartz phenocrysts are largely corroded and rounded and sometimes show undulatory extinction.

Dikes of a dark quartz porphyry have been mapped within the granite body, near the contact of the pluton, cutting through granitic dikes and forming bordering zones of the latter. It is a dark rock of biotite and amphibole with quartz and plagioclase phenocrysts and a few K-feldspar phenocrysts. Under the microscope this rock proved to be a tonalite porphyry. Large rounded, corroded and undulatory quartz phenocrysts, zonal, Carlsbad-, albite- and pericline-twinned, corroded andesine, brown biotite, hornblende and occasionally orthoclase phenocrysts are enclosed in a fine-grained groundmass, often with fluidal texture, of andesine, biotite, hornblende and some quartz.

As mentioned above different types of basic rocks have been observed. They show difference in darkness, in quantity of feldspar and in size and orientation of biotite. Usually they are dark coloured, fine-grained, glittering rocks, largely composed of biotite and feldspar. In dike outcrops they often show rounded blocks caused by weathering along joints or they may be weathered all through into yellow-brown, spotted, sandy material. In some dikes the rock has an oriented texture, due to relatively large biotite crystals, being arranged parallel to the dike contacts.

Most dikes have kersantite-like composition; one consists of greenish-grey porphyrite.

The aplite dikes normally contain quartz, orthoclase and some biotite; no exceptional minerals have been found in the aplites, nor in the few pegmatite or runite dikes and veins.

The country rock is usually microfolded slate with quartz veins, phyllitic with sericite and recrystallised quartz, blastophyllitic with garnet and kyanite, and schistose to almost gneissic with sericite, muscovite, biotite, chlorite, quartz and some albite. In the narrow contact zone a fine grained gneiss is locally developed with orthoclase and plagioclase. Andalusite, sillimanite and cordierite also have been observed near the contact.

5. *Granite contacts.*

Many exposures allowed a detailed observation of the pluton borders. The western contact forms a nearly straight line in the plane of the structure map. Slates border the granite along a sharply defined contact plane which dips, at an angle of 70° to 55°, under the slate. This contact has all the aspects of a set of joints, a pre- or syn-intrusive joint system without doubt, because of the existing contact metamorphism in the slate. A narrow zone of slightly metamorphosed slates and phyllites borders the contact with penetrating veins of aplite and pegmatite. No offshoots such as granitic dikes are to be found on this side of the pluton.

Joint-like contact planes have been observed nearly everywhere around the pluton. The northern border is complicated by the branching off of many dikes. These offshoots, splitting apart euhedral blocks of slate, could be observed in detail. It has not been feasible however to reproduce these complications in the structure map; the curved lines merely represent a general outline of the granite body in these places. The northern contact planes show great variety of orientation; steep discordant and low angled often concordant contacts have been measured. Blocks of slates, surrounded by granite dikes could be observed.

Contact metamorphism in the north and northeast of the pluton may locally be stronger than near the western border, though more than one meter of the country rock has usually not been changed megascopically. The slates are transformed in these places in a fine-grained gneiss often veined or brecciated with aplite and occasionally with pegmatite. The slates and metamorphosed country rock near the contact show variations in strike and dip. Dips proved to be usually steeper and strikes are systematically bent to northeasterly direction.

Parts of the eastern and southeastern contacts are hidden by hillside waste. Where visible the same joint-like contact planes with shallow metamorphism, acid veins and offshoots of granitic dikes occur. Here too, strikes and dips of the slates change near the contact. The contact plane usually dips under the slates with varying angles.

On the map there are two gaps in the southern border. In the eastern one the contact loses itself under debris. In the western gap there has

been no occasion for mapping further south; it seems quite possible however that across this track a bottleneck may join up the Mt. Aigoual pluton with the St. Guiral massif. The southern contact too has little contact metamorphism. Gneiss and acid veins are observed; mostly there is hardly any change beyond a hardening of the country rock.

Though the contact may be clean and sharp as in the western border, complicated contacts have been found. In a river exposure of the northern contact the following details have been observed. The granite near the contact, being quite normal with dark inclusions and at most a little less large orthoclase crystals is bordered by a small tonalite porphyry dike of 20 cm followed by a quartz porphyry dike of 30 cm thickness with inclusions. Then, along the contact there is a kind of conglomerate zone, 25 cm thick with rounded pieces of granite and metamorphosed slate in a fine-grained crystalline matrix. On the outer side of the contact and parallel to it a second tonalite porphyry dike cuts the slightly metamorphosed and hardened slate. In the south an exposure is found with the succession of normal granite, a 3 m zone of somewhat darker granite, a 50 cm zone of granite, normal in colour but more crowded with large orthoclase crystals than usual, a 75 cm dike of tonalite porphyry in contact with hardened slate of which a slice of 5 m is cut off by a quartz porphyry dike running parallel with the contact.

Still less of metamorphism has been found near the contacts of the granite or granite porphyry dikes, though local differences occur.

The contacts of the granite massif, usually cross-cutting and occasionally concordant with the slaty cleavage and the slight but never missing contact metamorphism points undoubtly to an intrusive character of the granite. As a whole the pluton seems to be bordered by joint systems. They must have been developed before or during the intrusion. During the intrusion movement along these joint systems has taken place. The intrusion has been accompanied by an uplift of the country rock. This is proved by strike and dip alterations near the contact. Post-intrusive movements along contact planes cannot have been of much importance because of the uninterrupted zone of contact metamorphism.

The contact zone described above with rounded granite and gneissic pebbles in a fine-grained crystalline mass, points to intrusive movements along this plane by which parts of both sides of the contact were crushed, rounded and embedded in a fluidal mass, causing an intrusion bordering mylonite.

6. *Outline of tectonic phenomena.*

The main point of the investigations has been to collect tectonic data in order to work out the movements and origin of the granite pluton. A summary is given in the structure map at the back. The detailed mapping in a relatively small area, with heights between 800 and 1400 meters, made it desirable to have all data transposed in one horizontal plane of 1000

meter. Topographic distortion is eliminated in this way. The structure map shows as it were a hypothetical peneplain at 1000 m in this area. Most measurements have been made near this 1000 m plane.

A fairly close network of tectonic data has been collected in the granite massif. Special attention was given to fluidal phenomena and fracture systems in order to be able to reconstruct the intrusive movements. Slickensides and directions of dikes were likewise of much importance with regards to these movements. Marginal observations on contact planes and inclusions complete the network of structural data.

In the country rock many important tectonic features could be measured. Strike and dip of cleavage planes of the slates are disturbed near the contact as mentioned in the preceding paragraph. Joint systems, ribs and minor folds in the slates give details of pre-intrusive tectonics. Dike measurements will possibly reveal relations between pre-intrusive tectonics and intrusive movements. Faults with drag phenomena may be connected with block movements during the intrusion.

These tectonic data, plotted in equiareal diagrams, will be discussed systematically in the following paragraphs.

7. *Flow structures.*

Flow structures in the Mt. Aigoual granite are mainly marked by oriented orthoclase crystals and, in its marginal parts, also by small inclusions.

The orthoclase crystals are mostly tabular after (010) and elongated in the direction of the *c*-axis. Their orientation may be linear with parallelism of the *c*-axes or planar with parallelism of the (010) planes. Usually they are twins after the Carlsbad law, showing interrupted (001) cleavage on their narrow sides.

Primary flow phenomena in crystalline rocks may be divided into linear and planar structures. Ordinarily one of the two is predominant or exclusive in a massif. Only when there are suitable minerals can both these flow structures be seen. Feldspar is one of these, because of its elongated tabular shape. In the Mt. Aigoual granite planar structures are favoured for its feldspars are distinctly more tabular than columnar in shape.

In spite of the possibility of recognizing flow structures by measuring the directions of the phenocrysts, their orientation at a first glance seems to be chaotic in many places. Only a careful investigation of several surfaces of different orientation of the granite reveals a predominant arrangement. A judicious choice of the order in which the surfaces are investigated, e.g. horizontal planes first, followed by surfaces at right angles to it assists in deciding between linear and planar orientation. In the latter case a surface parallel to this plane of flow was selected in order to reveal any tendency to a linear arrangement within this plane. As a rule only after a prolonged scrutiny and with many measurements of generally existing, local directions on many different planes of the granite, could

the predominant orientation be detected. Thus the field observations do not consist of measurements of single feldspar crystals which could only give reliable information if a large number (e.g. 100) were treated at each locality, but of measuring predominant directions on fairly large surfaces of granite outcrops.

Parallelism of minerals is caused by differential motion in the intrusive mass. Consolidation preserved a record of the ultimate movements. Linear parallelism is originated by preponderant one-dimensional elongation of the mass. Stretching in one direction results in a parallel orientation of the longest axes, the *c*-axis of the feldspars, in that direction. Their (010) planes have arbitrary positions rotated about the *c*-axes (fig. 2b). If differential motion in the mass effects equal stretching in all directions within (shortening normal to) a plane, planar parallelism will develop.

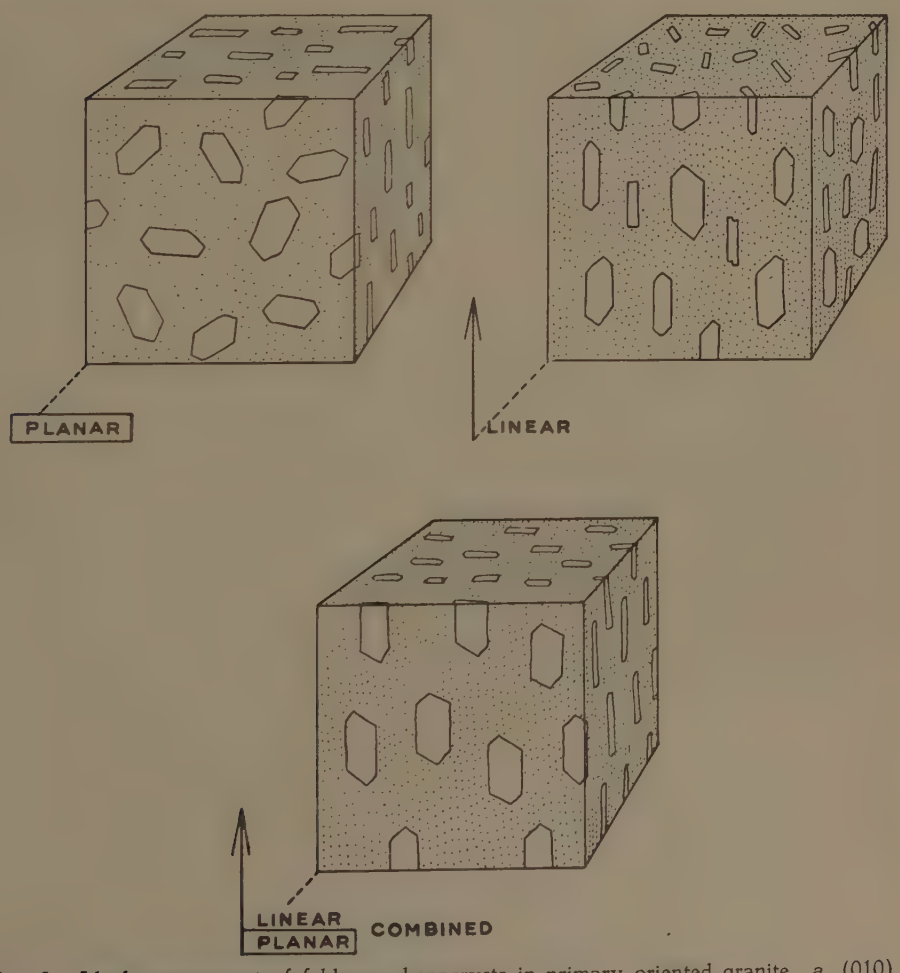

Fig. 2. Ideal arrangement of feldspar phenocrysts in primary oriented granite. *a.* (010) planes of feldspars in planar arrangement. *b.* c-axes of feldspar crystals in linear orientation. *c.* combination of linear flow structure by parallelism of c-axes and planar flow structure by platty arrangement of (010) planes.

Feldspars will tend to have (010) parallel to this plane, while their elongated *c*-axes show haphazard orientation (fig. 2a).

In the intermediate case, when planar structures are developed together with somewhat stronger stretching in a certain direction within this plane, both (010) planes are oriented in planar parallelism and *c*-axes in linear parallelism in the same plane (fig. 2c). Only locally are linear and planar orientation found associated; usually one of the two is predominant and the other weak or absent.

Because differential motion is strongest near the contacts of intrusions flow structures will be developed very well in their marginal parts. Conversely strongly oriented structures in the central part of the intrusion indicate that considerable differential movements also in these parts of the mass have existed. Usually these structures are planar. If linear parallelism exists too, strong one-dimensional stretching has been predominant. In parts of the intrusion where no planar structures are developed a weak linear orientation may be formed by distinct expansion of the pluton in a certain direction.

The movements of flow are very well determined if both planar and linear flow structures could be measured. Planar parallelism shows the plane along which flow has taken place and linear parallelism the direction of flow in that plane.

8. *Intrusive flow.*

The general aspect of the registered and interpolated flow data in the structure map of the pluton suggests comparison with a pan of boiling porridge. In at least three sections of this relatively small pluton upward culmination of flow is recorded.

This reconstruction is based on about 65 flow determinations. Construction of flow planes and lines is done by interpolation of the measured data in the least complicated way. These lines record in a nice manner the last movements of the intrusive mass before ultimate consolidation. The given interpolation is a reconstruction in the simplest way; in reality the flow structures may be much more complicated in detail.

West of the centre of the pluton a half concentric doming is made visible by flow phenomena. It has varying but mostly rather steep flow structures, planes as well as lines. The planar structure has conformable contacts with the westerly border, dips to the south against another, incompletely-known doming and continues to the E.N.E. To the north, structures are more complicated but presumably still conformable with the pluton contacts, continuing into dike offshoots. Conformable structures are also well-developed in granite dikes. Linear parallelism in north and west cross flow plane strikes nearly perpendicularly, indicating probably a strong upward flow. Near the top of the doming the lineation grows parallel with planar structures.

In the north-east of the pluton the continuation or easterly flank of the

doming is found. As far as observed it has identical conformable structures. Flow lines here may show stronger convergence in upward flow, also from northerly directions.

Flow structures in the south-east are different. They seem to be conformable to parts of the southern contact but disconformable to the easterly wall rock, representing a mass with parallel oriented planar structures, complicated by vertical and changing dip directions. They suggest a lacking or hidden part of the mass still S.E. of the southern pluton border.

These structures might have been caused by motion of a mass ascending from south-easterly direction; a northward motion which produces at the same time a drawing-out of the northern doming or elongation of the northern part of the pluton in S.W.—N.E. direction. Such an elongation may have originated the flow lines in that direction, which are bent in the central part of the pluton.

In the south-western part of the pluton a fragmentarily-known small doming is visible. The same parallel and steep flow lines as in the south-eastern section have been found in the south-western appendix or bottle-neck.

All together the flow structures in the pluton suggest an upward moving mass, converging from all directions, which was strongly affected by the ascending mass from the south, causing the elongation and bending out of the northern doming.

9. *Fracturing of granite.*

In the pluton joint systems are found in amazing quantity. Normally the Mt. Aigoual granite is fractured by about six different systems of joints in each locality. Up to twelve systems have been measured in some places. By fracturing the granite falls apart in different sized and irregular blocks, frequently parallelepipe and column shaped. In fresh rock, joint planes are hardly visible; in a few cases faint marks of dislocation are observed. The explanation of the existence of fracturing may be contraction during cooling of the granite, or continued motion within the pluton after consolidation of the upper shell, or a combination of both causes. In either case, however, the resulting fracture systems cannot be quite arbitrary, there certainly will be a relation with the fabric of the rock and the shape of the massif.

The connection of flow structures and some joint systems is advocated by HANS CLOOS, BALK and others. They make a distinction between e.g. cross joints perpendicular to flow lines and longitudinal joints parallel to them. Many joint systems could not be placed systematically by these authors.

In the case in question it proved always to be possible to find some of the six or twelve joint systems in regular association with flow structures. But there is nothing specific which marks the thus found "cross" or "longitudinal" joints; apart from their relations to flow structures nothing

may distinguish them from the other fractures. Most joints however cannot be explained with reference to these directions of use; they seem to be useless from tectonic point of view. In this case it would be a rather arbitrary application, to select and use "cross" joints, etc., according to recipe.

In the method here applied all measured joint data are used in a statistical diagram. This is done in order to bring out clearly the possible regularities of jointing in the pluton as a whole. Though it has proved, so far, not to be possible to arrange all existing joint systems according to structural or other principles, this of course in no way excludes the possibility of a systematic arrangement. There may be suggested here a systematic coincidence between the fracturing of the rock and its mechanical properties in different directions. Any alteration in equilibrium of the mass, e.g. during cooling, contraction, renewed motion etc., will thus cause systematic joint systems. They cannot all be explained locally, but they will relate as a whole to the fabric of rock and massif.

Measurements of joint systems have been made at regular intervals throughout the pluton outcrop. An average diagram of fracturing of the pluton may reveal special regularities in the structure of the massif. Projections of poles of all joint planes are plotted in an equal area net, thus giving a petrofabric analysis of the whole pluton as far as its joints are concerned. Fig. 3 shows the statistical pole diagram of 80 measured joint planes.

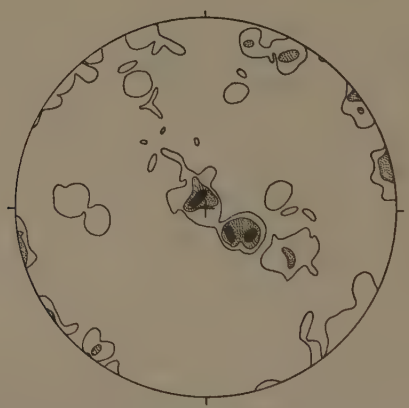

Fig. 3. Pole diagram of 80 joints throughout the pluton. Contours 5—4—2½ %
(Southern hemisphere as in fig. 5, 6, 7, 9 and 10.)

The first striking regularity is the evident symmetry of the diagram. The N 120 E. central line of the diagram shows the same density distribution at both sides. The direction of this symmetry plane harmonizes with shape and directions of flow structures of the pluton except for the south-western corner. Probably this symmetry in the diagram is connected with the predominant motion in the direction of the line of symmetry and with the mentioned probability of supply of granite mass from a south-easterly direction.

By further analysis of the diagram two girdles may be observed. They resemble *B*-tectonites or a cross girdle diagram in petrofabrics, one NW—SE and the other horizontal, crossing each other at right angles. This indicates an orientation of nearly all measured joints either parallel to a horizontal NE—SW axis or in a more or less vertical arrangement.

Because joints largely will be related to, or oriented as a result of the fabric of the rock, in this case the only visible variable viz. flow structures, this diagram may show an average orientation of joints associated with the average orientation of flow. A glance at the structure map shows a predominance of flow lines in NE—SW direction which may be associated here with domination of cross joints in the densest parts of the horizontal girdle viz. in the NE and SW of the diagram.

In the same way a relation does not seem accidental between the densest part of the vertical girdle in the middle and south-east of the middle of the diagram with the ascent of mass from a south-easterly direction. This densest part of the diagram indicates the nearly everywhere observed "bedding planes" or primary flat-lying joints throughout the pluton.

10. *Dikes and faults in the pluton.*

Besides numerous ordinary fractures described in the preceding paragraph, dikes and faults have been observed in the pluton. In this paragraph joints filled with aplite, lamprophyre and porphyry and faults with well-developed slickensides or with visible dislocation will be discussed. More than fractures they may be expected to furnish information about motion in the rigid or semirigid upper part of the pluton. These data are plotted in the structure map.

The discussion of these phenomena is hampered however, by their limited number. The pluton body proved to be relatively poor in aplite dikes. Three of them may be called of cross joint origin, two are along primary flat-lying joints, two others show affinity to longitudinal joints and the few remaining cannot be labelled according to flow structures and shape of the massif. It will be clear that use of this nomenclature has no practical value here for tectonic purposes because of the small quantity of data. The few measurements of lamprophyre and porphyry dikes cannot be used either.

Faults usually with striae could be observed clearly in the north-western sector of the pluton. They are plotted in tectonogram fig. 4. The diagram is composed of equiangular projections of: a fault zone striking N 37 E, dipping steeply W; the sharp bisectrix N 50 E, 7 S of a system of diagonal joints or faults, crossing each other nearly perpendicular (84°); horizontal striae in a fault zone striking N 45 E; and three sets of striae on different fault planes in one locality, striking in a north-western direction and dipping S. The last three fault systems with striae are likely to represent the result of the same direction of motion recorded on different planes in this locality; combined they may give the direction of the original

motion, viz. *S* (1.2.3.) in the diagram, striking N 38 E and dipping 25 SW.

These plotted data show remarkable conformity; they have uniform directions between N 35 E and N 50 E, with gentle dips, mostly to the

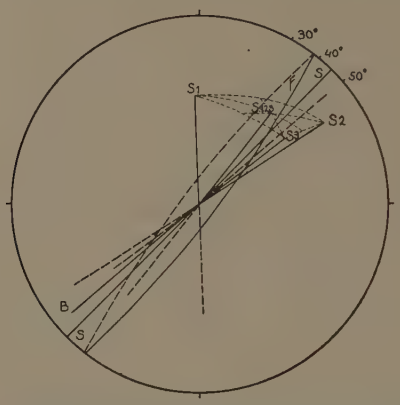

Fig. 4. Tectonogram of faulting and slickensiding in the north-eastern sector of the pluton. Equiangular projections of striae (*S*), the sharp bissectrix of diagonal joints (*B*) and a fault zone without striae (*F*). (Projections in the northern hemisphere.)

SW. Thus, motion is recorded in the rigid upper shell of the granite in SW—NE direction, slightly upward to the north-east.

In an earlier phase of the consolidation, motion in the same direction has taken place in the area north-west of the centre of the pluton. Two aplite dikes are several times broken and irregularly dislocated by sets of parallel steep faults, striking about N 40 E. Bent parts of the aplite dikes and fixing of the fault planes indicate a semirigid condition of the granite in which SW—NE motion has occurred.

The SW—NE motion thus found in the northern part of the massif may be interpreted as a result of differential expansion of the pluton in that direction during the last phases of the intrusion. Similar indications have been found by means of flow structures in earlier intrusive phases.

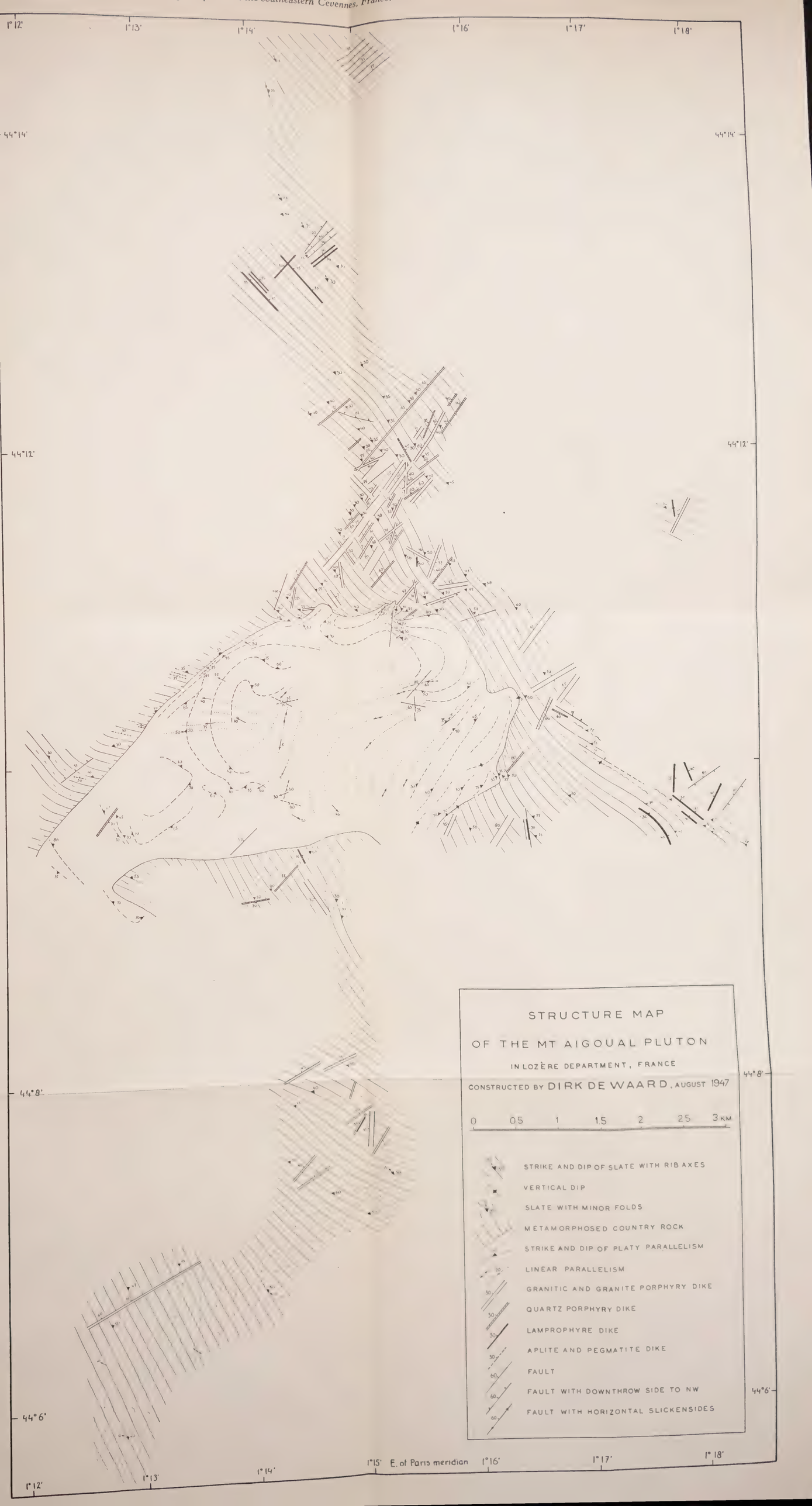
1°12'
1°13'
1°14'
1°15' E. of Paris meridian
1°16'
1°17'
1°18'
44°14'
44°12'
44°8'
44°6'
STRUCTURE MAP
OF THE MT AIGOUAL PLUTON
IN LOZÈRE DEPARTMENT, FRANCE
CONSTRUCTED BY DIRK DE WAARD, AUGUST 1947
0 0.5 1 1.5 2 2.5 3 KM
STRIKE AND DIP OF SLATE WITH RIB AXES
VERTICAL DIP
SLATE WITH MINOR FOLDS
METAMORPHOSED COUNTRY ROCK
STRIKE AND DIP OF PLATY PARALLELISM
LINEAR PARALLELISM
GRANITIC AND GRANITE PORPHYRY DIKE
QUARTZ PORPHYRY DIKE
LAMPROPHYRE DIKE
APLITE AND PEGMATITE DIKE
FAULT
FAULT WITH DOWNTHROW SIDE TO NW
FAULT WITH HORIZONTAL SLICKENSIDES

Anatomy. — *The digital formula in relation to age, sex and constitutional type.* I. By J. HUIZINGA. (Communicated by Prof. M. W. WOERDEMAN.)

(Communicated at the meeting of March 26, 1949.)

I. *Introduction.*

If we ask various persons to lay the pronated hand on a flat surface in such a way that the longitudinal axis of the hand is a prolongation of that of the forearm we shall find that:

1. The third finger ends the most distally.
2. The first finger ends the least distally.
3. The fifth finger follows the first in this respect.
4. Sometimes the second finger ends more distally than the fourth, sometimes the converse is true and sometimes these fingers are equal in length.

We may represent a given case as follows:

$$III > IV > II > V > I$$

This WOOD JONES (1944) terms the 'digital formula'.

If we confine ourselves to man, we find that the interindividual difference in digital formula consists in the varying relation between the fingers II and IV.

Although it is far from our intention to recommend memoirs such as those of CASANOVA as a source of scientific information, we feel justified in quoting CASANOVA's description of his conversation with the painter RAFAEL MENGS by way of introduction to our problem, the more so as it is our experience that the same dispute about the digital formula can be provoked in any group of people at the present day.

CASANOVA writes as follows (1871):

"Je me souviens qu'un jour je pris la liberté de lui faire observer, en voyant un de ses tableaux, que la main d'une certaine figure me paraissait manquée. En effet, le quatrième doigt était plus court que le second.

— Voila une plaisante observation, me dit-il, voyez ma main! et il l'étendit.

— Voyez la mienne, répondis je, je suis convaincu qu'elle ne diffère pas de celle des autres enfants d'Adam.

— De qui donc me faites vous descendre? répliqua-t-il.

— Ma foi! lui dis-je après avoir examiné sa dextre, je ne sais à quelle espèce vous rattachez, mais vous n'appartenez pas à la mienne.

— Alors votre espèce n'est pas l'humaine, car la forme manuelle de l'homme et de la femme est bien celle que voilà.

— Je parie 100 pistoles que vous vous trompez, lui dis-je. Furieux de mon défi, il jette palette et pinceaux, sonne ses gens, et leur fait à tous exhiber leurs mains; sa colère fut grandi quand il reconnut que chez tous le doigt annulaire était plus long que l'index. Cependant il voulut bien sentir le ridicule de sa conduite et termina la scène par cette plaisanterie:

— Je suis charmé du moins d'être unique en mon genre sur un certain point."

In 1875 ECKER, was the first anatomist-anthropologist to bring up the problem of the individually-differing prominence of the fingers. Since then numerous publications have appeared; these may be classified as follows on the basis of certain general principles:

1. Prominence and sexual dimorphism
2. Prominence and age
3. Prominence in the light of typology
4. Prominence in the light of racial differences
5. Prominence in the light of problems of evolution
6. Prominence differences between the two hands.
7. Discussion of the causation of differences in prominence.

No single author, however, has dealt with all these aspects at once; this is partly due to the lack of due insight into anthropologo-phenomenological problems. In some cases the contradictory nature of the statements made can be ascribed to the fact that the groups studied were non-comparable. For instance, data furnished by the study of a group of females aged 4 to 71 years, in the absence of any previous investigation of differences according to age, may well lead to premature conclusions about the phenomenon in women.

Although the population of the Netherlands can certainly not be regarded as racially homogenous (in addition to definite Nordic, Alpine and Mediterranean characteristics we also find Baltic and Dinaric features), analysis of our material from this point of view is vitiated by so many uncertainties of race-diagnosis that its results are not worth reporting.

The amount of anthropoid material available was so small that we do not feel justified in including it in our study.

To give some idea of the scope of the problem of prominence, a discussion of the points 1 to 7 mentioned above will precede the description of our own observations.

WOLOTZKOI (1924) devised a useful nomenclature and we shall follow him in speaking of hands of the *radial* type (Rd.) when the *index finger extends more distally* than the ring finger, and of hands of the *ulnar* type (Uln.) when the converse holds. The results of our own investigations

lead us to use the term transitional type (T.) for hands in which the index and ring fingers extend equally far distally. This nomenclature will also be used in discussion of the work of other authors.

II. *Survey of the literature.*

1. *Prominence and sexual dimorphism.*

ECKER, who was the first anthropologist to publish an article on this 'oscillating character in the hand of men' (1875), found 24 examples of the ulnar type and one of the T. type in 25 outlines of the hands of American negroes aged 19 to 65 years. In his group of negresses (age 4 to 71 years) he found 15 Uln., 6 Rd. and one T.

With a total absence of criticism as to the age-composition of his groups (note the women) he concludes that there is an unmistakable sex difference: Rd. occurs more in women than in men. From a group of Europeans (composition unknown) he drew the same conclusions, although with some reservations.

The data reported by MANTEGAZZA (1877) (ages not stated) make it possible to calculate 75 % Uln. for 258 Italian women and 92 % Uln. for 336 Italian men. In these groups of individuals examined by him, only Rd. or Uln. is found. Thus the Uln. type predominates in both sexes, as found by ECKER (1875).

PFITZNER (1893) found just the contrary for skeleton hands of adult Alsatians: 70 % of 175 male hands were of the Rd. type and 79 % of 90 female hands, while RUGGLES (1930) and BAKER (1888) found in white Americans that more Uln. types on the whole occurred among men and more Rd. types among women.

WEISSENBERG (1895) is more inclined to agree with MANTEGAZZA; he found more Rd. in women than in men but the the percentage of Rd. was always below 50 %, so that Uln. predominated in both sexes.

The next publication on sex differences in the digital formula did not appear until 1924 (WOLOTZKOI): in adult Russians Rd. was found in 62 % of 190 men and 77 % of 159 women. For adult Russian Jews the figures are 59 % Rd. in 29 men and 62 % Rd. in 58 women. These figures agree with those of PFITZNER (1893).

WOLOTZKOI then draws the inaccurate conclusion 'that the radial form is a special property of the female hand'.

RUGGLES (1930) concluded from a study of 402 male and 218 female 'white adults' that 'In white adults the ring finger in males is generally longer than the index finger and in females the reverse is found', a conclusion which he (*wrongly*) believes to be identical with those of PFITZNER, ECKER and MANTEGAZZA and contradictory to those of SCHULTZ (1924) and WOOD JONES, neither of whom, however, (the latter at any rate not in his book published in 1944) makes any mention of sexual dimorphism in a comparative sense. As we have not been able to obtain

a copy of the publication of BAKER (1888), we are doubtful as to what RUGGLES describes as BAKER's results (see above).

WECHSLER (1939) found more Uln. types in men than in women.

A number of the older anatomists (e.g. GEGENBAUER (1885), KOLLMANN (1886) believed Rd. to occur more in women than in men, although they did not give quantitative expression to this. The more frequent occurrence of Rd. in women together with the greater beauty of form (in the opinion of many) of the female hand, led various investigators to study the way in which artists depict the hands of their models. ECKER (1875) makes the following pronouncement: ... 'wherever a great artist has endeavoured, whether instinctively or consciously, to depict a hand of perfect beauty ..... he certainly never makes the index finger appreciably shorter than the ring finger as this formation definitely gives the stamp of a lower type'.

WEISSENBERG (1895) did not confirm this in his study of Egyptian and Assyrian art. However, we shall confine ourselves to the mere outline of this aspect of the problem. Summing-up we may remark that the literature fails to provide us with unequivocal information on the sex differences in the digital formula. We shall return to this question in connection with our own investigations.

2. *Prominence and age.*

Much less has been written about the connection between relative length of fingers and age than about the difference between the sexes in this respect. We have already seen how ECKER (1875) put females aged 4 to 71 years in a single group labelled 'women' and then came to the conclusion that there was an unmistakable difference between the sexes.

WEISSENBERG (1895) classified his 574 male Jews according to age as well as sex. For the right hand he gives:

	5-10 yr.		11-20 yr.		21-30 yr.		31 yr. and older	
Rd.	30	45.5%	57	18.9%	29	23.6%	21	25.0%
Uln.	34	51.5%	222	73.8%	86	69.9%	59	70.2%
T.	2	3.0%	22	7.3%	8	6.5%	4	4.8%

From this it follows that boys from 5 to 10 years of age show the Rd type more frequently (45 %) than older boys (25 % for age about 20 yr.). Although the proportion of Rd types is higher between the ages of 5 and 10, WEISSENBERG's data show it to remain still below 50 %. He also remarks 'both types of hand may be found even in new-born infants'.

WOLOTZKOI (1924) arranged his Russian and Jewish men and women in age-groups as proposed by STRATZ (1903). In the periods from 1 to 4 and 8 to 10 years growth in breadth is regarded as predominating over that in height (first and second filling-out periods; turgor primus et turgor secundus), while those of 5 to 7 and 11 to 14 years correspond to relatively

greater increase in height (first and second periods of extension; proceritas prima et secunda). Then follows the maturation period from 15 to 20 years.

In order to facilitate comparison with our own findings we give WOLOTZKOI's figures in full:

Russians.

age-groups	Males				Females			
	number	%/%/% Rd.	%/%/% Uln.	%/%/% *T*	number	%/%/% Rd.	%/%/% Uln.	%/%/% *T*
1—5	13	77	21	2	18	60	28	12
5—7	59	81	15	4	67	76	21	3
8—10	53	64	30	6	53	77	21	2
11—14	78	50	42	8	184	63	29	8
15—20	61	53	44	3	52	67	33	—
21—older	190	62	34	4	159	77	21	2

Jews (Moscow).

age-groups	Males				Females			
	number	%/%/% Rd.	%/%/% Uln.	%/%/% *T*	number	%/%/% Rd.	%/%/% Uln.	%/%/% *T*
5—7	9	99	10	—	9	100	—	—
8—10	10	70	30	—	13	46	38	16
11—14	10	20	80	—	25	64	28	8
15—20	13	54	38	8	20	80	20	—
21—older	29	59	27	14	58	62	31	7

WOLOTZKOI concludes that the hands of children show a predominance of the Rd. type, but that with increasing age the number of Uln. forms increases. He also remarks that after the 20th year the converse phenomenon appears and the number of Uln. decreases in favour of Rd. forms. (This is not the case with the Jewesses, J. H.).

Although both WEISSENBERG and WOLOTZKOI examined Russian Jews, there is an enormous difference between their percentages for the different hand-types. WEISSENBERG finds 70 % of Uln. forms in adult males, whereas WOLOTZKOI gives 27 %. To what extent the cause of these discrepancies is to be sought in the number of subjects examined, we need not discuss here. It seems justifiable to conclude from both these investigations that the *Rd. type* is more frequent in *youth* than at a more advanced age, although the actual percentage reported by these two authors differ widely.

We shall discuss this conclusion further in connection with our own work.

As far as we know the only publication in which mention is made of the hands during intrauterine life is that of MIERZECKI (1946). Without specifying the number of subjects examined or their sex, he gives the following percentages for negroes (N) and whites (W)

	3th. month		4th. month		9th. month		10th. month	
	W	N	W	N	W	N	W	N
Uln.	33.3	57.1	14.7	50.0	33.5	63.2	31.8	54.6
T.	64.7	42.9	69.0	50.0	53.4	36.8	54.6	45.4
Rd.	2.0	—	16.3	—	13.1	—	13.6	—

In whites, thus, it appears that the index finger is longer than the ring finger in the third month in only 2 % of cases, whereas at birth the occurrence of this relation is 14 %. According to MIERZECKI, in negroes the hand during intrauterine life is invariably *non*-Rd. 'In the development of the hand of the negro, as in that of apes, no tendency whatever is seen for the length relation between the fingers to change in favour of the index finger.'

The high percentage of T. in the above table is remarkable. The number of cases in which the investigator is unable to make a decision is largely dependent on the method of examination used. What looks like a T form on simple inspection may be shown by accurate measurements to be Rd. or Uln., or vice versa. We may also agree to use the terms Rd. or Uln. only in cases where the difference in prominence exceeds a given number of millimetres. MIERZECKI is silent on this point.

In addition to this, the uncritical fashion in which he makes use of ECKER's data makes it impossible for us to have very great faith in his percentages.

3. *Prominence in the light of typology.*

In 1875 (long before the time of Kretschmer) ECKER remarked in his publication that, where the Rd type occurs in European men, this 'is found more frequently in tall, thin individuals than in those of short, stocky build'. We understand him to mean that this does not hold for women.

The Viennese investigator ROMICH (1932) describes the distribution of the two hand forms among the constitutional types distinguished by him.

The *progressive* constitutional type (P. T.) 'includes the sum of all progressive characteristics that are necessary for the static functions and that find expression in the transformations of the entire locomotor apparatus which are brought about by and adapted to these functions'. This part of his definition will, we believe, suffice to show the direction in which the characteristics are oriented.

The *conservative* constitutional type (C. T.) 'adapts itself, with respect to the locomotor apparatus, for the dynamic function and shows a pronounced accentuation of the rudimentary formation'.

Among 300 adults of both sexes (proportions not stated, J. H.) consisting of 150 P. T. and 150 C. T. individuals, 40 % showed Uln.,

51 % Rd. and 9 % T. forms. Classifying these according to C. T. and P. T. types, however, ROMICH found:

	P.T.	C.T.
Uln.	60%	20%
T.	8%	10%
Rd.	32%	70%

The percentage of Rd. forms for the whole group (51 %) appears thus to result from the occurrence of Rd. in 70 % of the conservative and 32 % of the progressive groups (these groups being numerically equal). ROMICH further states that in his progressive type (i.e. that in which the static function is to the fore) a narrow, gracile hand with long fingers is usually found, while the hand of the conservative type is short and broad with short fingers.

This would mean that the progressive hand corresponds to that of the leptosome type, in which, therefore, the Uln. form must predominate (60 %). If we are really justified in using the term leptosome here, it seems that this conclusion conflicts with the findings of ECKER already mentioned.

We are, further, inclined to believe that ROMICH's typology is no great acquisition.

4. *Prominence and racial differences.*

We have already mentioned the distribution of the two hand forms found by ECKER (1875) in American negroes. Although ECKER makes no definite statement, SCHAAFFHAUSEN (1884) after comparing the 'so-called savages with civilized human beings' considers himself justified in remarking that it is 'as ECKER was the first to show, a characteristic of culture versus savagery that the index finger increases in length relative to the fourth or ring finger'. Although we ourselves have not investigated racial differences, we do not wish to cast doubt on the possibility that differences may exist, even to a very large extent. But we see in the fact that judgements on this problem, pronounced at the end of the 19th century, were frequently based on the examination of 2, 3, 4 or 5, individuals of little-known races — and often without any attention to age or sex — a reason for not attaching undue value to such statements.

VIRCHOW (as stated by WECHSLER in 1939) asserted in 1898 that cultured peoples have the Rd. type while primitive peoples show the less elegantly proportioned hand of the Uln. type. VIRCHOW also remarked (in our opinion humorously): 'the tendency to a longer index finger happened to be greatest in the chief of the negro tribe studied: in him there was no difference between these two fingers'.

We have already mentioned the results of PFITZNER (1893) with Alsatians and those of WOLOTZKOI (1924) with Russians and Jews, as

well as those of WEISSENBERG (1895) with Jews. According to SCHULTZ (1924) the rule that primates (see below) have the Uln. type holds for negroes.

RUGGLES (1930) states in connection with his American whites: 'There is no indication of any relationship betwee the finger type and (either handedness or) eye color'.

Comparison of the results of racial investigations gives a confused picture.

5. *Prominence and problems of evolution.*

Here again we must mention ECKER who was the first to include anthropoids in his investigations. He remarks that in all the apes examined — but least in the Gorilla — the Uln. type occurs. The number of apes examined was very small.

SCHAAFFHAUSEN (1884), the student of 'savages' already mentioned, states in connection with the occurrence of the Rd. type 'this is seen in none of the anthropoid animals; in these the ring finger is invariably the longer and the index finger the shorter'.

HARTMANN (1883) whom WEISSENBERG calls one of the greatest experts on the anthropoids, states, however, that Rd. prominence does occur in apes.

SCHULTZ (1924) remarks: 'Among all primates, except in a large percentage of white men and perhaps of some other human races, the fourth finger surpasses the second in length'. WOOD JONES (1944) also describes the Uln. form as typical of all 'monkeys and apes'. The Rd. type is 'definitely non-simian and constitutes a characteristic human specialisation'. He also remarks that, although the Rd. type is found only in man 'this formula is found only in a certain number of cases, that it may be present in one hand and not in the other and that it depends upon the greater development of the index finger'.

It is precisely this 'elongated index' that we may regard as a 'distinctly human specialisation'. In this connection WOOD JONES points to the differentiation of a separate deep index flexor muscle from the musculus flexor digitorum profundus vel perforans. 'The factor underlying the differentiation of this portion is undoubtedly the human specialisation of the index.'

From the literature it seems justifiable to conclude that, while the Rd. type may perhaps occur sometimes in anthropoids, the Uln. type is the rule in apes and anthropoids.

6. *Difference in prominence between the two hands.*

Little attention seems on the whole to have been paid to a possible difference in prominence between the right and the left hand. According to WEISSENBERG (1895) the Rd. type is commoner in the left hand. We quote the figures for his 574 Jewish boys and men.

RUGGLES (1930) comes to exactly the opposite conclusion, stating that the Rd. type predominates in the right hand in both men and women.

Rd. type (WEISSENBERG 1895).

	5—10 yr.		11—20 yr.		21—30 yr.		31 yr. ond older	
Right	$n = 30$	45.5%	$n = 57$	18.9%	$n = 29$	23.6%	$n = 21$	25.0%
Left	$n = 29$	43.9%	$n = 75$	24.9%	$n = 39$	31.7%	$n = 27$	32.1%

We have already seen that WOOD JONES (1944) says of the Rd. type 'that it may be present in one hand and not in the other'.

According to RUGGLES (1930) there is no relation between hand type and 'handedness'.

Rd. type (RUGGLES 1930).

	Men		*Women*	
Right	$n = 56$	28%	$n = 57$	52%
Left	$n = 40$	20%	$n = 51$	47%

As is the case with practically all the aspects of the prominence problem which we have discussed here, a study of the literature once again presents us with contradictory opinions.

WOLOTZKOI (1924) determines the 'mean' prominence of the two hands of an individual by placing the hands, each with its longitudinal axis along the prolongation of that of the forearm, in the same plane, with the middle fingers tip to tip. If the distance between the tips of the index fingers is smaller than that between the the tips of the ring fingers we have a (mean) Rd. type. As this method doubles the difference in prominence between II and IV and thus shows it more clearly, we also used it for our investigations (see photo).

Physiology. — *Phosphate-exchanges in purple sulphur bacteria in connection with photosynthesis.* By E. C. WASSINK, J. E. TJIA and J. F. G. M. WINTERMANS. (From the Laboratory of Plantphysiological Research, Agricultural University, Wageningen.) (21st Communication on Photosynthesis) *). (Communicated by Prof. A. J. KLUYVER.)

(Communicated at the meeting of March 26, 1949.)

Introduction.

Since the time VOGLER and his collaborators made the important discovery that in cultures of the chemo-autotrophic sulphur bacterium *Thiobacillus thiooxidans* the shift from the energy-producing to the energy-consuming phase of metabolism is accompanied by a phosphate exchange (1), suggestions as to something analogous in photo-autotrophic metabolism have not been lacking (2—7). Already VOGLER himself put the question: "..... is it possible to irradiate photosynthetic organisms in the absence of CO_2 and to store at least a portion of the radiant energy within the cell in a form which can later be used for CO_2 fixation in the dark?" (2). A certain uptake of CO_2 in the dark by photosynthetic organisms had already been demonstrated by sensitive methods (8), so that there appeared to be a fair chance that VOGLER's question would be answered in the affirmative. Nevertheless, the attempts undertaken so far to furnish direct proof herefor cannot be said to have shown very definite results (5, 9).

These attempts all made use of green cells. Now, in our opinion, there are some good reasons to give preference to purple sulphur bacteria for these studies. In the first place they are more closely related to the organisms VOGLER used. Some strains of purple bacteria even have been shown to be capable of an anaerobic, photosynthetic mode of life as well as of a heterotrophic, oxydative one. In the second place, in purple bacteria, both carbon dioxide and the hydrogen donor can be supplied at will. In the third place, previous studies had given some general idea of the kinetics of the metabolism of at least one strain (*Chromatium*, strain D).

We, therefore, decided to look for possible connections of photosynthesis and phosphate exchange in suspensions of *Chromatium*, strain D.

The method of phosphate determination was worked out chiefly by the second author, the results reported below were collected by the last mentioned author.

Methods.

The bacteria were grown in the medium, described earlier as "combination 23",

*) 20th Comm.: Ann. Rev. Biochem. **17**, 559—578 (1948).

containing 0.24% sodium-l-malate and 0.16% sodium thiosulphate in an inorganic stock-solution (10). In the reported experiments, cultures from a small amount of dense inoculum were used after 1 day of incubation at about 27° in a light cabinet. They were centrifuged, suspended in the medium used in the experiments (see below), and centrifuged again. After this, the bacteria were resuspended in the same medium, and the experiments were started.

The general trend of an experiment was very simple. A suspension of bacteria in a glass cylinder of about 20 cm height and about 50 ml. contents was ventilated with a suitable gas stream, mostly consisting of oxygen-free nitrogen with either hydrogen or carbon dioxide added, and exposed either to light or to darkness. At the moment of changing conditions, or at intervals during an exposition, inorganic phosphate-P in the suspension medium was determined.

To this purpose, it was deemed advisable to separate the cells from the suspension medium as quickly as possible, and under sensibly the same conditions as during the experiment. In view of the experiments in light, centrifuging appeared unsuitable in this respect. At first, an experimental set-up was made in which the bottom of a glass cylinder was replaced by a cylindrical funnel with glass filter plate. Suspension liquid could be removed by suction during the fully undisturbed experiment.

Unfortunately, however, bacteria entered into the pores of the filter plate — of about 1 μ width — soon preventing rapid filtering. After a few trials the following simple procedure was found satisfactory. Cylindrical glass funnels were made, about 5 cm in diameter, and 6 cm in height, with a nearly flat bottom and a tube of about 1 cm width. A stiffly rolled strip of ordinary filter paper, about 2 cm broad and 30 cm long, was pressed into the upper end of the tube. About 5 ml. of suspension were now removed from the glass cylinder in which the bacteria were exposed to the experimental conditions, introduced into the funnel — which was either illuminated or in darkness — and ventilated with the same gas stream as used in the experiment. Then suction was quickly applied, upon which the suspension medium rapidly went through clear.

In order to have a chance upon measurable relative changes in PO_4–P, solutions of low phosphate contents had to be used; in general about 10 μ g P/ml was taken. Initially, dilute phosphate buffers of pH ~ 8.0, according to CLARK and LUBBS, and to SÖRENSEN were used. Since the bacteria soon became inactive in these dilute media, 1% NaCl was added. A remaining drawback was the weak buffering capacity of the medium. In case of ventilation with gas containing CO_2, the buffering capacity could be increased by addition of sodium bicarbonate, which, however, had the disadvantage of preventing subsequent removal of CO_2 — *e.g.*, when applying $N_2 + H_2$ afterwards — and, moreover, turned out to have an influence upon the phosphate determination.

In search for other suitable buffering systems it has to be observed that systems containing organic acids, as *e.g.*, acetate, citrate, *etc.* are less advisable since these substances are likely to be used as sources of hydrogen and/or of CO_2 by the bacteria. Finally, a borate mixture was found suitable and was stood very well by the bacteria; PALITZCH' mixtures were used. Ten ml. solution containing 3 ml. M/20 borax, and 7 ml. M/5 boric acid + M/20 NaCl, pH ~ 8.0 were added to 40 ml. of a phosphate mixture containing about 10 μ g P/ml. When ventilated in dark with $N_2 + 1\%\ CO_2$, a decrease of pH was observed which, after about 3 hours, remained at about 7.15. B-concentrations used did not interfere with P-determination.

Phosphate-P was determined colorimetrically, according to the phospho-molybdic acid method first devised by OSMOND (1887). BELL and DOISY (1920) first used this method in connection with an organic reductant. Several modifications, differing in the sort of reductant, have since been described. We used that of LOWRY and LOPEZ (11), with ascorbic acid as reductant. Advantages of this method are the operation at moderate pH and the use of a rather dilute solution of molybdate.

Two ml. of suspension medium sucked through the filter (*cf.* above) were introduced into a measuring flask of 25 ml., and some acetate buffer, pH 4.0, was added. Subsequently,

2 ml. of a solution containing 1 % of ammonium molybdate in 0.05 N. sulfuric acid, and 2 ml. of a 1 % solution of ascorbic acid were added, and filled up to 25 ml. with acetate buffer. A stopwatch is started after addition of the reductant, and the blue color, gradually developing, is measured after 5 and 10 minutes with a "lumetron, model 400 A" colorimeter, using the red filter, and a solution without molybdic acid as reference. In general, the readings after 5 and 10 minutes turned out to be the same, so that each moment between was suitable for the determination. About 10 readings were taken from each sample, yielding one measurement. The phosphate content according to the reading was computed from a calibration curve obtained by submitting solutions of known phosphor contents to the same procedure.

The accuracy obtained may be indicated by the following figures: 20 measurements of blank P + B-solution (before introducing bacteria into it) yielded $P = 8.9 \pm 0.05$; $\sigma = 0.23\ \mu$ g P/ml.

The following experimental details still have to be mentioned. In the earlier experiments glass cylinders were used to take up the bacteria in the experiments (*cf.* above). As a rule two of these were used in each experiment, submitted to different conditions (*e.g.*, light *versus* darkness, $N_2 + H_2$ *versus* $N_2 + CO_2$). The suspensions contained about 5 cmm bacteria/ml. The cylinders stood in a thermostatic water bath with glass sides, at about 29°, illuminated from 2 opposite sides with a 100 Watt incandescent lamp, yielding on either side an intensity of 8—9000 lux. In later experiments flat glass boxes of about $20 \times 10 \times 0.6$ cm were used instead of the cylinders.

During the experiments a flow-meter-controlled gas stream from a bomb was passed through the suspensions. Either $N_2 + 30\ \% H_2$, $N_2 + 30\ \% H_2 + 5\ \% CO_2$, or $N_2 + 1\ \% CO_2$, obtained by mixing pure nitrogen with nitrogen containing 5 % of carbon dioxide, were applied. The gasses were freed from oxygen by passing them over electrically heated copper gauze. With the aid of flow meters the gas streams in both cylinders or glass boxes were adjusted to equal velocity. At the top the vessels were closed except inlet and outlet of gas, the first ending in the suspension near the bottom. Before entering into the vessel with the bacteria, the gas passed a washing bottle with water at room temperature, to control evaporation of the suspension.

Unfortunately, so far, we were not in a position to follow simultaneously the gas exchange of the cells used, owing to the lack of suitable apparatus herefor. This is planned for a subsequent part of this investigation.

Experimental results and their preliminary discussion.

The first experiments tended to "translate" VOGLER's crucial experiments in terms of photosynthesis as closely as possible. A suspension of *Chromatium*, Strain D, in a borate mixture with about 10 μg PO_4–P/ml., pH $\sim$ 8.0, under $N_2 + 30\ \% H_2$ was submitted to a short dark period for "adaptation", and then illuminated. During the illumination period, a decrease of phosphate in the external medium is observed. After some hours, the light is turned off, and the gas phase replaced by $N_2 + 5\ \% CO_2$. Then, an increase in external phosphate is observed. The procedure may be repeated with the same result (fig. 1, curve *a*). It is obvious that these observations are concordant with a concept, analogous to the one proposed by VOGLER for the chemo-autotrophic sulphur bacteria. In the light, hydrogen may be taken up, and fixed in some form, involving phosphate uptake. If this form is an "energy rich phosphate", able to aid in the reduction of carbon dioxide in the dark, release of phosphate in a subsequent dark period may be expected.

It may be remarked already now that, in a M/15 phosphate buffer of pH ~ 8.0, WASSINK and KUIPER observed a long-lasting uptake of gas from $N_2 + H_2$, in the absence of CO_2, even in cells submitted to special "starvation" treatments (in an investigation on the relation between redox potential and photosynthesis [12—14]). So far studies

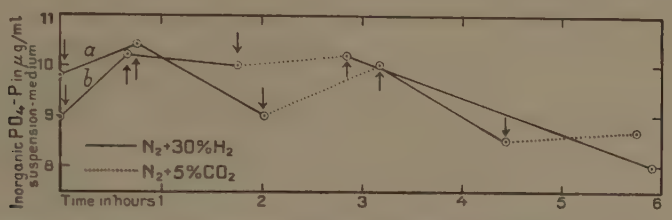

Fig. 1. Phosphate changes in suspension medium with *Chromatium*, strain D, in relation to light and darkness, and under various gas phases. Exp.s of 13, 14. 10. 48.
↓ : shift to darkness. ↑ : shift to light.

as to a "dark pick-up" of CO_2 have not yet been made. In the course of the mentioned investigation some incidental indications were obtained that cells, allowed to take up hydrogen in the light for a long time, already quickly thereafter produce considerable amounts of CO_2 in the dark.

Not always, however, the cells showed clear responses as to phosphate in the various phases of the above mentioned type of experiment (*cf.*, *e.g.*, fig. 1, curve *b*). This forced us to a more systematic study of the various phenomena involved.

The next observation made was a release of PO_4 in the dark (increase in the external medium) when freshly harvested, and washed cells were suspended as described. This PO_4-liberation starts at once, and shows a tendency to decrease with time. In $N_2 + 30\ \% H_2$, and in $N_2 + 1\ \% CO_2$ it was studied in greater detail and only little difference between these two gas phases was found (fig. 2, 3, 4, 5, 6, 8, 10; Table I). This release

TABLE I.

Release of PO_4–P (increase of P in suspension medium) by *Chromatium*, strain D, in darkness under various gas phases.
Suspension medium: borate buffer, pH ~ 8.0, with ~ 10 µ g P/ml.

	Ventilated with	Time	Total PO_4–P released	Number of observations
a	$N_2 + 30\%\ H_2$	35′	0.53 ± 0.05	15
		120′	1.1 ± 0.13	12
		180′	1.8 ± 0.14	5
		285′	2.15 ± 0.25	2
b	$N_2 + 1\%\ CO_2$	120′	1.08 ± 0.18	12
		270′	2.19 ± 0.55	5

of PO_4 probably may be compared with that accompanying "endogenous respiration" in VOGLER's experiments. Notwithstanding the fact that, owing to the absence of oxygen, the *Thiorhodaceae* can not show a respiration-proper, some form of energy liberating metabolism is likely to continue in darkness, which may well be accompanied by a release of PO_4.

Since neither hydrogen nor carbon dioxide are likely to be active in the dark in these bacteria — unless, eventually, after special treatments — it is perhaps not very surprising that the rate of release is fairly independent of the gas phases applied.

Next, the behaviour of the cells after admitting light, in $N_2 + 30\ \% H_2$, was studied in greater detail. The phosphate release is now replaced by phosphate uptake (fig. 1, 2, 3, 4, 7*b*, 8*b*); after a short dark period, when the tendency to release phosphate apparently still was strong, the uptake at first was sometimes small or even slightly negative still (*cf.* fig. 4, 7*b*) especially in dense suspensions (low average light intensity). Some typical experiments are represented in fig. 2 and 3; in each case, after a short dark period, the two halves of the same suspension were submitted oppositely to light and darkness, whereas, some 2 hours later, the conditions were reversed (fig. 2) or continued (fig. 3) without changing the gas phase.

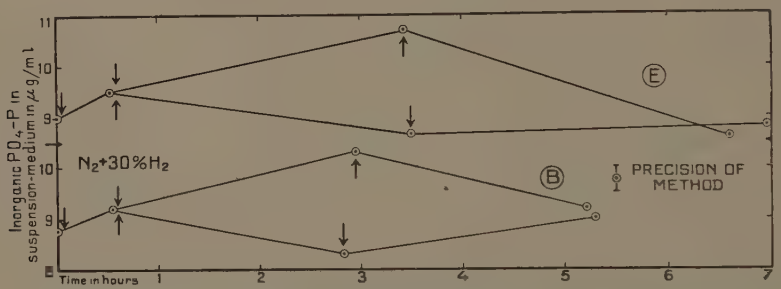

Fig. 2. Phosphate changes in suspension medium with *Chromatium*, strain D, in relation to light and darkness. Flushed with $N_2 + 30\ \% H_2$. E: Exp. of 17.11.48; B: Exp. of 10.11.48.
↓ : shift to darkness. ↑ : shift to light.

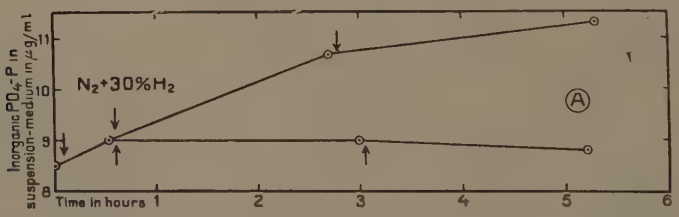

Fig. 3. Phosphate changes in suspension medium with *Chromatium*, strain D, in relation to light and darkness. Flushed with $N_2 + 30\ \% H_2$. Exp. of 9. 11. 48.
↓ : shift to darkness. ↑ : shift to light.

A number of experiments of the type-fig. 2 is summarized in fig. 4, showing the different behaviour in light and darkness very clearly. It may be concluded too, provisionally, that the rate of phosphate uptake in the light is higher after a longer dark period (fig. 4, Table II, *a*). The reaction upon renewed darkness will be discussed below.

Also in $N_2 + 1\ \% CO_2$, illumination as a rule causes uptake of phosphate, replacing the release occurring in the dark (fig. 5, a few experiments are summarized in fig. 6). Here, too, after a prolonged dark period the rate of uptake appeared increased (*cf.* Table II, *b*).

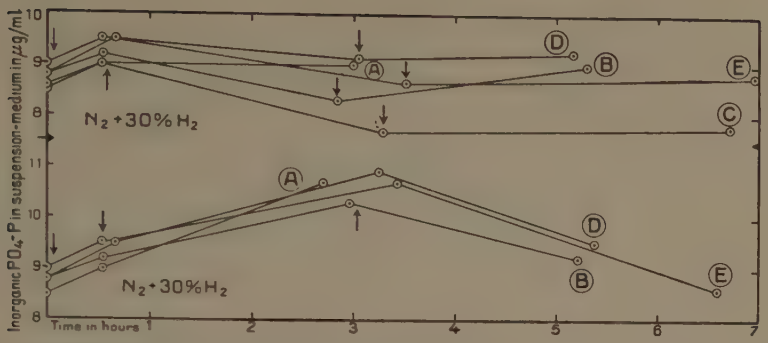

Fig. 4. Phosphate changes in suspension medium with *Chromatium*, strain D, in relation to light and darkness. Flushed with $N_2 + 30\,\% H_2$. Aliquots of the same culture indicated by equal characters. Exp.s of various dates.
↓ : shift to darkness. ↑ : shift to light.

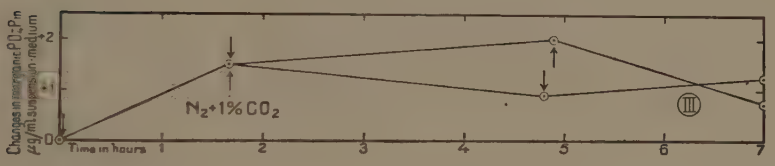

Fig. 5. Phosphate changes in suspension medium with *Chromatium*, strain D, in relation to light and darkness. Flushed with $N_2 + 1\,\% CO_2$. Exp. of 2. 12. 48.
↓ : shift to darkness. ↑ : shift to light.

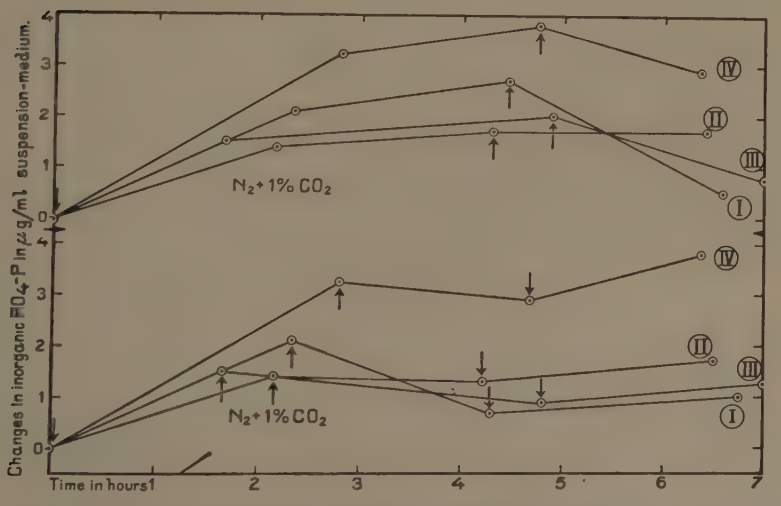

Fig. 6. Phosphate changes in suspension medium with *Chromatium*, strain D, in relation to light and darkness. Flushed with $N_2 + 1\,\% CO_2$. Aliquots of the same suspension indicated by equal numbers. Exp.s of various dates.
↓ : shift to darkness. ↑ : shift to light.

TABLE II.

Uptake of PO_4–P (decrease of P in suspension medium) by *Chromatium*, strain D, in illumination under various gas phases.

Suspension medium: borate buffer, pH ~ 8.0, with ~ 10 μ g P/ml.

	Condition during dark period	Duration of dark period	Condition during subsequent illumination	Time of exposure to light	Total PO_4–P taken up in light	Number of observations
a	$N_2 + 30\%\ H_2$	30′	$N_2 + 30\%\ H_2$	75′	0.29 ± 0.1 μg/ml.	12
				135′	0.49 ± 0.15 „	12
				195′	0.80 ± 0.32 „	5
				235′	1.38 ± 0.70 „	3
	same	2 hours	same	120′	0.80 ± 0.26	6
				240′	1.11 ± 0.16	5
	same	3 hours	same	120′	1.20 ± 0.10	3
	same	4.5 hours	same	120′	2.40 ± 0.2	2
b	$N_2 + 1\%\ CO_2$	2 hours	$N_2 + 1\%\ CO_2$	120′	0.31 ± 0.16	11
				240′	0.20 ± 0.17	5
	same	4.5 hours	same	120′	1.0 ± 0.4	5
c	$N_2 + 30\%\ H_2$	30′	$N_2 + 30\%\ H_2 + 5\%\ CO_2$	150′	0.0 ± 0.14	5

However, another feature is very obvious, *viz.*, that the uptake in light under $N_2 + 1\ \%\ CO_2$ is much smaller than under $N_2 + 30\ \%\ H_2$ (fig. 8). In some cases with CO_2 it even hardly reaches significantly positive values (*cf.* Table II, *b*). The same can be said, comparing $N_2 + H_2 + CO_2$ with $N_2 + H_2$, also here the presence of CO_2 reduces the phosphate uptake in the light practically to zero, and the difference in the general trend of the curves is very obvious, notwithstanding some incidental exceptions (fig. 7, Table II, *c*).

It should be emphasized that most of the curves of *a* and *b* in fig. 7 and 8 have been obtained one by one in the same experiment so that the variable "activity" of the cells to take up and give off phosphate cannot have interfered with these results.

In the type of experiment as shown in fig. 2 and 5 (*cf.* also fig. 4 and 6) darkness was again given after light in one of the two aliquots of suspension. The number of these observations is still too small to draw definite conclusions. It is obvious, however, that phosphate uptake stops or is converted into release. It would seem that in $N_2 + CO_2$ the release is somewhat more definitely pronounced than in $N_2 + H_2$ (*cf.* fig. 4 and 6). The reaction upon darkness after light without changing the gas phase throws some doubt upon the meaning of the release of phosphate after changing from H_2 to CO_2. More and quantitative studies, taking into account the gas exchange, are required here. In general, however, it may be admitted that under all conditions the cells are provided with organic

substances, which may be converted under release of phosphate and probably of CO_2, as soon as conditions for active rebuilding of ~ph are absent, especially when the source of energy: light, is lacking.

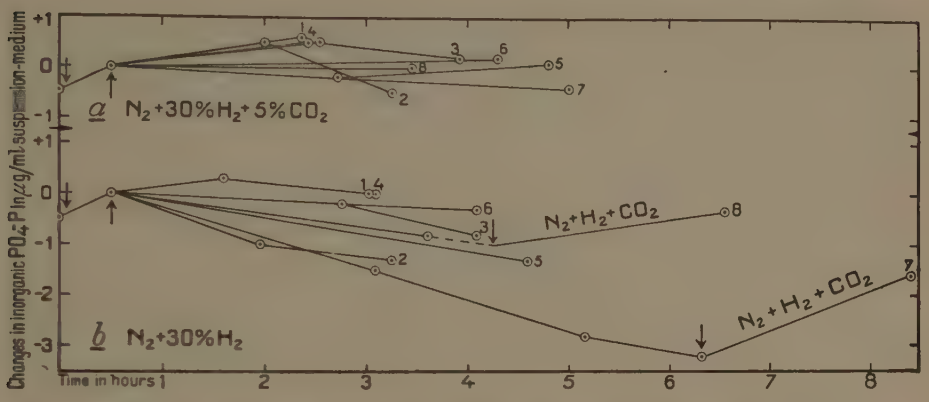

Fig. 7. Phosphate changes in suspension medium with *Chromatium*, strain D. Influences of various gas mixtures during illumination and eventually subsequent darkness. Aliquots of suspensions were separated after ± ½ hour adaptation in dark with $N_2 + 30\% H_2$. (Numbers indicate parallels with the same culture.) Exp.s of various dates.
↓ : shift to darkness. ↑ : shift to light.

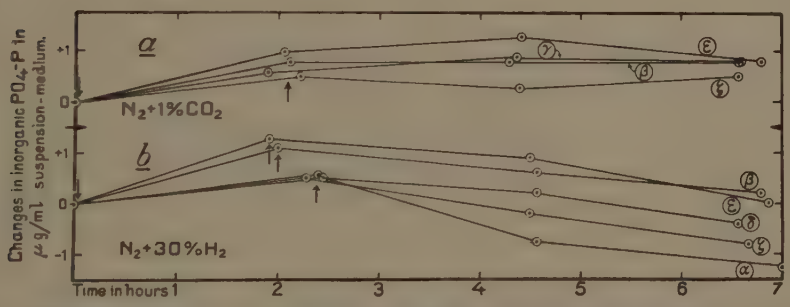

Fig. 8. Phosphate changes in suspension medium with *Chromatium*, strain D. Influence of various gas mixtures in dark and in light in parallel experiments (indicated by characters.) Exp.s of various dates.
↓ : shift to darkness. ↑ : shift to light.

General Discussion.

In the foregoing, uptake and release of phosphate have been observed. It is obvious, *a priori*, that neither of the two can last infinitely with the same speed, even under as such favorable conditions. It is obvious too, therefore, that both uptake and release will show an asymptotic course in relation to time. Furtheron, it may be admitted that the rate of reversion upon a change of conditions also depends upon the nature and duration of the condition before the change. Finally, if indeed there is a relation between phosphate metabolism and photosynthesis of the type VOGLER found in *Thiobacillus thiooxidans*, we may expect that in the light, in the

absence of carbon dioxide, cells will accumulate phosphate to a higher degree than in its presence. In darkness, we may expect phosphate bond energy to be released as part of the energy reserve of the cell, used up in darkness.

From these general statements, and founded upon the results of VOGLER and UMBREIT, we would expect purple sulphur bacteria to influence the phosphate content of a limited amount of medium in which they are suspended, in a way schematically represented in fig. 9.

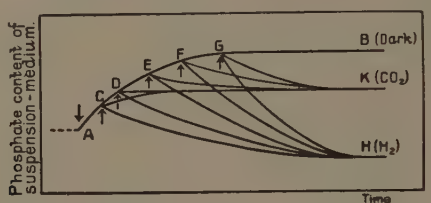

Fig. 9. Schematical representation of expected PO_4-shifts under different conditions. See text.

↓ : shift to darkness. ↑ : shift to light.

Cells brought into darkness from a well-fed condition will start releasing phosphate from a level A, which phosphate accumulates in the medium. Since neither hydrogen nor carbon dioxide are known to act as energy sources in the dark for *Chromatium*, there is no reason to expect that the release of phosphate will depend either on the presence of hydrogen or of carbon dioxide. The release will show an asymptotic course (AB). Upon illumination, *e.g.* in $N_2 + H_2$, an uptake of phosphate will occur which may be expected to start at higher rate, the more phosphate has been released before, so, *e.g.*, the longer the dark period has lasted. The curves starting at C, D, E, *etc.*, will be expected to strive towards virtually the same level, indicated by H. The probability that this level is, *e.g.*, dependent on light intensity, will not be discussed here. Under $N_2 + CO_2$ we may expect a behaviour fundamentally analogous to that under $N_2 + H_2$, only pointing to a significantly higher ultimate phosphate content in the external medium (level K).

In fig. 10 we have collected from our total experimental material, the

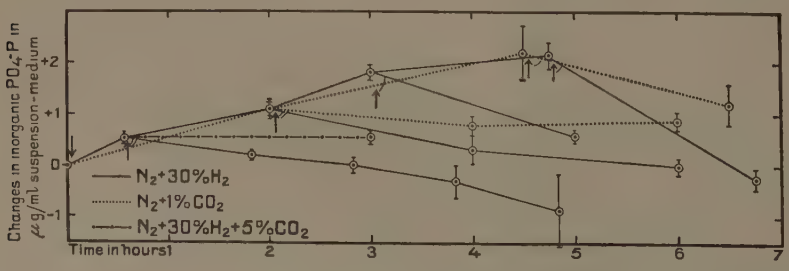

Fig. 10. Summarized representation of actual PO_4-shifts from table I and II. Cf. fig. 9 and text.

↓ : shift to darkness. ↑ : shift to light.

data pertaining to the points outlined above. Notwithstanding the fact that on various points the material still is somewhat scanty (expressed by the large mean errors of some points and the lack of data on shorter intervals) it is clear that, in general, fig. 10 shows a very distinct analogy with the scheme of fig. 9. This would seem to indicate that, in general, the situation answers to the outline given.

It should, however, not be overlooked that the experiments made so far, do not *prove* that, in photosynthesis of *Chromatium*, in the absence of CO_2, part of the energy of the light actually is accumulated as phosphate bond energy. To prove this would require recovery of these energy rich phosphates from the cells which determinations have not yet been attempted. The findings merely are very well in accordance with the supposition that indeed light energy *is* accumulated in this form.

It may be useful still to emphasize a rather fundamental difference between VOGLER's case and that of the photosynthetic bacteria. In *Thiobacillus*, the oxidation of the hydrogen donor is achieved by oxygen, and is, or at least may be conceived to be fundamentally independent of carbon dioxide. This easily leaves room for a storage of energy from the oxidation process in some form which may, or may not, be used for the reduction of carbon dioxide. In *Chromatium*, on the other hand, carbon dioxide itself is the ultimate oxidant of the hydrogen donor; for the transfer of hydrogen light is essential. This, however, would seem to leave much less room for an independent storage of (light) energy at the expense of the hydrogen donor, and requires a much more specialized mechanism. The observation, alluded to above, that excessive hydrogen uptake may occur without supply of carbon dioxide (13, 14), indicates that indeed under certain conditions — *e.g.* pH $\sim$ 8.0 — hydrogen may be assimilated more or less independent of carbon dioxide. It is interesting in this respect that so far no indications were found for an appreciable CO_2-uptake without hydrogen during prolonged illuminations. The results reported in the present paper suggest that the mentioned uptake of hydrogen — which was not measured in the present study — is connected with phosphate uptake. It is perhaps most plausible to assume, that phosphate-shifts are connected with the transfer of energy from the pigment-protein system (*cf.* [15, 16, 12]).

In view of an estimation of the quantitative importance of the phosphate shifts observed, it may be of interest to compare their magnitude with the presumable phosphate content of the cells. If we suppose a "normal" phosphor content in *Chromatium*-cells, this may be fixed at $\sim$ 5 % of the dry weight, as P_2O_5; the dry weight may be 15 % of the fresh weight. This would mean that the bacteria contain 0.75 % of their fresh weight as P_2O_5, or 0.33 % P. The suspension density as a rule was about 5 cmm/ml., or about 5 mg/ml. Thus, the bacteria in 1 ml. contain about 17 μg P. On exposure to $N_2 + H_2$ in the light, an uptake of 1.5 μg P/ml is not rare. It thus appears that the bacteria may underly shifts in phosphate amounting to about 10 %. In order to achieve that these shifts will definitely surpass

the limits of the method of determination, rather dense bacterial suspensions are advisable. In order to obtain sufficient illumination inside the suspension, in our more recent series we used glass boxes instead of cylinders to suspend the bacteria.

Summary.

In suspensions of *Chromatium*, strain D, in borate buffer, pH ~ 8, containing some phosphate, shifts in phosphate content of the medium were found correlated with shifts from light to darkness, and from a gas phase consisting of $N_2 + H_2$ to one containing $N_2 + CO_2$.

The principal observations were as follows. Bacteria taken from the culture medium ("comb. 23", see [10]) release phosphate in darkness, at about equal rates under $N_2 + H_2$ as under $N_2 + CO_2$. Shift to light results in a marked uptake of phosphate under $N_2 + H_2$ and in a much smaller one under $N_2 + CO_2$. Shift from light under $N_2 + H_2$ to darkness under $N_2 + CO_2$ results in a marked release of phosphate. Change from light to darkness without change of gas phase results in a certain release, too.

As a whole the data collected so far show a marked similarity with VOGLER's findings with *Thiobacillus thiooxidans*, if $N_2 + H_2$ in light is parallelized with sulphur oxidation. They thus form a preliminary support for the hypothesis that *Chromatium* in the light is capable of building up energy rich phosphate bonds which are broken down in part when CO_2 becomes available and/or light is withdrawn. The phosphate exchanges observed so far can amount to 10 % of the phosphate content of the bacteria.

Correlations with gas exchange were not made so far. The investigation is being continued.

REFERENCES.

1. K. G. VOGLER and W. W. UMBREIT: J. Gen. Physiol. **26**, 157—167 (1943).
2. ————: J. Gen. Physiol. **26**, 103—117 (1943).
3. S. RUBEN: J. Amer. Chem. Soc. **65**, 279—282 (1943).
4. C. B. VAN NIEL: Physiol. Reviews **23**, 338—354 (1943).
5. R. L. EMERSON, J. F. STAUFFER and W. W. UMBREIT: Amer. J. Bot. **31**, 107—120 (1944).
6. H. GAFFRON: Currents in biochem. research 325—348, (Interscience Publishers, N. Y., N. Y., 1946).
7. B. KOK: Enzymol. **13**, 1—56 (1948).
8. E. D. MCALISTER and J. MYERS: Smithsonian Inst. Publ. Misc. Coll. **99** (6) (1940).
9. S. ARONOFF and M. CALVIN: Plant Physiol. **23**, 351—358 (1948).
10. J. G. EYMERS and E. C. WASSINK: Enzymol. **2**, 258—304 (1938).
11. O. H. LOWRY and J. A. LOPEZ: J. Biol. Chem. **162**, 421—428 (1946).
12. E. C. WASSINK: Antonie v. Leeuwenhoek, J. Microbiol. Serol. **12**, 281—293 (1947).
13. ————: Abstracts Comm. 4th Intern. Congr. Microbiol. 173—174 (Copenhagen, 1947) and 4th Intern. Congr. Microbiol. Rep. Proc. 455—456 (Copenhagen, 1949).
14. E. C. WASSINK and F. J. KUIPER: Enzymologia (in preparation).
15. E. C. WASSINK, E. KATZ and R. DORRESTEIN: Enzymol. **10**, 285—354 (1942).
16. R. DORRESTEIN, E. C. WASSINK and E. KATZ: Enzymol. **10**, 355—372 (1942).

Botany. — *De hypothese voor de erfelijkheidsformules van de twee zuivere lijnen I en II van Phaseolus vulgaris op grond van kruisingsproeven.* I. By G. P. FRETS. (Communicated by Prof. J. BOEKE.)

(Communicated at the meeting of January 29, 1949.)

In een vroegere mededeling (Proceed. 50, p. 798, 1947) stelden we voor de bonen van de I- en II-lijn de formules $L_1 L_1 \ldots L_6 L_6 B_1 B_1 \ldots B_3 B_3 b_4 b_4 \ldots b_6 b_6 th_1 th_1 \ldots th_6 th_6$ en $l_1 l_1 \ldots l_6 l_6 b_1 b_1 \ldots b_6 b_6 \ldots Th_1 Th_1 \ldots Th_3 Th_3 th_4 th_4 \ldots th_6 th_6$ op, of eenvoudiger geschreven $L_1 L_2 B_1 b_2 th_1 th_2$ en $l_1 l_2 b_1 b_2 Th_1 Th_2$. De bonen van de I-lijn zijn lang, breed en dun, die van de II-lijn zijn kort, iets minder breed en dik. Het verschil van de lengten is veel groter dan dat van de breedten en de dikten. Bij de formules worden voor de erfelijkheid van de verschillen der afmetingen 6 paar genen aangenomen. De grootte-toename door één gen is voor alle 3 afmetingen relatief even groot. Steeds zijn één gen voor de lengte, één voor de breedte en één voor de dikte tegelijk werkzaam. Om het zoveel grotere verschil van de lengten dan van de breedten en de dikten te verklaren, wordt aangenomen, dat bij de bonen van de I-lijn er 6 genen voor de lengte in de homozygote, dominante vorm (als LL) aanwezig zijn, terwijl er slechts 3 genen voor de breedte in de homozygote, dominante vorm (als BB) aanwezig zijn. Bij bonen van de II-lijn zijn er slechts 3 genen voor de dikte in de homozygote, dominante vorm (als Th Th) aanwezig. Van de 6 genen voor de afmetingen komen dus de genen 4—6 bij de breedte en bij de dikte alleen in de homozygote, recessieve vorm (als b b en th th) voor. Daarom schrijven we de formules ook $L_1 L_2 B_1 b_2 th_1 th_1$ voor de bonen van de I-lijn en $l_1 l_2 b_1 b_2 Th_1 th_2$ voor de bonen van de II-lijn. Volgens deze schrijfwijze hebben we te doen met een kruising volgens het tetrahybride schema. Na de kruising ontstaan er in de splitsingsgeneraties verschillende nieuwe vormen als resultaat van genencombinaties op grond van het kruisingsschema zo b.v., voor de lengte en de breedte de vormen $L_1 L_2 B_1 b_2$ en $L_1 l_2 B_1 b_2$. Er zullen dus, — we wezen hier reeds op in onze eerste mededeling (l.c.) —, erfelijke variaties met een zeer grote lengte en een grote breedte en ook die met een niet zeer grote lengte en een grote breedte voorkomen, m.a.w. onder de bonen met de grootste breedten ($B_1 b_2$) zullen er zijn met zeer grote lengte ($L_1 L_2$), doch ook met een niet zeer grote lengte ($L_1 l_2$). De grens tussen bonen met een zeer grote en die met een niet zeer grote lengte, legden we bij 15.5 mm. Van bonen met een grote breedte is de breedte groter dan 8.5 mm. Bonen van de 2e groep, dus met de form. $L_1 l_2 B_1 b_2$ hebben een hoge LB-index.

In onze eerste mededeling voegden we hieraan de opmerking toe, dat

individueel voortkweken van verschillende varianten de beslissing over de juistheid der hypothese zou kunnen brengen (l.c., p. 804). Met het oog op dit gezichtspunt bespreken we hier de varianten van de lengte en de breedte $L_1 L_2 B_1 b_2$ en $L_1 l_2 B_1 b_2$ van F_3-1935. We bedenken daarbij, *1e* dat er duidelijk erfelijkheid is bij de op elkaar volgende generaties, — er is een vrij grote positieve correlatie, l.c., p. 800 —, doch er is ook een grote niet-erfelijke variabiliteit, blijkende uit de hoge standaard-deviatie en variatie-coëfficiënt (tab. 1 en 2). De grote niet-erfelijke variabiliteit zal het resultaat van ons onderzoek minder evident maken. Ook is het volstrekte bewijs der juistheid onzer hypothese niet te leveren. *2e* De grond voor onze aanname, dat steeds een gen voor de lengte, één voor de breedte en één voor de dikte tegelijk werkzaam zijn, vinden we in de positieve correlatie tussen de afmetingen voor een willekeurig materiaal en voor de negatieve correlatie in groepen bonen met een zelfde gewicht, als uiting van „compensational growth". Er is bij de groei der bonen een regulerende factor

TABLE 1. The variation of beanyields of the F_3- and the F_4-seedgenerations and of the I- and the II-line of 1935. (Only the variation of the length is given in this table.)
The length

	Pl.	n	M ± m	σ ± m	V	Gr. var.	Sm. var.	Var. r.
I-line	11	39	16.59 ± 0.24	1.54 ± 0.18	9.3	18.5	12.0	6.5
	3	38	15.19 ± 0.26	1.61 ± 0.18	10.6	18.3[1]	11.1[2]	7.2
	9	58	14.33 ± 0.22	1.59 ± 0.15	11.1	19.1	11.1	8.0
	7	60	14.3 ± 0.14	1.08 ± 0.1	7.6	17.5	11.3	6.2
II-line	22	48	12.08 ± 0.09	0.64 ± 0.07	5.3	13.0	9.8	3.2
	25	87	11.02 ± 0.09	0.87 ± 0.07	7.9	12.9	8.6	4.3
	30	30	10.49 ± 0.13	0.73 ± 0.1	7	11.9	8.6	3.3
F_3-seedgeneration	73	35	15.9 ± 0.24	1.39 ± 0.17	8.8	18.3	12.0	6.3
	38	52	14.58 ± 0.17	1.21 ± 0.12	8.2	17.2	11.9	5.3
	44	90	13.66 ± 0.09	0.84 ± 0.06	6.2	15.4	10.9	4.5
	61	122	12.72 ± 0.06	0.65 ± 0.04	5.1	15.0	10.4	4.6
	97	58	12.01 ± 0.12	0.94 ± 0.09	7.8	14.3	10.2	4.1
F_4-seedgeneration	119	51	16.32 ± 0.17	1.18 ± 0.11	7.2	19.2	13.2	6.0
	133	51	15.16 ± 0.11	0.78 ± 0.08	5.2	16.5	13.5	3.0
	150	46	14.21 ± 0.16	1.1 ± 0.11	7.7	16.3	11.9	4.4
	178	45	13.26 ± 0.11	0.72 ± 0.08	5.4	14.5	11.8	2.7
	187	42	12.19 ± 0.1	0.63 ± 0.07	5.2	13.5	10.1	3.4
	198	41	11.04 ± 0.1	0.67 ± 0.07	6.1	12.8	9.5	3.3

[1]) Then follows 17.6. [2]) Then follows 12.

The variation of the beanyields of the pure lines I and II, — that is non-hereditary variation —, is great; it is greater of the I-line than of the II-line. The variation of the beanyields of the F_3- and the F_4-generation, that is hereditary and non-hereditary variation is not greater than that of the I-line and of the II-line (cf. tab. 2, p. 425).

TABLE 2. The mean dimensions and weights and the variation of the beans of the I- and the II-line in 1935—1937. (Only the lengths and the weights are mentioned in this table) [1].

Year	The lines	n	M ± m	σ ± m	V	Gr. var.	Sm. var.	Var. r.
			The length					
1935	I-line	774	15.2 ± 0.07	1.78 ± 0.05	11.7	21.6[2]	10.1	11.5
1935	II-line	802	11.1 ± 0.03	0.84 ± 0.02	7.5	13.7	8.6[2]	5.1
1936	I-line	1617	14.2 ± 0.02	0.99 ± 0.02	7	18.1	10.2	7.9
1936	II-line	605	11.16 ± 0.03	0.81 ± 0.02	7.3	13.3	7.3	6
1937	I-line	2383	15.2 ± 0.02	1.13 ± 0.02	7.4	19.0	9.7	9.3
1937	II-line	1292	11.0 ± 0.02	0.80 ± 0.02	7.3	14.9[3]	6.4	8.5
			The weight					
1935	I-line	895	52.5 ± 0.5	16.4 ± 0.4	31	127[4]	10	117
1935	II-line	799	42.4 ± 0.3	7.9 ± 0.1	19	63	15	48
1936	I-line	1610	50.7 ± 0.3	10.4 ± 0.2	21	89	21	68
1936	II-line	605	45.1 ± 0.4	8.6 ± 0.2	19	66	10	56
1937	I-line	1303	63.8[5] ± 0.4	13.1 ± 0.3	21	99	22	77
1937	II-line	1298	43.8 ± 0.2	6.5 ± 0.1	15	64	15	49

[1]) The F_3- and following generations are not included in the table. The averages are not comparable here: at the basis of the material is the selection of the initial beans.

[2]) Then follows 19.6 mm.

[3]) Then follows 13.2 mm.

[4]) Then follows 105 cg.

[5]) The mean weight of 1937 is much greater than that of 1935. The mean thickness is also very great, whereas that of 1935 is small.

tussen de afmetingen (1947,l.c.). *3e* Onder de uitsplitsingen van de F_3- en F_4-zaadgeneratie zullen ook bonen als de oudervormen zijn. Dergelijke uitzonderlijke uitsplitsingen zullen echter phaenotypisch als regel verschillen van de uiterste varianten van de I- en de II-lijn (1947).

We groepeerden van het materiaal van F_3-1935 de bonen met de grote breedten volgens breedte-klassen en tekenden de bij de bonen van iedere breedte-klasse behorende lengte aan. Hetzelfde deden we voor vergelijkmateriaal van de I- en de II-lijn. We gaan dan na, of in de groepen van bonen met de grootste breedten meer bonen met een niet zeer grote of kleine lengte voorkomen dan in de overeenkomstige groepen van bonen van de I-lijn. We vinden het volgende: In tab. 3 zijn van het F_3-materiaal van 1935 de bonen met de grootste breedten opgenomen. Ter vergelijking zijn bonen van de I-lijn en van de II-lijn er naast geplaatst. We zien (tab. 3), dat de grootste breedte van bonen van de II-lijn van 1935 is, b = 9.8 mm. De bonen van de II-lijn komen welhaast voor ons onderzoek niet in aanmerking. Er zijn in het I-materiaal 5 bonen met een breedte van b = 13.0—11.5 mm, dit zijn grotere breedten dan bij de F_3-bonen van 1935 voorkomen. Al deze 5 bonen hebben een zeer grote lengte; ook der-

TABLE 3. The F_3-seedgeneration of 1935. The number of beans with a length that is not very great (15.5 mm and smaller) and with a very great length (15.6 mm and greater) for beans with a great breadth (8.6 mm and greater) and comparison beans of the I- and the II-line. sm. l. = number of beans with a length of 15.5 mm and smaller. gr. l. = number of beans with a length of 15.6 mm and greater. gr. v. = greatest variation; sm. v. = smallest variation.

1935

F_3-seedgeneration							I-line[1])					
Br.	n	Sm.l.	Gr.l.	m_l	Gr. v.	Sm.v.	n	Sm.l.	Gr.l.	m_l	Gr v.	Sm.v.
130							1	0	1		216	
121							1	0	1		179	
117							1	0	1		193	
115							2	0	2	184.5	186	183
113	1	1	0			152	2	0	2	179	191	167
112	1	0	1		183		5	0	5	180.8	196	161
111	1	0	1		164		5	1	4	161.6	173	148
110	4	1	3	162.3	172	144	6	0	6	173.8	183	162
109	3	1	2	159.3	170	141	6	0	6	168.8	182	158
108	4	0	4	167.8	172	160	9	0	9	170.9	183	156
107	7	4	3	158	176	146	15	2	13	164.7	180	146
106	2	1	1	149.5	158	141	9	1	8	174.7	185	155
105	12	3	9	162.3	183	146	11	1	10	166.3	177	148
104	10	6	4	154	166	141	18	1	17	168.8	186	147
103	34	19	15	154.6	176	137	20	2	18	168.8	196	153
102	31	20	11	151.8	166	136	19	0	19	165.4	181	157
101	32	22	10	151.8	178	136	12	1	11	171.2	183	155
100	47	38	9	149.1	174	130	17	1	16	167.1	184	148
99	61	49	12	148.6	182	132	16	0	16	166.9	176	160
98	77	63	14	149.3	175	136	26	5	21	165.2	192	142
97	97	80	17	147.1	169	127	39	4	34	163.6	187	151
96	134	115	19	146.5	167	132	20	6	14	160.5	181	140

[1]) We find for the material of the II-line that there are 2 beans with the great breadth (i.e. the greatest breadth that occurs) b = 9.8 mm, the length is resp. 12.0 and 11.8 mm. There is one bean with the breadth, b = 9.7 mm; the length is l = 13.0 mm. There are 3 beans with the breadth, b = 9.6 mm; the length is resp. 12.6, 12.4 and 12.2 mm.

gelijke zeer grote lengten ontbreken onder de F_3-bonen. Onder de 57 bonen van de I-lijn van 1935 met een breedte van 11.3—10.6 zijn er twee met een lengte van resp. 14.8—14.6 mm, d.w.z., dat er onder de bonen met de grote breedten 11.3—10.6 mm, van de I-lijn, d.i. van bonen met de form. $L_1 L_2 B_1 b_2$ van de lengte en breedte, er 2 zijn met de niet zeer grote lengte 14.8 en 14.6 mm, als niet-erfelijke varianten hier. Bovendien is er één boon met de lengte l = 15.5 mm, d.i. de grenswaarde. Er zijn 23 bonen in het F_3-materiaal van 1935 met de grote breedten 11.3—10.6 mm. Deze aantallen bonen van de F_3-generatie en van de I-lijn zijn niet direct vergelijkbaar: het totale aantal bonen van de I-lijn is veel kleiner dan van de F_3-generatie. De I-lijn echter is een zuivere lijn en bevat slechts niet-

erfelijke variaties, terwijl de F_3-generatie een zeer heterogene erfelijke samenstelling heeft.

Onder deze 23 F_3-bonen met de breedten 10.6—11.3 mm, zijn 8 bonen met een niet zeer grote lengte (d.w.z. l = 15.5 mm, en kleiner). Er zijn daarbij met een lengte van 14.1—14.4 mm, d.i. met een zo kleine lengte, als ze onder bonen van de I-lijn met deze breedten niet voorkomen. Onder de 11, resp. 18 bonen van de I-lijn met een breedte van 10.5 en 10.4 mm,

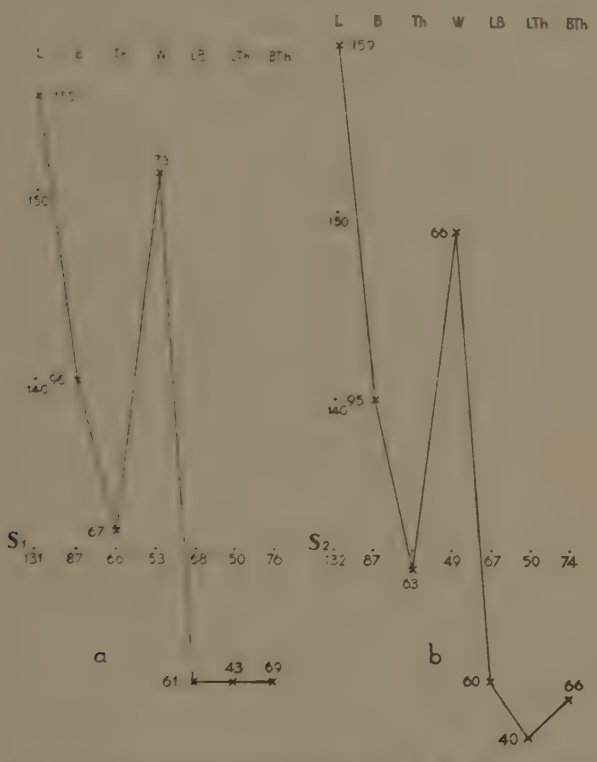

Fig. 1. *a*. Characterogram of 4 p l b. initial bean of pl. 81, F_2-1934 for pl. 73, F_3-1935. *b*. Idem of the averages of the beanyield of pl. 73, F_3-1935. S_1 = Standardcharacterogram of 1934. S_2 = Standardcharacterogram of 1935.

vinden we in ieder van deze groepen slechts één boon met een niet zeer grote lengte, l = 14.7 en = 14.8 mm. Onder de 12, resp. 10 bonen van de F_3-generatie van 1935 vinden we 3, resp. 6 bonen met een niet zeer grote lengte. De kleinste lengte van de 1ste groep is 14.6, die van de 2de is 14.1 mm.

In de volgende breedte-klassen b = 10.3 mm e.v. (tab. 3) blijven we in de groepen van de I-lijn slechts zeer enkele bonen met een niet zeer grote lengte aantreffen. De kleinste lengte, l = 14.8 mm, is van een boon met de breedte b = 10.0 mm. Van de bonen van de breedte-klassen b = 10.3 mm, e.v. van de F_3-generatie wordt de gemiddelde lengte regelmatig kleiner; het aantal bonen in ieder van deze klassen is vrij groot. Van de bonen

met een breedte b = 10.3, b = 10.2 en b = 10.1 mm, is de kleinste lengte resp. l = 13.7, = 13.6 en = 13.6 mm.

We vinden dus onder de bonen met een grote breedte, b = 11.3—10.1 mm, van de F_3-generatie meerdere bonen met een niet zeer grote lengte, l = 15.5—13.6 mm.

Bij bonen met een dergelijke grote breedte b = 11.3—10.1 mm van de I-lijn van 1935, vinden we slechts een zeer enkele boon met een niet zeer grote lengte. De boon met de kleinste lengte is l = 14.6 mm.

Bij het F_3-materiaal zijn bonen met een zo kleine lengte, als ze onder de bonen van de I-lijn niet voorkomen. Deze verschillende bevinding laat zich verklaren uit de verschillende erfelijke samenstelling van deze groepen van bonen van de F_3-generatie en van de I-lijn, iedere groep met dezelfde grote breedte. De formule voor de lengte en de breedte is van alle bonen van de I-lijn dezelfde, nl. $L_1 L_2 B_1 b_2$. Onder deze bonen van de F_3-generatie zijn er met de formule $L_1 L_2 B_1 b_2$ als van de I-lijn (of tot dit gebied behorend), maar ook met de formule $L_1 l_2 B_1 b_2$.

De geleidelijke afname van de gemiddelde lengte der bonen van de op elkaar volgende breedte-klassen (tab. 3) wijst in de eerste plaats op de positieve correlatie van de lengte en de breedte, — we treffen de geleidelijke afname ook aan voor de I-lijn —, en ook op de erfelijkheid door polymere factoren. L_1 en L_2, B_1 en b_2 staan ieder voor een groep polymere factoren (L_1—L_3 en L_4—L_6; B_1—B_3 en b_4—b_6).

Het aantal bonen van ons F_3-materiaal is voor de breedten 10.0—9.6 mm, vrij groot, het aantal bonen met een niet zeer grote lengte neemt, vergeleken bij dat met een zeer grote lengte, zeer toe. Onder de bonen van de I-lijn met dezelfde breedten van 10.0—9.6 mm, zijn naar verhouding veel meer bonen met een zeer grote lengte. Dit verschil van bonen van de F_3-generatie en van die van de I-lijn, berust hierop, dat in de formule van de lengte en de breedte van deze bonen met geleidelijk minder grote breedte, de homozygotie der bonen afneemt. Het best voor ons onderzoek lenen zich de groepen der grootste breedten en hier vinden we een goede aanwijzing voor het voorkomen, in het F_3-materiaal, van bonen met voor de lengte en de breedte de formule $L_1 l_2 B_1 b_2$ naast bonen met de formule $L_1 L_2 B_1 b_2$, d.w.z. onder de bonen met de grootste breedten zijn er met de formule $L_1 L_2 B_1 b_2$ en $L_1 l_2 B_1 b_2$.

In onze eerste mededeling (1947) groepeerden we de bonen volgens afnemende lengte en als aanwijzing voor de bevestiging van onze hypothese, vonden we daar, dat in de groepen met de grootste lengten, de gemiddelde breedte dezelfde was; eerst in de latere groepen, daalde met de lengte, de gemiddelde breedte der bonen regelmatig. Ook hier de aanwijzing, dat bonen met de grootste lengten (formule $L_1 L_2$), dezelfde grote gemiddelde breedte ($B_1 b_2$) hebben als bonen met minder grote lengten (formule $L_1 l_2$). In tab. 4 zijn enige voorbeelden van F_3-bonen van 1935 met de grootste breedten en één met zeer grote lengte bijeengebracht en

TABLE 4. F_3-1935. Some examples of beans with great breadths and not very great lengths and comparisonbeans of the I and the II-line.

Pl.	Bean	L	B	Th	W	LB	LTh	BTh
36	1p 1b	148	107	66	70	72	45	62
36	1p 3b	146	107	65	66	73	45	61
87	6p 2b	141	106	59	60	75	42	56
68	9p 1b	146	105	77	83	72	53	73
87	10p 2b	146	105	73	74	72	50	70
87	6p 6b	141	104	71	74	74	50	67
87	6p 4b	137	103	56	59	75	41	54
58	5p 2b	139	102	65	67	73	47	64
82	3p 3b	136	102	69	73	75	51	68
65	9p 3b	137	101	76	73	74	56	75
103	1p 2b	140	101	65	65	72	46	64
	Comparisonbeans of the I-line (very rare)							
1	4p 3b	148	111	65	78	75	44	69
4	8p 2b	146	107	66	70	73	45	62
20	5p 2b	148	105	61	64	71	41	58
4	1p 4b	147	104	52	55	71	35	50
10	16p 2b	153	103	67	72	67	44	65
	Comparisonbeans of the II-line (very rare)							
28[1]	5p 4b	118	98	75	58	83	64	77
28[1]	12p 2b	122	98	74	59	80	61	76
22	8p 2b	130	97	67	55	75	52	69

enkele zeer zeldzame vergelijkbonen van de I- en de II-lijn. Deze F_3-bonen hebben een hoge L B-index, evenals de bonen van cl. 5 met de formule l B Th van ons schema. De dikte is verschillend. Van bonen met een kleine dikte is de B Th-index laag, ze komen overeen met de bonen van cl. 6 met de formule 1 B th. Deze F_3-bonen met een grote dikte hebben een matig hoge B Th-index. Ze komen overeen met bonen van cl. 1a met de formule $L_1\, l_2$ B Th. Bonen met de formule $L_1\, l_2\, B_1\, b_2$ voor de lengte en de breedte hebben een grote absolute breedte en een hoge L B-index.

De hypothese (1947, l.c., blz. 800), waarbij aangenomen wordt, dat het grootte-verschil der lengten op de werking van een even groot aantal polymere factoren in de dominante homozygote vorm berust als dat der breedten en dikten, doch dat de werking van een factor voor het grootte-verschil van een lengte-factor beduidend groter is dan die van een factor voor de breedte en voor de dikte *kan* het voorkomen van bonen met een grote breedte en een niet zeer grote lengte ook verklaren, maar de verwachting van dergelijke bonen (dus met de formule voor de lengte en de breedte $L_1\, l_2\, B_1\, b_2$ naast die met de formule $L_1\, L_2\, B_1\, b_2$) is bij de door ons aangenomen hypothese veel groter.

De verschillende erfelijke samenstelling van F_2-bonen brengt mee, dat de F_3- bonenopbrengsten onderling zeer zullen verschillen. In tab. 5 zijn

enige bonenopbrengsten van de F_3-zaadgeneratie met de grootste gemiddelde breedten en enkele vergelijk-bonenopbrengsten van de I- en de II-lijn bijeengebracht. We vinden, dat van de bonenopbrengsten met de grootste gemiddelde breedten, de gemiddelde lengte van de bonenopbrengsten van de I-lijn steeds zeer groot is (l_m = 16.6—15.8 mm, eenmaal

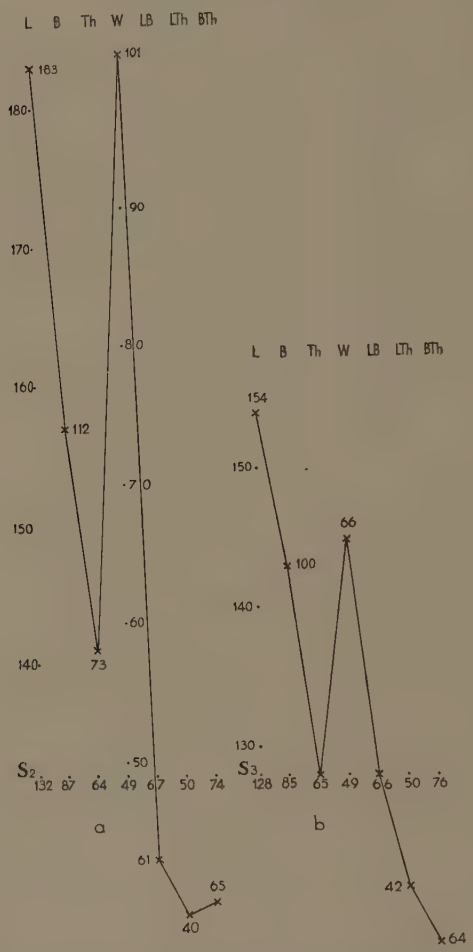

Fig. 2. *a.* Characterogram of 2 p l b, initial bean of pl. 73, F_3-1935 for pl. 309, F_4-1936. *b.* Idem of the averages of the beanyield of pl. 309, F_4-1936. S_3 = Standardcharacterogram of 1936.

is l_m = 151.9 en = 149.3 mm). Onder bonenopbrengsten van de F_3-zaadgeneratie zijn er enkele, die, — ofschoon de gemiddelde breedte zeer groot is —, een niet zeer grote gemiddelde lengte hebben. De grootste gemiddelde breedte van bonenopbrengsten van de II-lijn is 9.04 mm, d.i. kleiner dan de gemiddelde zeer grote breedten, die we hier beschouwen; de gemiddelde lengte is 12.08 mm.

Bij de F_3-bonenopbrengsten van 1935 met een grote gemiddelde breedte

zijn er enkele, met een kleine gemiddelde lengte, zoals ze bij de bonenopbrengsten van de I-lijn met eenzelfde grote gemiddelde breedte niet voorkomen. Deze bevinding wijst er weer op, dat, onder de F_3-bonenopbrengsten met een grote gemiddelde breedte, er met een andere erfelijke samenstelling van de lengte en de breedte zijn dan bij de bonenopbrengsten van de I-lijn. Van alle bonenopbrengsten van de I-lijn is de formule voor de lengte en de breedte $L_1 L_2 B_1 b_2$, onder die van de F_3-zaadgeneratie zijn er met de formule $L_1 L_2 B_1 b_2$ en ook andere met de formule $L_1 l_2 B_1 b_2$.

Statistics. — *Random sampling frequencies; an implement for rapidly constructing large-size artificial samples.* By H. C. HAMAKER. (Laboratorium voor Wetenschappelijk Onderzoek der N.V. Philips' Gloeilampenfabrieken Eindhoven–Nederland.) (Communicated by Prof. H. B. G. CASIMIR.)

(Communicated at the meeting of March 26, 1949.)

Artificial sampling is, no doubt, the chief purpose to which tables of random sampling numbers have been constructed and applied. To fix our argument, let us suppose that we wish to sample the Poisson distribution with parameter $m = 2$, which yields the cumulative frequencies listed below.

TABLE I.

Cumulative frequencies of the Poisson distribution with $m = 2$.

0	.1353	5	.9834
1	.4060	6	.9955
2	.6767	7	.9989
3	.8571	8	.9998
4	.9474	9	1.0000

Then referring to a table of random sampling numbers arranged in sets of 4 digits, we score a 0 for each number lying between 0000 and 1353, we score a 1 for numbers between 1353 and 4060, a 2 for those between 4060 and 6767, and so on; this is a common procedure which does not need further explanation.

If it is our purpose to investigate certain properties of small samples, the taking of individual scores will be unavoidable, even though this may involve some tedious labour; but if we intend to study the properties of large samples, the work involved will soon become prohibitive, and the question arises whether it is possible to devise a more rapid and convenient method for the constructing of random samples of a large size. Such a method will be described below.

We begin by observing that as we score a 0 for all numbers from 0000 to 1353, we may score a 0 for all numbers beginning with 00 to 12 without any further knowledge of the two digits that follow; likewise all numbers beginning with a pair between 14 and 39 will score a 1 regardless of the two final digits. It is only for numbers beginning with 13, 40, etc., that we require to know the last two digits as well.

Let us then for a moment neglect the last two digits . We take 1000 pairs of two-digit random sampling numbers and we score these in a 10×10 array, thereby obtaining the frequencies recorded in table II.

The classes and the frequencies in this table will be designated as the array-classes and the array-frequencies, to distinguish them from the sample-classes and the sample-frequencies relating to the sample that we are going to construct from them.

TABLE II.

1000 two-digit random sampling numbers scored in a 10×10 array.

First digit	Second digit										Totals
	0	1	2	3	4	5	6	7	8	9	
	Array-frequencies										
0	13	14	9	7	5	11	5	11	10	10	95
1	4	5	9	7	10	14	9	11	9	9	87
2	12	9	7	11	8	9	4	5	15	10	90
3	9	9	16	11	9	9	7	8	10	8	96
4	8	8	5	11	10	8	10	17	16	15	108
5	16	14	14	9	8	17	5	9	13	7	112
6	10	7	7	13	10	11	10	6	12	14	100
7	7	6	5	11	12	11	11	7	10	14	94
8	4	15	9	15	15	9	11	14	7	13	112
9	8	8	14	10	7	14	11	15	6	13	106
Totals	91	95	95	105	94	113	83	103	108	113	1000

With the aid of the array of table II we may now rapidly construct a random sample of 1000 scores of the population specified by table I in the following manner:

The frequencies in the array-classes 00 to 12 are added giving a score of 113 entirely belonging to sample-class 0. In the array-class 13 we have a score of 7 and to allot these to sample classes 0 and 1 we have to tag two more digits behind them, and then to divide the resultant set of 4-digit numbers into those below and those above 1353 (see table I); from a table of random sampling numbers we select a random set of 7 two-digit figures, for instance

12 17 77 82 46 33 97;

four of these are less than 53, and hence we decide that of the seven scores in array-class 13, 4 have to go into sample-class 0, and the other 3 into sample-class 1. The total score in sample class 0 will then be $113 + 4 = 117$.

Next we add the frequencies in the array-classes 14—39, giving a total of 248; the score of 8 in array-class 40 is again subdivided by a set of 8 two-digit random sampling numbers, 3 going into sample-class 1, and 5 into sample-class 2. The total in sample class 1 is now also complete, viz: 3 (from array-class 13) + 248 (from array-classes 14—39) + 3 (from array-class 40) = 254.

Thus we proceed until we have reached the array-class 99, which has to be subdivided into four sets, those below 55, those between 55 and 89,

those between 89 and 98, and those above 98, going into the sample-classes 6, 7, 8 and 9 respectively (compare table I). The sample will then be complete. The entire procedure is illustrated in table III.

TABLE III.

Illustrating the construction of a random sample of 1000 from the distribution of table I by means of the array-frequencies of table II.

Sample class	Array classes	Array frequencies	Sample frequencies	Theory
0	00—12	113	117	135
	13	7 → 4, 3		
1	14—39	248	254	271
	40	8 → 3, 5		
2	41—66	280	291	271
	67	6 → 6, 0		
3	68—84	178	185	180
	85	9 → 7, 2		
4	86—93	85	92	90
	94	7 → 5, 2		
5	95—97	40	43	36
	98	6 → 1, 5		
6			9	17
7	99	13 → 4, 7, 2	7	
8			2	

$\chi^2 = 6.28$; $\nu = 6$; $P = 0.395$

So far this method cannot claim to effect much saving of labour. In constructing our sample, however, we started in the left-hand top corner of the array of table II, and we proceeded from left to right and from the top to the bottom of this array; and a considerable saving of labour can be achieved by observing that there is no reason for using the array-frequencies precisely in this order. All the array-frequencies are equivalent to one another, and in constructing a sample we may start at any point in the array and proceed in any direction; or, more general still, we may rearrange the frequencies of table II at random in any of their 100! permutations before we start making up our sample. The simplest method to achieve this is to write the array frequencies on 100 chips of card board, mix these thoroughly and lay them out in random order while constructing the sample.

If we use invariably the same set of array-frequencies (for instance those of table II) we may expect our samples to be on the average slightly biassed in one way or another, though the variability obtained by rearrranging is so large that serious bias is hardly to be expected. Nevertheless it seems inadvisable to use one set only, and I have therefore constructed ten independent arrays (as that in table II), from which one may be chosen at random every time we wish to construct a sample; thereby the possibility of systematic bias should be ruled out.

TABLE IV.

Ten sets of random sampling frequencies for sample size 1000.

Set Nr	1	2	3	4	5	6	7	8	9	10
Array-freq. f	Frequencies of the array-frequencies = n									
2	—	1	1	—	—	—	—	—	—	—
3	1	—	1	1	—	1	—	1	—	1
4	2	1	4	1	3	1	1	3	5	3
5	3	7	4	4	7	2	5	3	5	8
6	4	6	5	8	3	7	9	9	6	3
7	8	9	6	3	11	9	10	11	10	8
8	11	11	8	17	9	12	7	6	8	6
9	16	14	15	11	15	9	12	12	14	14
10	17	9	17	13	12	19	14	13	10	13
11	8	10	5	10	12	9	9	8	9	20
12	9	7	15	12	3	13	11	10	3	2
13	11	9	6	6	5	8	10	8	15	5
14	5	7	3	6	9	6	5	5	5	7
15	1	5	7	6	6	1	2	6	5	4
16	2	—	—	1	3	1	3	4	2	3
17	1	2	1	1	2	—	2	1	2	2
18	—	—	—	—	—	1	—	—	1	1
19	1	2	—	—	—	1	—	—	—	—
20	—	—	1	—	—	—	—	—	—	—
21	—	—	1	—	—	—	—	—	—	—
Σn	100	100	100	100	100	100	100	100	100	100
Σnf	1000	1000	1000	1000	1000	1000	1000	1000	1000	1000
s_f^2	8.42	11.26	11.50	8.62	10.50	8.20	9.14	10.54	11.32	10.70

If we use the array-frequencies not in the form of table II, but as a lottery with 100 lots drawn without replacement, the actual array will be quite immaterial; it will only be important to know the frequencies of the array-frequencies. These I shall call the "*random sampling frequencies*"; for the ten arrays actually constructed they have been recorded in table IV above; set Nr 5 corresponds to table II.

Also in table V an independent set of random sampling frequencies have been provided for the construction of samples of size 500, and in table VI a set for sample size 200.

Samples of other sizes may be obtained by combination; for instance, if we require a sample of 1500 we may construct two samples, one of

1000 and one of 500 scores, and then add their frequencies; or alternatively by laying out one set of 100 random sampling frequencies for sample size 1000 and one set for sample size 500 in a 10×10 array, and by adding the array-frequencies we obtain a set of random sampling frequencies for sample size 1500, from which by permutation any number of samples of this size may be constructed. If we desire a sample of exactly 1537 scores we have only to add 37 more made up in the usual way. Thus the sets of frequencies in tables IV, V, and VI should be amply sufficient for a great variety of purposes.

TABLE V.

Ten sets of random sampling frequencies for sample size 500.

Set Nr	1	2	3	4	5	6	7	8	9	10
Array freq. f	Frequencies of the array-frequencies = n									
0	1	2	—	—	1	—	—	—	—	2
1	3	3	2	3	6	—	3	3	1	2
2	9	9	5	13	7	10	10	5	11	8
3	13	13	15	20	10	19	21	19	12	13
4	23	17	25	11	21	17	15	15	18	15
5	15	13	19	16	16	18	16	23	17	20
6	8	19	13	12	16	13	10	12	20	18
7	12	12	10	6	10	11	7	12	11	12
8	8	6	3	5	5	4	10	7	7	5
9	5	3	6	10	5	5	2	1	1	2
10	1	1	—	2	1	1	3	1	—	1
11	2	—	2	1	—	1	1	1	2	1
12	—	2	—	1	1	1	—	—	—	1
13	—	—	—	—	1	—	2	1	—	—
Σn	100	100	100	100	100	100	100	100	100	100
Σnf	500	500	500	500	500	500	500	500	500	500
s_f^2	5.34	5.40	4.10	6.32	5.64	4.66	6.36	4.48	3.96	4.74

TABLE VI.

Ten sets of random sampling frequencies for sample size 200.

Set Nr	1	2	3	4	5	6	7	8	9	10
Array-freq. f	Frequencies of array-frequencies = n									
0	18	12	16	14	10	14	16	12	14	14
1	18	30	21	26	27	24	27	24	28	27
2	30	25	32	31	31	33	25	32	24	30
3	18	18	18	12	24	13	16	21	21	12
4	12	10	7	12	3	11	9	7	7	11
5	4	4	3	3	3	3	5	3	3	4
6	—	1	3	1	2	2	1	1	3	1
7	—	—	—	1	—	—	—	—	—	1
8	—	—	—	—	—	—	1	—	—	—
Σf	100	100	100	100	100	100	100	100	100	100
Σnf	200	200	200	200	200	200	200	200	200	200
s_f^2	1.92	1.88	2.06	2.10	1.62	1.92	1.76	1.64	2.08	2.16

It may be added that these random sampling frequencies were all derived from tables of random sampling numbers constructed as described in a previous paper [1].

To conclude this paper let us briefly discuss a practical application. In tables VII and VIII we have represented two sets of ten samples each of 1000 units taken from the population specified in table I; the first set (table VII) was constructed by using the random sampling frequencies of set Nr 1 in table IV in ten different permutations, while the second set (table VIII) was obtained by using the ten sets of table IV each once. For each sample we have computed the first, second and third moments about the origin, and χ^2, and from these the average moments and the standard deviations have been calculated.

TABLE VII.

Ten random samples of the Poisson distribution with $m = 2$ constructed from *one set* of random sampling frequencies in ten different permutations.

Sample class	10 samples constructed from set Nr 1, table IV — Frequencies										Theory
0	127	146	147	148	155	146	145	128	138	129	135
1	282	267	257	301	247	272	270	265	264	277	271
2	285	271	259	236	269	265	253	271	276	266	271
3	157	178	178	170	178	190	183	177	176	179	181
4	90	88	98	91	89	89	97	110	89	100	90
5	42	35	40	31	48	29	36	30	38	30	36
6	14	10	17	18	11	8	11	13	17	13	} 16
7	1	4	3	4	3	1	3	5	2	6	
8	2	1	1	1	—	—	2	1	—	—	
	1000	1000	1000	1000	1000	1000	1000	1000	1000	1000	
m'_1	2.000	1.966	2.032	1.946	2.002	1.928	2.996	2.049	2.006	2.016	
m'_2	6.01	5.86	6.29	5.91	6.09	5.53	6.05	6.23	6.04	6.06	
m'_3	22.2	21.3	23.6	22.3	22.3	18.9	22.4	23.0	22.0	22.2	
χ^2	5.85	1.21	4.22	13.03	9.53	6.26	2.52	6.30	0.98	3.09	

$$\overline{m'_1} = 1.994; \qquad s_{m'_1} = 0.036$$

$$\overline{m'_2} = 6.007; \qquad s_{m'_2} = 0.200$$

$$\overline{m'_3} = 22.02\ ; \qquad s_{m'_3} = 1.19$$

In computing χ^2 the frequencies of the last three rows were pooled, which reduces the number of classes to seven and the number of degrees of freedom to six; the 95 % and 5 % points of the χ^2-distribution are then 1.64 and 12.59 respectively. On comparing with tables VII and VIII we see that out of a total of 20 values of χ^2 two (0.98 and 1.21) lie below the 95 % point and one (13.03) lies above the 5 % point: quite an acceptable result. It will be noted that these three somewhat outlying

[1]) H. C. HAMAKER, Proc. Kon. Ned. Akad. v. Wetensch., Amsterdam, **52**, 145—150 (1949).

values all occur in table VII, and if we restrict our attention to this table, we have an event with a chance 1/10 that has occurred 3 times in a series of 10 trials; the binomial probability of three or more such events is easily computed to be 0.07, which is still above the customary significance limit.

TABLE VIII.

Ten random samples of the Poisson distribution with $m = 2$ constructed from *ten different sets* of random sampling frequencies.

Set Nr	1	2	3	4	5	6	7	8	9	10	Theory
Sample class	Frequencies										
0	123	131	138	124	143	132	131	141	146	121	135
1	276	249	253	288	265	285	257	267	268	295	271
2	267	279	278	273	267	278	296	263	247	264	271
3	199	187	173	176	194	162	174	178	187	185	181
4	77	88	98	90	84	91	90	91	98	86	90
5	41	45	38	34	37	34	32	38	42	35	36
6	12	19	12	11	10	14	14	16	7	10	
7	4	1	7	3	—	3	5	4	4	4	
8	1	1	1	1	—	1.	1	2	1	—	16
9	—	—	2	—	—	—	—	—	—	—	
	1000	1000	1000	1000	1000	1000	1000	1000	1000	1000	
m'_1	2.028	2.074	2.057	1.987	1.962	1.974	2.018	2.021	2.003	1.985	
m'_2	6.08	6.38	6.44	5.86	5.71	5.88	6.06	6.23	6.07	5.82	
m'_3	22.3	23.7	25.1	21.1	19.8	21.5	22.3	23.6	22.2	20.8	
χ^2	5.71	5.86	4.45	2.36	4.59	3.23	4.61	2.57	6.19	4.43	

$$\overline{m'_1} = 2.011; \qquad s_{m'_1} = 0.024$$
$$\overline{m'_2} = 6.053; \qquad s_{m'_2} = 0.230$$
$$\overline{m'_3} = 22.24 : \qquad s_{m'_3} = 1.47$$

Moreover, the ten samples of table VII were derived from the set of random sampling frequencies Nr 1 in table IV which possesses a standard deviation somewhat below the theoretical value; if anything, we should therefore expect the variability between the samples of table VII to be less than normal, though it is extremely unlikely that such a tendency should already be apparent in so small a series of samples. These arguments render it highly probable, however, that the comparatively large variations in χ^2 in table VII are accidental, and are not in any way connected with the particular method by which the samples were obtained.

The average moments in tables VII and VIII lie close to their theoretical values, which are 2.00, 6.00, and 22.00 respectively. The standard deviation of the moments computed from each of these tables separately are in satisfactory agreement, and these standard deviations offer perhaps the best illustration of the usefulness of the methods described in this paper;

by constructing a set of large-size samples we may rapidly estimate the standard error of any statistic computed from them, while avoiding involved mathematical arguments which are all too often incomprehensible to the practical statistician; and the method also applies to cases not amenable to mathematical treatment.

I should like to express my indebtedness to Mr. H. A. C. v. d. LINDEN for his careful assistance in carrying out this investigation.

Eindhoven, 19 December 1947.

Crystallography. — *Transformation of gnomograms and its application to the microchemical identification of crystals.* I. By D. W. DIJKSTRA. (Memorandum of the Crystallographic Institute of the Rijks-Universiteit at Groningen.) (Communicated by Prof. J. M. BIJVOET.)

(Communicated at the meeting of February 26, 1949.)

Summary. The method of construction, dealt with in this article, allows: 1° the transition to another plane of projection, crystallographic axes of reference and parametral plane remaining the same (rotation, Umwälzung), 2° the transition to other axes and parametral plane (transformation in a narrower sense).

Here it is not the crystal, that will be rotated (as usual) into another position with respect to the plane of drawing, which does not alter its position, but the crystal remaining stationary the projecting lines are made to cut out another gnomogram in a new plane, which may have any position with respect to the original plane of drawing. This plane is revolved to coincide with the picture plane, and then the old gnomogram and the new one will be found to be related by the principle of central collineation. The form of the collineation is a very simple one, so the constructions can be effected with only few lines and practically only with a ruler (§ 6, 8, 9 and 10).

The most usual types of gnomogram are considered to be particular cases of one general gnomogram (§ 1, 2 and 3).

As an application the identification of a crystal of silverdichromate, measured by microscope, will be described (§ 11*b*).

§ 1. In the most usual gnomogram the zone lines are equidistant parallel lines because of the particular position of the plane of projection, the latter being perpendicular to one of the axes of reference.

In the general form of the gnomogram, however, the plane of projection may have any position.

In practice this may occur inter alia in the under mentioned cases:

a. In measuring efflorescent or deliquescent crystals time may be insufficient to adjust the crystal on the two-circle goniometer. Measurements are taken with the crystal in an arbitrary position and this will result in a general gnomogram.

b. With some crystals the planes are arranged in a small number of zones, intersecting in a face actually occurring on the crystal. In measuring these "face adjustment" [1]) will be profitable. When plotting the measure-

[1]) M. H. HEY, Min. Mag. **23**, 560 (1932).

ments one will find a gnomogram with the plane of projection coinciding with a face of the crystal, and the latter being in general not perpendicular to a possible edge, the form of the gnomogram will be the general one.

c. When reducing Laue photographs one often meets with gnomograms with arbitrary planes of projection [2].

§ 2. When passing from the particular to the general gnomogram the normal pattern of fig. 1*a* changes into that of fig. 1*b*.

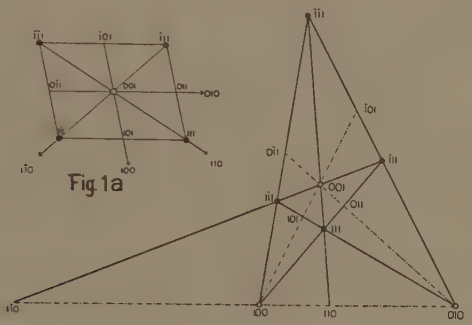

Fig. 1a

Fig. 1b

This figure 1*b* is a complete quadrangle with as its angular points the "octahedral faces": (111), ($\bar{1}$11), ($\bar{1}\bar{1}$1) and (1$\bar{1}$1) (for the sake of clearness its sides are represented by full lines, its diagonals by dotted ones). The "cube faces" (100), (010) and (001) are the diagonal points; the four zone lines through each "cube point" form a harmonious pencil of lines, being two sides and two diagonals of the complete quadrangle.

In order to construct in this general gnomogram the zone lines corresponding to the equidistant parallel zone lines of the ordinary gnomogram represented in fig. 2*a*, the rays (100)–(001) and (100)–(111) in

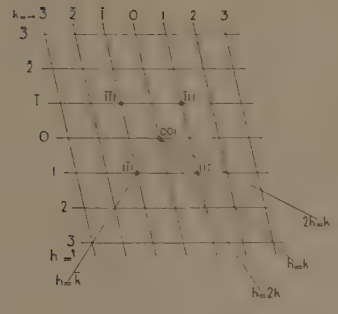

Fig. 2a

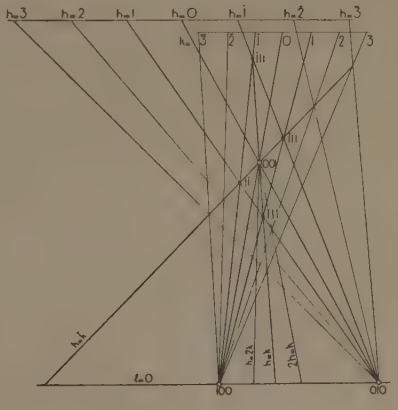

Fig. 2b

[2] See e.g. R. W. G. WYCKOFF, "The structure of Crystals" (1924) p. 139, fig. 108.

fig. 2*b* (the points (100), (010), (001) and (111) being given) are intersected with a line parallel to the ray (100)–(010), and then on this line pieces are laid off equal to the piece cut off by the rays just mentioned (fig. 2*b*). The connection of the division points, found in this way, with the point (100) results in the pencil through (100), and then a corresponding construction gives the one through (010).

§ 3. *a.* The first particular case of this general gnomogram mentioned here, is the ordinary gnomogram; the line (100)–(010) in this case is the line at infinity of the plane, and that converts the pencils into systems of equidistant parallel lines.

b. Another particular case is that of the trigonal notation according to MILLER. Here the "dodecahedron zone" $(1\bar{1}0)$–$(0\bar{1}1)$–$(\bar{1}01)$ [3]) is the line at infinity (fig. 3).

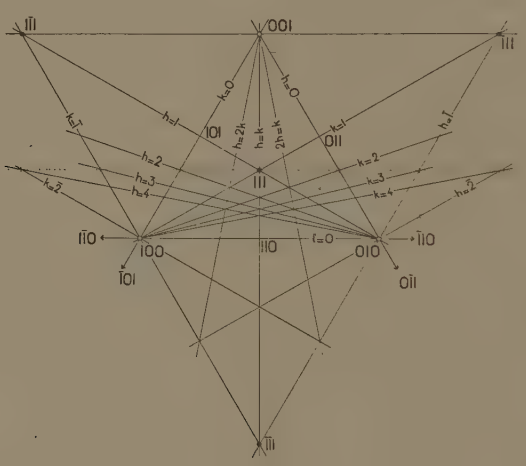

Fig. 3

c. In the regular system the "triangular gnomograms" are identical with those according to MILLER's notation; in the other systems their form is the general one [4]).

§ 4. In the usual methods [5]) of transforming gnomograms the crystal will be made to rotate the plane of drawing remaining stationary (Umwälzung), which results in the gnomogram thus constructed having the same gnomon circle as the original one. The new place of the pole is found by construction or by means of a "gnomonic net".

---

[3]) This is the zone [111].

[4]) R. L. PARKER, Schw. Min. Petr. Mitt. XVII, 475 (1939).
P. TERPSTRA, "Kristallometrie", p. 103 seqq.

[5]) See e.g. V. GOLDSCHMIDT, "Über Projection und graphische Krystallberechnung" (1887) p. 68.
H. E. BOEKE, "Die gnomonische Projection etc." (1913) p. 26.
F. E. WRIGHT, Am. Min. **17**, 422 (1932).

Let us take WRIGHT's method by way of example. (In § 7 WRIGHT's construction will be shown to become formally identical with this method of ours, by only a slight alteration.)

In fig. 4 the crystal is to be rotated, the result being the coincidence of the pole P' with the centre of the gnomon circle. First thing to do is to construct the angle of rotation $P'C_nO$; this is bisected by the line $C_nR_{p'}$, and in $R_{p'}$ the line i_1 is drawn perpendicular to $P'O$. At the same distance from O, but this time on the other side, the line $i_2 \parallel i_1$ is drawn. These lines i_1 and i_2 are WRIGHT's "isometric lines".

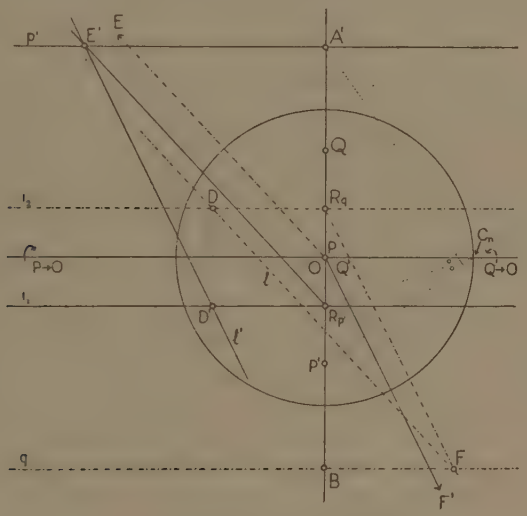

Fig. 4

The rotation makes a point D' on i_1 coincide with a point D on i_2.

Next the trace p' of the plane P' is constructed; now the point $R_{p'}$ will be the angle point of the line p' ($\angle A'R_{p'}C_n = 90° - \frac{1}{2}\angle OC_nP'$, $\angle A'C_nR_{p'}$ is so too; so $A'C_n = A'R_{p'}$). By rotation p' goes to infinity, making O the new angle point. This means that after the rotation a point E' on p' has come at the point at infinity of the line drawn through $O \parallel R_{p'}E'$. Thus the point at infinity of the line $R_{p'}E'$ will represent the point E corresponding to the point E'.

The zone line l conjugate to a given zone line l' through D' and E' is obtained by connecting D and E, this being the line through D parallel to $R_{p'}E'$.

§ 5. In our method the crystal itself is not rotated; the projecting rays from the centre O, however, are made to intersect not only the original plane of drawing but another one too, which may have any position with respect to the former, provided that its distance to the centre of projection — as that of the former plane — is equal to the radius of the gnomon-circle. Each pair of corresponding points lying on the same ray from the

centre of projection, the figures in both planes are in perspective with one another.

In fig. 5 τ' represents the original plane of drawing in which lies the gnomogram to be transformed, and τ the new plane of drawing. Both planes are tangent to the sphere, having the centre of projection O for centre and the gnomon for radius, and their intersection is the line d. The plane through O perpendicular to d is the plane of drawing in our figure. O' is the centre of the gnomon circle and P' is the pole of the plane τ in the original gnomogram. The plane τ_p, through O parallel to τ, intersects τ' by the vanishing trace v'; the plane τ'_p, through O parallel to τ', intersects τ in the vanishing axis w.

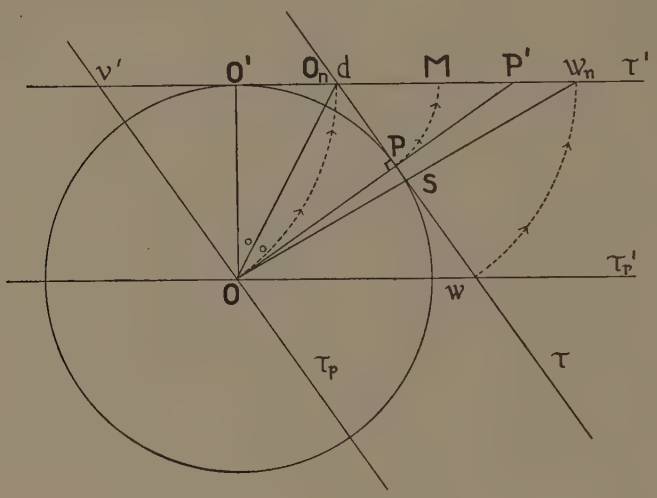

Fig. 5

The distances of the parallel sides in the parallelogram $v'Owd$ being equal $v'Owd$ is a rhomb, which makes $v'O = v'd$ and $v'd = dw$.

Now τ_p is revolved round v' into τ', and τ in the same direction round d, likewise into τ'. This revolution makes O (afterwards called O_n) come on d and the vanishing axis w at w_n, $v'd$ being equal to dw_n. The centre P of the gnomon circle in the new plane τ comes at M, while $O'd = dP = dM$. Now the figure in the plane τ' will look like fig. 9 without the point O drawn there.

The revolution has made the old gnomogram in τ' and the new one in τ, formerly being in perspective to one another, now to be related by the principle of central collineation, the line d being the principal axis of the collineation, the lines v' and w_n, on either side of and at an equal distance from d, being the secondary axes and the point O_n on the line d the centre of collineation.

The central collineation has the following properties, as will be proved in § 6:

a. Each line l' of the original gnomogram intersects its conjugate l of the new one in a point on the principal axis d.

b. Each line through O_n coincides with its conjugate.

c. A set of parallel lines l' changes into a pencil l through Q, the point of intersection of the secondary axis w_n and the line through O_n parallel to l' (fig. 6*a*).

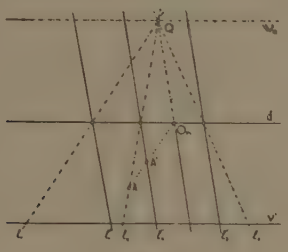

Fig 6a

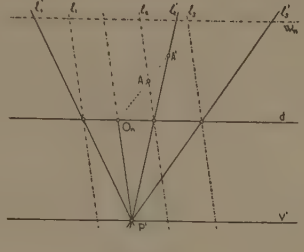

Fig. 6b

d. A pencil l' through the point P' on the secondary axis v' changes into a set of parallel lines l, parallel to the line connecting P' and O_n (fig. 6*b*).

e. Conjugate points A' and A lie on one straight line through O_n.

§ 6. In order to prove these properties fig. 5 has been copied stereometrically in fig. 7. The letters are the same as in figg. 5 and 6, in figg. 5 and 7 the index n being added after revolution.

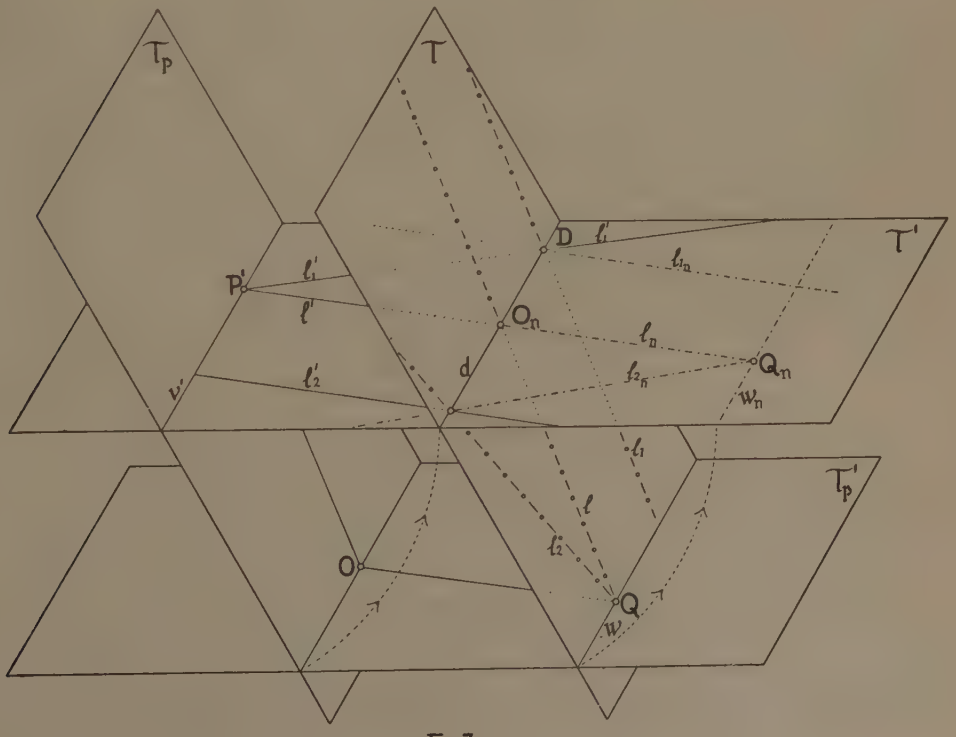

Fig. 7

a. The rays from O, projecting the line l_1, describe a plane through O and l_1; the intersection of this plane and τ' is the line l'_1 conjugate to l_1. The intersection D of this plane and the line d is a point common to l_1 and l'_1 and this point D remains stationary during the revolution; so the point of intersection of l'_1 and l_{1n} too will lie on the principal axis d.

b. The rays from O projecting the line l through O_n will lie in a plane through O and l. The parallelogram $O_nP'OQ$ formed by the intersections of this plane with the planes τ, τ', τ_p and τ'_p will be a rhomb.

During the revolution $P'O_n$ remains stationary, the parallelogram hinges in its corners, OQ remaining parallel to $P'O_n$. When finally O has come at O_n, Q coincides with Q_n on $P'O_n$ produced, so O_nQ $(= l)$ becomes O_nQ_n $(= l_n)$, l_n being l' produced.

c. The intersections of any set of planes through OQ with τ will form a pencil of lines $l, l_2 \ldots$, having Q for its vertex, and those with τ' a set of parallel lines $l', l'_2 \ldots$. After the revolution the pencil will lie in the plane τ' with Q_n for its vertex, O_nQ_n being parallel to the set $l', l'_2 \ldots$.

d. The intersections of any set of planes through OP' with τ' will form a pencil of lines $l', l'_1 \ldots$, having P' for its vertex, and those with τ a set of parallel lines $l, l_1 \ldots$, forming, after revolution into τ', a set of lines parallel to $P'O_n$.

e. The line O_nA' is transformed into a conjugate line O_nA, coinciding — as shown in section (b) — with O_nA'; which is another way of saying that O_n, A' and A will lie on one straight line.

§ 7. In this passage will be shown, that only a slight alteration in WRIGHT's construction will bring about formally the same results as those obtained in § 5.

In fig. 4 all the zone lines l', meeting at the point E' on p', are shown to change into a set of lines l, parallel to one another because they are all parallel to $R_{p'}E'$.

In order to deduce from the unaccented zone lines the corresponding accented ones the rotated crystal is to be turned back through the same angle, which results in Q coming at O (fig. 8). q, the trace of the plane Q, being located, the construction is an analogous one.

The zone line l meets i_2 at D and q at F; so l' is drawn through D' and E', that is through $D' \parallel OF^* \parallel R_qF$.

This way of constructing results in a set of accented lines, parallel to one another, all of them being parallel to R_qF, corresponding to a set of unaccented ones, meeting at the point F on q. In order to complete the conformity with the method based on the principle of central collineation, another modification is made in the drawing represented in fig. 4. The full lines in fig. 8 are the same as those in fig. 4 and the letters too are placed in the same way. In fig. 4 two gnomograms are drawn with the same gnomon circle, one accented, the other one unaccented.

The unaccented gnomogram is, as a whole, shifted downwards across a

distance $a = OR_q = OR_{p'}$; the accented one is translated upwards across this distance a. After translation lines and points all have got an asterisk and the lines have been changed as follows: ———— into - - - - - - - - and ···· into ····. Now the gnomon circles will be separated and i_1 and i_2 will coincide with one another.

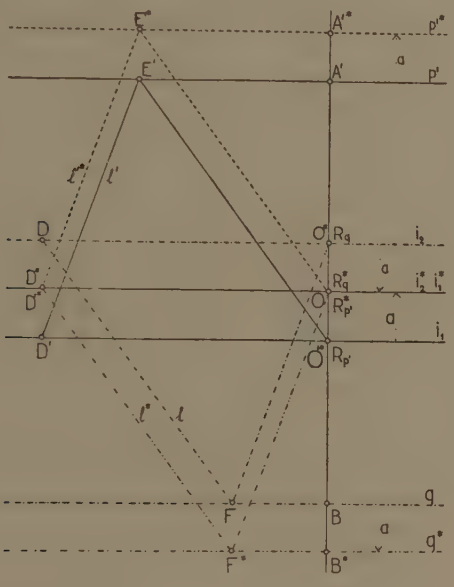

Fig. 8

The way of constructing conjugate lines is now identical with that described above in § 5; i_1^* i_2^* taking the place of the principal axis of the collineation (fig. 7), p'^* that of the vanishing trace v' and q^* that of the vanishing axis w_n. $R_{p'}^*$ (R_q^*) is the centre of the collineation O_n.

§ 8 The transformation dealt with in § 5 can be performed easily, when the lines d, v' and w_n and the centre O_n have been located.

In most cases these lines and the point O_n will have to be constructed. Three of them will be described here:

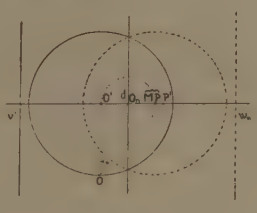

Fig 9

a. A given gnomogram is to be transformed into a gnomogram on a plane indicated by its pole P' (fig. 9). With regard to an arbitrary plane

one has to solve this problem, when wishing to reproduce a face in its true form by means of orthogonal parallel projection onto the plane of drawing, e.g. for the construction of a model of some crystal or other in pasteboard.

The zone line to the pole P' (cf. fig. 5) is constructed; this is the secondary axis v'. The line bisecting $\angle O'OP'$ intersects the original plane of projection at O_n; the line through $O_n \parallel v'$ will be the principal axis d; the other secondary axis w_n is the line parallel to d and at an equal distance from d as v'. The centre M of the new gnomon circle is found by making $O'O_n = O_nM$, the radius not being changed. In the gnomogram now constructed the pole of face P will coincide with M.

b. A transformation of a given gnomogram is required, resulting in a certain line v' in the original one changing into the line at infinity of the new one, this being the case when a gnomogram in the general form is to be transformed into one with equidistant parallel zone lines.

First P', the pole to the zone line v', is located and then the construction is completed as above (problem (*a*)).

If the zone line v' should lie beside the drawing paper and so the pole close to the centre of the gnomon circle, to begin with, a transformation should be performed promoting an arbitrary but farther removed point to centre of the gnomon circle, which then should be followed by another transformation converting the line v' of the second gnomogram into line at infinity.

c. For the sake of completeness the case will be dealt with, that the line at infinity is to be transformed into a given line w_n (figg. 5 and 10). In fig. 10 only the line w_n and the point O' are given.

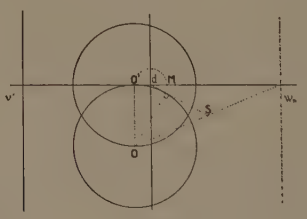

Fig 10

Now (fig. 5) O_nw_nwO will be a parallelogram, Ow and O_nw_n being parallel and equal to one another. The point of intersection S of the diagonals bisects the line Ow_n. So from S (fig. 10) the tangent to the circle is drawn and the point d results. The point M and the line v' are constructed as above (problem (*a*)).

§ 9. In order to change to other axes of reference and another parametral plane the complete quadrangle through the given poles is constructed, as indicated in the first part of this article, and this is transformed into an ordinary gnomogram as in § 8*b*.

§ 10. The construction is performed as follows. The line l conjugate to the given line l' is to be constructed.

a. The line l' (fig. 11) can be regarded as one out of the pencil through B (cf. fig. 6*b*), which will change into a set of parallel lines. The ray BO_n out of this pencil coincides with its conjugate and the line l conjugate to l' can be drawn through $A \parallel BO_n$.

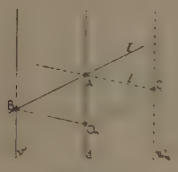

Fig. 11

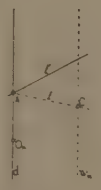

Fig. 12

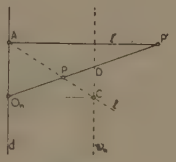

Fig. 13

b. The line l' (fig. 12) can be regarded as one of a set of parallel lines (cf. fig. 6*a*), which will change into a pencil with its vertex on w_n. The ray O_nC out of this set coincides with its conjugate, which makes C the required vertex. The line l conjugate to l' is drawn through A and C.

This construction of the point P conjugate to P' (fig. 13) turns out to be quite the same as that of the image formed by a negative lens, O_n performing the function of the optic centre and C that of the focus. Accordingly the relation between the positions of conjugate points complies with the well known formula for lenses, giving here $\frac{1}{O_nP} - \frac{1}{O_nP'} = \frac{1}{O_nD}$.

Physics. — *Photons in extensive Cosmic-Ray-Showers.* By J. CLAY. (Natuurkundig Laboratorium Amsterdam.)

(Communicated at the meeting of March 26, 1949.)

Summary.

The results are given of 6 and 8-fold coincidence measurements of extensive showers with layers of lead above and between the counters, by which the absorption of the electrons and the production of electrons in the showers could be estimated. It is clear that there are a great deal of energetic photons in these showers and the amount increases with the density of the shower particles.

By measuring 4- and 6-fold coincidences for surfaces of relative sizes from 1 to 6 the value of the coefficient S in the frequency-density relation $I = I_0 \cdot N^{-S}$ could be found and we come to the conclusion that S is not constant but varies from $S = 3{,}0$ for very small densities to $S = 1{,}5$ for high densities, which is in agreement with the frequency-density relation for bursts.

Some time ago in the extensive atmospheric showers we found an indication of a great number of photons. We were carrying out an experiment for measuring on one hand the absorption of the electrons in these showers and on the other hand the percentage of the particles therein which penetrate at least 10 cm Pb. To this purpose we were using 4 trains of two counter-sets each, which were placed in a quadrangle, each train arranged so, that the lower box could be protected by 10 cm Pb. We were anxious to measure afresh the number of penetrating particles in relation to the total number of particles, as we had found in two separate sets of measurements this relation to be 1 to 10. At the Pasadena congress of 1948 COCCONI protested that he had found a relation which was totally different from the one found by us. Therefore we repeated our experiments with two different counter arrangements in two different places, in our laboratory and in a wooden shed with a thin wooden roof where we had already made several measurements before. In both places we again found the relation 1 to 10. Vide table.

We have already stressed that when we observe two particles there are two possibilities. It may be two particles belonging to one extensive shower and it may be two coherent mesons produced in one and the same process. The variation with distance found while measuring 4-fold coincidences caused by two particles in two vertical counter-trains at not too large a distance from each other appears in either case. We thought however that we would be able to distinguish between the two cases when measuring 2 or 3 particles. And indeed when we suppose the variation of frequency of the coincidences with distance to be given by $N = N_0 e^{-ax}$, we find in the case regarding 2 particles at distances of 120 cm and 60 cm $a = 0{,}47$

and $a = 0{,}37$ respectively and in the case of 3 particles at the distances mentioned $a = 0{,}62$ and $a = 0{,}64$ cm^{-1} resp. In the frequency-distance curve for the coincidences we find a very distinct difference between the variation for slightly larger distances (up till 5 m) for two penetrating particles of extensive showers and the variation of the frequency of coincidence of two coherent mesons which here are measured together [1]). Above 5 m distance the influence of the coherent mesons is negligible. JÁNOSSI [2]) is of opinion that also the showers are to be divided in two groups, viz. extensive showers and locally more limited ones.

Two years ago already we came to the conclusion that the extensive showers were very rich in photons. We therefore tried to find the proportion of the photons to the electrons in the following way. We used four trains of two sets of counters each, these sets separated by a space of 10 cm designed to be filled with lead screens of different thickness. In case there is no lead between the counters, the particles, mesons and electrons, give coincidences and we can measure at the same time 4 and 6-fold (2 and 3 particles) and 6 and 8-fold (3 and 4 particles). When we apply lead between the counters, the absorption of the soft part of the radiation, the electrons, can be measured. From the absorption curve the energy distribution may be derived. With 10 cm of lead the electrons are practically all absorbed, and we find that the incident radiation contained a number of mesons equalling about 1/10 of the number of electrons. This ratio between the two kinds of particles is totally different from their ratio in the radiation of the atmosphere outside the showers.

When next we put a sheet of lead above the upper set of counters we find an increase. This is on account of the photons in the shower which produce in the top layer of lead Compton electrons or electron-pairs. These secondaries are able to operate the counters under the layer. The absorption of the primary electrons is known from measurements with lead between and above the counters. To determine the number of photons we proceed in the following way.

We know that when the active area of m counters, each of an area f, is called F and N is the density per m^2, the probability of an n-fold coincidence is $(1-e^{-mfN})^n$ or $(1-e^{-FN})^n$. If there are P photons which have an opportunity of producing in the top layer an electron able to operate the counters under the layer, with an efficiency λ, then the probability of an n-fold coincidence in which n_1 counter-sets are discharged by either primary electrons or photon-produced electrons and $n-n_1$ by primary electrons only, is

$$\{1-e^{-F(N+P\lambda)}\}^{n_1}(1-e^{FN})^{n-n_1}; \qquad 0 \leqslant n_1 \leqslant n.$$

For each value n_1 this expression has a special weight g_{n_1} and the total probability for an n-fold coincidence with lead on top of the counter-sets is given by

$$\sum_{n_1=0}^{n_1=n} g_{n_1}\{1-e^{-F(N+P\lambda)}\}^{n_1}(1-e^{-FN})^{(n-n_1)}.$$

The experimental results however gave us an indication that this formula might be simplified in the following way. The $\frac{1}{n}$ th power of the ratio a of n-fold coincidences with and without a layer of lead on top is nearly a constant, as appears from the table hereunder:

N	a	$\sqrt[n]{a}$
2	1,20	1,10
3	1,39	1,12
4	1,80	1,16

Consequently we may conclude that in the case with lead above the counter-trains, the electron density N increases by λP, giving $(1-e^{-F(N+\lambda P)})^n$ for the probability of an n-fold coincidence.

The ratio of n-fold coincidences with and without lead may therefore be expressed as

$$\frac{(1-e^{-F(N+\lambda P)})^n}{(1-e^{-FN})^n} = a$$

in agreement with the above-mentioned experimental results.

If F is known, we can compute N from the measurements without lead, so that e^{-FN} is known too. Substituting then $e^{-F\lambda P} = x$ and $e^{-FN} = y$ enables us to calculate λP in the following way:

$$a = \frac{(1-e^{-FN-F\lambda P})^n}{(1-e^{-FN})^n}$$

$$\sqrt[n]{a} = \frac{1-yx}{1-y}$$

$$\sqrt[n]{a} - y\sqrt[n]{a} = 1-yx$$

$$x = \frac{y\sqrt[n]{a} - \sqrt[n]{a} + 1}{y}.$$

From earlier experiments we found for counters $0{,}03 < \lambda < 0{,}06$. If we now introduce $\lambda = 0{,}06$ the value may turn out to be too small in this case. But we are experimenting at the time to find a more appropriate value.

The measurements treated in the present paper were made in two series. One of them was made in our laboratory under a roof with a concrete ceiling of 20 cm. Four vertical trains of two sets of counters each were used, so that it was possible to measure 2, 3 and 4 particles mainly in a vertical direction.

Next we experimented with the counter-sets placed side by side and 6 and 8 coincident particles were measured. These measurements were repeated with 1 cm Pb above the counter trains. With this arrangement we measured the particles and photons from every direction.

Each set contained 3 counters of 30 cm length and 3,5 cm diametre so that the active area of a set was 315 cm². N was found 35 p m². Using this value, we find $\lambda P = 16$, giving $P = 320$ for $\lambda = 0.06$.

In a second series of measurements 4 and 6-fold coincidences were counted with sets of counters of 70 cm length and 3 cm diametre. 1, 2, 3, 4, 5 and 6 of these counters in turn were used in parallel. As we will see, the minimum density of the showers which we are able to measure depends on the active surface and is smaller when this area is larger, as we had already observed in 1941. In several cases the photons were measured too, with lead (1, 3, 5 and 6 counters in parallel). In all these cases the frequency of coincidence was measured moreover with a cover of 10 cm Pb to the counters.

In one case we have determined the photon-density of the showers using very small surfaces and in doing so we have found a mean density of 150 times the density of the total of the particles of the shower. The density of the photons in this case was 4000 per m² for $\lambda = 0{,}06$.

For the first mentioned experiments the results are given in the graph 1, which shows that the increase by the lead layer is considerable.

Likewise a very interesting result is that, when 1 cm Pb is placed between the upper and lower sets of counters, there is still an increase in the number of coincidences in comparison to that in counters without lead. How is this possible? This is a consequence of the coherence between electrons and

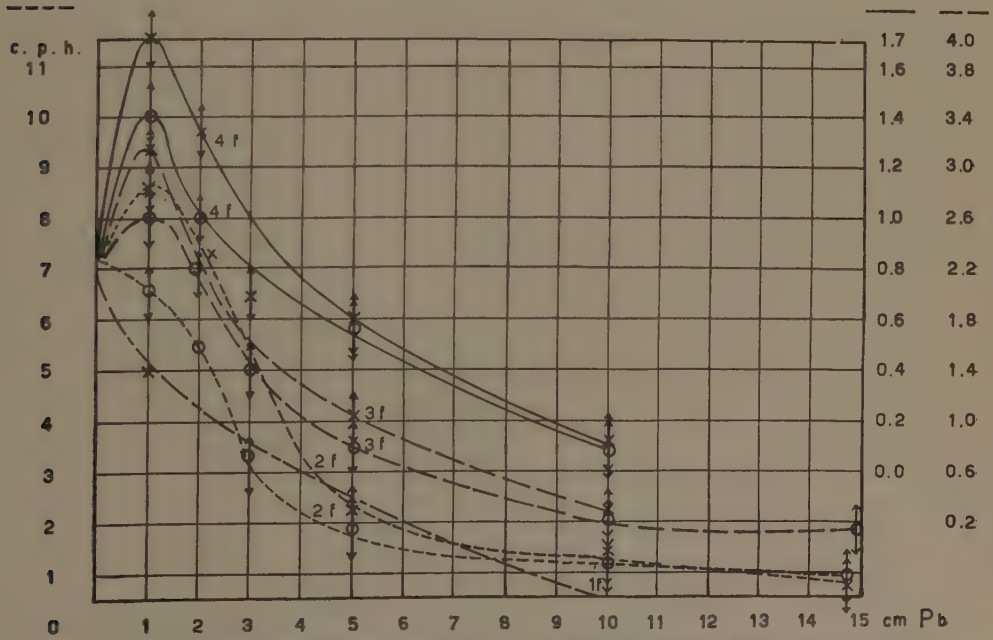

Fig. 1. 3 and 4-fold coincidences open and with different layers of Pb on top (drawn curves) and with Pb between the counter-sets (dotted curves). For comparison the absorption curve is given for the common soft electron component (1 f).

photons. Due to the absorption of the electrons by the lead sheet between

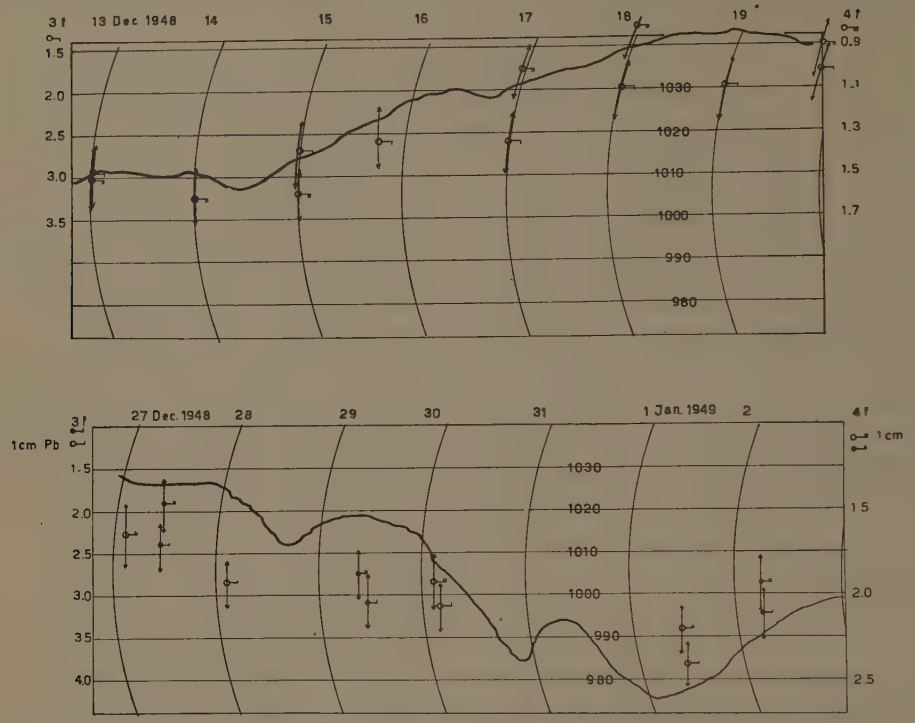

Fig. 2 and 3. The variation of 6 (3p) and 8 (4p) fold coincidences with barometric variations.

the counters a great number of the electrons cannot operate the counters under that sheet and this will decrease the number of coincidences. But there are photons in coherence with the electrons. And the presence of the lead sheet causes these photons to produce secondary electrons. Therefore a coincidence may occur caused by a primary electron traversing the upper set and by a secondary electron produced by a coherent photon traversing the lower set of counters. It may be possible to calculate the effect from the respective numbers of electrons and photons but it is difficult to estimate the energy spectrum of the electrons which is certainly different from that of the electron of the ordinary soft electron component in the radiation which is given also in the graph for comparison.

It is evident that one cannot measure the actual absorption of the primary electrons directly by putting lead over the counters nor by putting the lead between the counters.

Another interesting phenomenon is discernible in this series of observations, but this complicates the issues considerably. It became manifest that barometric fluctuations caused great variations in the frequency of the observed showers. This influence is given in the graphs 2 and 3 and the coefficient of the variation in frequency is 13 % for 1 cm Hg. Conse-

quently we can compare the results of different situations only for identical barometric pressure. This big coefficient is further quite in agreement with the increase of the frequency of showers with increasing altitude observed by HILBERRY in the lower part of the atmosphere and it indicates that the production of the showers may lie not very high in the atmosphere.

We also made a prolonged series of measurements in another building with sets arranged in a hexagon, observing 4 and 6-fold coincidences as mentioned above. Every set contained six counters and measurements were first made with one counter functioning in each box, then two, three ... up till six. From counting 4 and 6-fold coincidences in this manner we could compute the frequency of showers and their mean density. By putting 0,5 cm Pb over the counters the photon density could be estimated and by placing 10 cm Pb over these boxes the penetrating part was determined.

We know that with the increase of the active surface the ratio of the showers of low density to those of high density increases. It is even a well-known fact that with very small surfaces only the densest showers are found. There must be a relation between the frequency and the density of the showers and in analogy with what was found in the case of the meson and the electron spectrum, the most plausible assumption was to suppose that the frequency would be proportional to a power of the density. $I(N)dN = I_0 N^{-S} dN$. We may test by experiments whether the value of S is of the same order as the exponent for the energy for the mesons. This has also been done by COCCONI, LOVERDO and TONGIORGI [3]).

If N is the density and f the active surface of the counters, the chance that a counter system of m counters will be hit is $(1-e^{-mfN})^n$ and the total probability of the coincidence for an area $F = mf$ will be

$$I(F) = I_0 \int_0^\infty N^{-S}(1-e^{-FN})^n \, dN.$$

TABLE.

Number of counters	Absorber	Surface in cm²	$4f$	$6f$	$\frac{6f}{4f}$	N	P	M
	1—10 cm *Pb*	64				140	250 (4000)	
1	0	230	2,0	1,6	0,8	100		
	1 cm *Pb*	230	3,8	2,1		60	26 (410)	
	10 cm *Pb*	230						
2	0	460	4,6	3,1	0,68	38		
3	0	690	9,7	6,3	0,68	19		
	0,5 cm *Pb*	690	12,1	7,9		23	5 (80)	
	10 cm *Pb*	690	0,6	0,4				5
4	0	920	13,3	7,9	0,60	16		
5	0	1150	19,1	9,7	0,51	11		
6	0	1400	26,0	14,1	0,55	9		
	0,5 cm *Pb*	1400	30,1	17,0			1,5 (24)	
	10 cm *Pb*	1400	3,6	1,7				4

After the substitution of $FN = x$ this becomes

$$I(F) = I_0 F^{S-1} \int_0^\infty x^{-S} (1 - e^{-x})^n \, dx.$$

What we next want to find is the value of S. There are two ways: by varying F and by measuring for different values of n. The first has been done by COCCONI, LOVERDO and TONGIORGI and gives mathematically the simplest result, as the integrals for two values of F are the same and

$$\frac{I(F_1)}{I(F_2)} = \left(\frac{F_1}{F_2}\right)^{S-1}$$

gives directly the value of S which is constant for different N's, but it is more correct to derive the relation from different areas which have different observed mean densities. Therefore it is preferable to find S for different n's and use the same surface per set. We have made measurements in both ways, as we have observations of the relation of 4 and 6-fold coincidences with sets of 1, 2, 3, 4, 5 and 6 counters in every set.

For the relation of sixfold and fourfold coincidences the values which we found were:

S	Theoretical	Experimental	N (density)
1,5	0,89	0,84	100
2,0	0,78	0,68	19
2,5	0,63	0,60	16
3,0	0.58	0,55	9

The integrals $I(F)$ were calculated for a series of S and n values by Mr H. F. JONGEN to whom we are much indebted.

With these results it is obvious that we may not take the value of S constant for all densities, but that with the increase of density the value S decreases, and therefore our assumption about S in $I(F)$ is not perfectly correct, but this was a first attempt to solve the problem.

These different values of S are in agreement with our results for the track density of bursts [1]), which is for the low density of the order of 3,0 and for high densities 1,6. Also the value of proportion of two coincidences of different numbers n is different.

For one counter the value	6/4 f	5/4 f	4/3 f	3/2 f
theoretical	0,78	0,77	0,72	0, 33
experimental	0,8	0,6	0,36	0,11

This agreement is not too good, but the tendency in the calculations and the observations is the same.

Finally I wish to thank Mr G. KLEIN for his help with part of the experiments.

Amsterdam, Febr. 1949.

REFERENCES.

1. J. CLAY, Phys. Soc. Cambridge Rep. 47 (1947).
2. L. JÁNOSSY & ROCHESTER, Phys. Roy. Soc. A **181**, 399 (1943).
3. G. COCCONI, A. LOVERDO, V. TONGIORGI, Phys. Rev. **70**, 841 (1946).

Biochemistry. — *On stearate systems containing methyl-hexylcarbinol with viscous and elastic properties comparable to elastic viscous oleate systems containing KCl.* By H. J. VAN DEN BERG and L. J. DE HEER. (Communicated by Prof. H. G. BUNGENBERG DE JONG.)

(Communicated at the meeting of March 26, 1949.)

1. *Introduction.*

The results obtained in this laboratory [1]) with elastic viscous oleate systems containing KCl opened up the question if any systems with analogous properties also exist with other soaps. A priori one would be inclined to answer in the affirmative, as at sufficienlty high temperature palmitates and stearates also form elastic systems at KCl concentrations which are to low for coacervation.

Difficulties to be foreseen in the measuring technique at such high temperatures withheld us for some time to start with such an investigation.

The elastic systems obtained at high temperatures cannot be investigated after having cooled down to room temperature as they are no longer stable then (the soaps separate in an insoluble form). Prof. BUNGENBERG DE JONG informed us that the temperature at with the elastic stearate system of the composition 1.2 % *K*-stearate in 0.2 N KOH becomes unstable, can considerably be lowered by adding the proper amount of a suitable organic substance, e.g. methyl-hexylcarbinol. It was therefore decided to perform some measurements on the above stearate systems for which we used "*K*-stearat, doppelt gereinigt, RIEDEL DE HAEN", as this preparation makes it possible to get stable and clear systems at even 15°.

2. *Preparation of the elastic system.*

When the system (1.2 gr *K*-stearate p. 100 cc in 0.2 N KOH) has cooled down to room temperature, it is a thick semiliquid somewhat pasty system, of a white silky appearance. If at 15° one adds increasing amounts of methyl-hexylcarbinol and homogenizes it by vigorous shaking, it is found that gradually the white silky appearance becomes less and the system changes into a clear markedly elastic system, which on further addition of the alcohol grows turbid and finally looses its elastic properties completely. It was found in preliminary experiments (rotational oscillation in a spherical vessel with a radius of 3.58 cm) that as a function of the added amount of methyl-hexylcarbinol, the values

1) Cf. H. G. BUNGENBERG DE JONG and H. J. VAN DEN BERG, these Proceedings part I, **51**, 1197 (1948), parts II, III, IV, V, **52**, 15, 99, 363, 377 (1949).

ν ($= 1/T$), $1/\Lambda$ and n increase to a certain maximum and next decrease. The maxima, which nearly coincide, are situated in the region of the completely clear systems. For the experiments in the following section we made a large quantity of elastic system corresponding to the position of the above maxima, for which an addition of 0.42 cc methyl-hexyl-carbinol was needed per 100 cc. 1.2 % *K*-stearate in 0.2 N KOH.

3. *Period and logarithmic decrement as function of the radius of the sphere at 15.7°.*

The methods used and the calculations of the elastic constants were the same as described by H. G. BUNGENBERG DE JONG and H. J. VAN DEN BERG in their publication of their investigations on elastic viscous oleate systems (see note 1, Part I, II and III).

The results obtained with the rotational oscillation at 15.7° are collected in Table I and depicted in fig. 1.

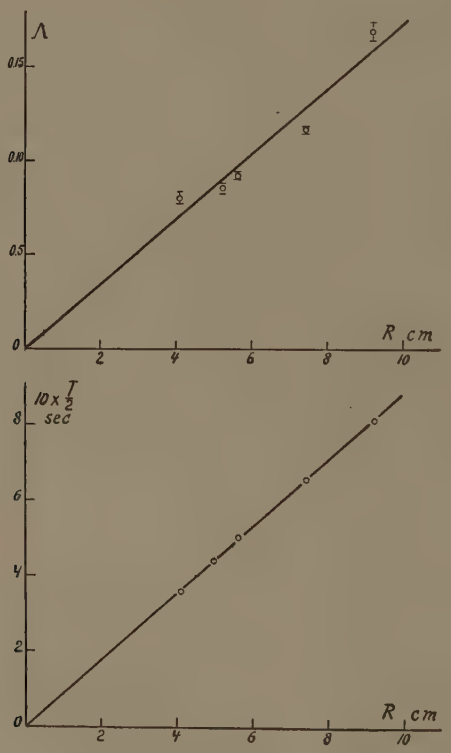

Fig. 1.

We see from fig. 1 lower that the period is proportional to the radius R of the sphere. Compared with oleate systems this is quite the same result.

In oleate systems we meet two different cases as regards the dependence of Λ on R. In 1.2 % systems it was found to be proportional to R, in 0.6 % systems, however, it was found to be independent of R. We

TABLE I.

Measurement with a 1.2 % stearate system (containing 0.2 N KOH and 0.42 cc methyl-hexylcarbinol per 100 cc) at 15.7° C (rotational oscillation).

R(cm)	n	$10 \times \frac{T}{2}$ (sec)	b_1/b_3	Λ	$\lambda = (T/2\Lambda)$ (sec)		G (dynes/cm^2)		
9.24	96.5	8.10	1.183	0.168 ± 0.005	4.82		64.2		
7.46	93.8	6.54	1.124	0.116 ± 0.002	5.64	mean	64.2	mean	$\eta = G \times \lambda =$
5.65	86.2	5.02	1.096	0.092 ± 0.002	5.47	5.12	62.5	63.9	$5.12 \times 63.9 =$
5.01	83.5	4.40	1.089	0.085 ± 0.003	5.16		63.9		**327 poises**
4.12	74.2	3.60	1.083	0.080 ± 0.003	4.51		64.6		

see from fig. 1 upper that in our 1.2 % stearate system too, Λ is proportional to the radius of the sphere. This means that here too the damping of the elastic oscillations must be ascribed to relaxation of the elastic stresses with a constant time of relaxation λ [2]). These values of λ (calculated from $T/2\Lambda$) are given in column 6 of Table I and fluctuate considerably around the mean value 5.12.

This is most probably connected with the relatively low damping (far lower values of Λ as were ever found in oleate systems). The lower the damping ratio b_1/b_3 the more experimental errors exert their influence on Λ (which is $ln\, b_1/b_3$). Such great fluctuations are not found in the calculated G values (Table I, column 7), which brings out that the b_1/b_3 measurements are far more difficult than the $10 \times T/2$ measurements.

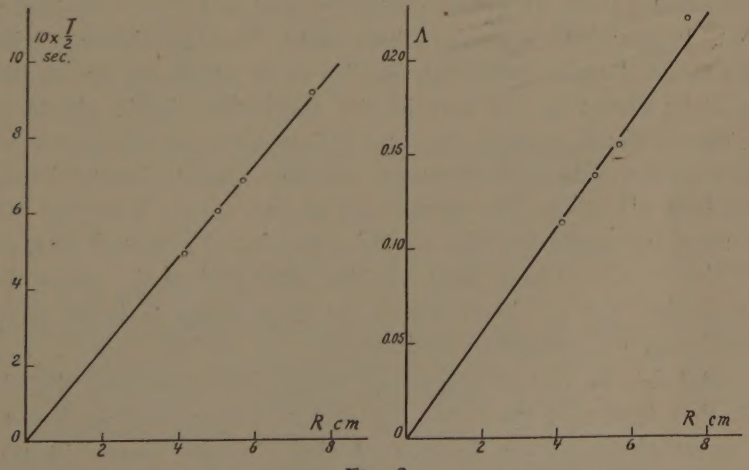

Fig. 2.

We therefore decided also to perform elastic measurements on a lower concentrated system, which we obtained by diluting three volumes of the above 1,2 % stearate system with one volume 0.2 N KOH. As it is highly probable that the methyl-hexylcarbinol is practically wholly bound to the stearate, an extra addition of it was deemed to be unnecessary.

---

2) J. M. BURGERS, Proc. Kon. Ned. Akad. v. Wetensch., Amstedram, **51**, 1211 1948).

TABLE II.

Measurements with a 0.9 % stearate system (containing 0.2 N KOH and 0.32 cc methyl-hexylcarbinol per 100 cc) at 15.7° C (rotational oscillation).

R(cm)	n	$10 \times \frac{T}{2}$ (sec)	b_1/b_2	Λ	$\left(\lambda = \frac{T}{2\Lambda}\right)$ (sec)		G (dynes/cm²)		
7.46	54.7	9.18	1.250	0.2232	4.11		32.6		
5.65	63.3	6.86	1.168	0.1553	4.42	mean	32.4	mean	$\eta = G \times \lambda =$
5.01	61.3	6.06	1.149	0.1389	4.36	4.30	33.7	33.3	$= 4.30 \times 3.33$
4.12	59.4	4.92	1.121	0.1138	4.31		34.6		**= 143 poises**

The results obtained with this 0.9 % stearate system are collected in Table II and depicted in fig. 2, from which we once more see that $T \sim R$ and $\Lambda \sim R$, the experimental Λ points now deviating much less from the drawn straight line than in fig. 1 upper. Therefore the calculated λ values (column 6) also show far smaller fluctuations percentually.

That is why we feel justified in assuming that the irregularities in the Λ and λ values met with in the 1.2 % stearate system, were caused by the difficulties in the measurement of the damping ratio.

In Table I we have also calculated the value $G \times \lambda$, which we will need in the next section.

4. *Viscous behaviour of the 1.2 % stearate system at 15.7°.*

For this investigation we used the same method as described by H. G. BUNGENBERG DE JONG, H. J. VAN DEN BERG and L. J. DE HEER (see note 1, Part. V). It may suffice to give here only the (logarithmic) viscosity-shearing stress diagram obtained. See fig 3, in which we notice the same characteristic shape as we met in the markedly elastic oleate system, though due to the very high viscosity at low shearing stresses it was not possible to make sufficiently accurate measurements to locate the η_0 level. The bending off at the left upper end of the curve, however, suggests that it must lie approximately as indicated by the dotted line. ($\log \eta_0 = 2.08$, that is $\eta_0 = 120$ poises). At the other end of the curve we have not yet reached the η_∞ level, which we may expect to lie at an η value in the order of 10 centipoises or lower.

The total fall in viscosity from η_0 to η_∞ by increasing the shearing stress is therefore very great, viz. at least to a thousandfold lower value.

The most characteristic feature of the viscosity curve in fig. 3 is, however, the occurrence of an intermediate level. The total fall in viscosity by increasing the shearing stress takes place in two separate steps, the first from ± 120 poises down to ± 4 poises, the second from ± 4 poises down to 0.1 poise. (or lower).

Such viscosity curves with three levels are characteristic of the markedly elastic oleate systems.

Finally we may discuss a further point of resemblance between stearate and oleate systems. It was found for the latter that the viscosity coefficient

calculated from the elastic measurements (using MAXWELL's formula $\eta = G \times \lambda$) is of the same order as the experimentally determined η_0 level, though η_0 was found to be always smaller than $G \times \lambda$ [3]).

We have drawn in figure 3 the level corresponding with the value $G \times \lambda$, which according to table I was found to be 327 poises (log η is therefore 2,51). Assuming the η_0 level to lie at approximately 120 poises (log $\eta = 2{,}08$), as drawn in figure 3, η_0 would be approximately 2,7 times smaller than $G \times \lambda$.

For oleate systems the disagreement between η_0 and $G \times \lambda$ has been found to increase with the absolute value of η_0 and from this one would have expected for an η_0 value of 120 poises a disagreement which comes near to the above mentioned value of 2,7 times smaller. (i.e. $\eta_0/G \times \lambda = 0{,}37$).

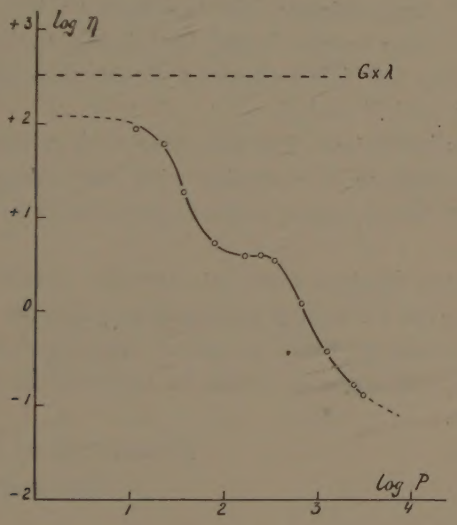

Fig. 3 [4])

5. *Final remarks.*

The investigations described above show that the characteristics of the elastic and viscous properties of the soap system used are the same as those of oleate systems containing KCl. They do not claim to give accurate figures for a pure stearate, however. In spite of the indication "doppelt gereinigt", the preparation of *K*-stearate used, appeared in further experiments to be anything but pure. BUNGENBERG DE JONG and DE HEER, in comparing a number of *K*-stearates and stearic acids of different origin, have found very great differences at to the damping under

[3]) Cf. paper quoted in note 1, part V.

[4]) P = shearing stress at the wall of the capillary in dynes/cm^2; V = mean rate of flow in cm^3/sec. In figure 3 the ordinate does not indicate log V, but log P—log V, which stands for the meaning of the logarithm of a viscosity coefficient η.

comparable conditions. Really pure stearate systems (using a preparation of Stearic acid "Kahlbaum" with m. p. 69°) cannot be transformed into clear elastic systems with methyl-hexylcarbinol at 15°, nor at 20°, but it does succeed at 40°. At 40° however, RIEDEL DE HAEN's preparation, which we used in this investigation, was no longer measurable because of the now very great damping (n, the number of turning-points being only 3) though it had a small damping at 15° (n having now values in the order of 60).

Summary.

1. It has appeared to be possible to make elastic-viscous systems, with analogous properties, with other soaps than oleates. One must slightly alter the methods of preparation though, in order to obtain systems which are measurable at a conveniently low temperature.

2. Analogous to the results found for elastic measurements of oleate systems of more than 1,1 % Na-oleate, a direct proportionality was found between A and R, and T and R.

3. The viscous behaviour was the same as has been found for oleate systems viz. a breakdown of viscosity with increasing shearing stress in a two-step process, which seems to be characteristic for these elastic soap systems.

4. There exists a disagreement between the viscosity η_0, measured at low shearing stress (at the wall of the capillary) and the viscosity predicted by MAXWELL's formula $\eta = G \times \lambda$, which disagreement is found to be of the same order of magnitude as could be expected from the behaviour of the oleate systems.

Department of Medical Chemistry,
University of Leiden.